EXPERIMENTAL STUDY ON EFFECT OF AGGREGATE SIZE ON THE HYDRAULIC PROPERTIES OF PERVIOUS CONCRETE

Thesis

Submitted in partial fulfilment of the requirements for the degree of

DOCTOR OF PHILOSOPHY

by

PREETI JACOB

DEPARTMENT OF WATER RESOURCES AND OCEAN ENGINEERING
NATIONAL INSTITUTE OF TECHNOLOGY KARNATAKA,
SURATHKAL, MANGALURU - 575 025

DECEMBER, 2023

EXPERIMENTAL STUDY ON EFFECT OF AGGREGATE SIZE ON THE HYDRAULIC PROPERTIES OF PERVIOUS CONCRETE

Thesis

Submitted in partial fulfilment of the requirements for the degree of

DOCTOR OF PHILOSOPHY

By

PREETI JACOB

145088AM14P02R

Under the guidance of

Dr. G S Dwarakish

Professor

Department of Water Resources and Ocean Engineering

NITK, Surathkal

DEPARTMENT OF WATER RESOURCES AND OCEAN ENGINEERING

NATIONAL INSTITUTE OF TECHNOLOGY KARNATAKA,

SURATHKAL, MANGALURU - 575 025

DECEMBER, 2023

DECLARATION

I hereby *declare* that the Research Thesis entitled **Experimental Study on Effect of Aggregate Size on the Hydraulic Properties of Pervious Concrete** which is being submitted to the National Institute of Technology Karnataka, Surathkal in partial fulfilment of the requirements for the award of the Degree of Doctor of Philosophy in the **Department of Water Resources and Ocean Engineering** is a *bonafide report of the research work carried out by me*. The material contained in this Research Thesis has not been submitted to any University or Institution for the award of any degree.

PREETI JACOB
(145088AM14P02R)
Department of Water Resources and Ocean Engineering
National Institute of Technology Karnataka, India

Place: NITK, Surathkal
Date: 15-12-2023

CERTIFICATE

This is to *certify* that the Research Thesis entitled **Experimental Study on Effect of Aggregate Size on the Hydraulic Properties of Pervious Concrete** submitted by **PREETI JACOB** (Register Number: 145088AM14P02R) as the record of the research work carried out by her, is *accepted as the Research Thesis submission* in partial fulfilment of the requirements for the award of degree of Doctor of Philosophy.

G. S. Dwarakish
18.12.23

Research Guide

(Name and Signature with Date and Seal)

Vanja K
22.12.23

Chairman – DRPC

Chairman (DRPC)
Dept. of Water Resources & Ocean Engineering

(Name and Signature with Date and Seal)

ACKNOWLEDGEMENTS

First and foremost, I am deeply thankful to my esteemed supervisor, Dr. G S Dwarakish, for his unwavering guidance, invaluable insights, and endless encouragement throughout the research endeavor. His mentorship has been a source of inspiration, and I am grateful for the knowledge and skills I have gained under his tutelage.

I am also indebted to the members of my thesis committee, Dr. Lakshman Nandagiri and Dr. C P Devatha for their valuable feedback and constructive criticism that significantly improved the quality of this work.

My gratitude extends to my colleagues in CMR Institute of Technology, Bengaluru for their camaraderie and stimulating discussions. Their support and friendship have made the academic journey more enjoyable and rewarding.

My gratitude also extends to my fellow researchers for accommodating me in the intervals, I have being in NITK Surathkal. Special thanks to Bindu mam, Ganasri, Dinu, Waleed, and Mukul. A special thanks to Waleed for running around for me for the formalities associated with PhD work.

I am deeply grateful to my family especially my husband Jaycobe C Cheeran, my parents K S Jacob and Jessie Jacob, my parents-in-law Molly Chummar and C I Chummar, and my niece, Suzanne for their unwavering love, encouragement, and patience throughout my years of study. Their constant support has been a pillar of strength during both the highs and lows of this challenging journey. I have to especially thank my kids Annmaria and Alex for understanding that their mother is doing some serious work.

Lastly, I wish to thank all those who have contributed to my work, directly or indirectly.

PREETI JACOB

ABSTRACT

Pervious Concrete is a distinct type of concrete in which narrow gradations of aggregates are used to increase the permeability. Though pervious concrete is green concrete that allows water passage through its pores, it tends to clog due to particles in the runoff. The study aims to evaluate the impact of clogging on pervious concrete mixes and explore a simple method to calculate permeability and clogging using the falling head method in a fabricated unit. The materials used are cementitious materials and aggregates, along with superplasticizers. The cementitious materials used are OPC Grade 53 cement and micro–Ground Granulated Blast Furnace Slag (μGGBS). Two separate narrow aggregate gradations are used - 2.36 - 4.75mm and 4.75 - 6.30mm. The water-binder ratio is taken as 0.25, and the aggregate-binder ratio is taken as 3.33. The clogging materials used are clay and sand with a concentration of 5g/l for six cycles. The pervious concrete's compressive strength, permeability, and clogging potential are calculated. In addition, the image analysis of the top surface of pervious concrete is done in ImageJ open-source software to understand the reduction of pores as the clogging cycle progresses. The R open-source software is used for statistical analysis through split violin plots by comparing the effect of clay and sand on the top surface.

The average compressive strength for 2.36 - 4.75mm and 4.75 - 6.30mm is 24MPa and 20MPa respectively. The average permeability for 2.36 - 4.75mm and 4.75 - 6.30mm is 4.78mm/s and 8.16m/s, respectively. The relationship between porosity and permeability is established. The introduction of clay slurry reduces the permeability by 69.8% and 74.9%, respectively, and with sand, it decreases by 74.7% and 71.7%, respectively in its first cycle. The sand particles are retained in the pervious concrete matrix for all clogging cycles in both the aggregate size gradation. The clogging potential of clay and sand are calculated for both the gradations.

The top surface of the pervious concrete was analyzed for the properties of area, perimeter, aspect ratio, circularity, roundness and solidity through image analysis. For the aggregate size gradation of 2.36 – 4.75mm, in the six clogging cycles of clay, the total percentage area reduced from 14.02% to 8.68%, whereas for sand, the total percentage area reduced from 13.16% to 4.11%. For the aggregate size gradation of 4.75 – 6.30mm, in the six clogging cycles of clay, the total percentage area reduced from 9.54 % to 6.90%, whereas for sand, the total percentage area reduced from 8.89% to 5.50%.

It concludes that the clogging cycle follows an exponential curve, and the maximum clogging occurs when the clogging material is introduced to the specimen for the first time. The values indicates that sand clogs the pervious concrete matrix more than clay particles. The clogging of pervious concrete is typically a top surface phenomenon. The degradation of permeability depends on the clogging particle's particulate size and the concrete matrix's pore size. The smaller aggregates in pervious concrete are not recommended in areas of high siltation. The pore analysis indicates that the pores are non-circular and cause delay in the permeability of pervious concrete.

Keywords: pervious concrete, permeability, clogging, image analysis, ImageJ, R.

TABLE OF CONTENTS

ABSTRACT.....i

TABLE OF CONTENTS.....iii

LIST OF FIGURES.....vii

LIST OF TABLES.....xi

LIST OF ABBREVIATIONS.....xiii

CHAPTER 1 INTRODUCTION 1

1.2. GENERAL.....1

1.3. MIX PROPORTION 3

1.4. ENVIRONMENTAL SIGNIFICANCE 4

1.5. RESEARCH SIGNIFICANCE.....5

1.6. LOW IMPACT DEVELOPMENT(LID) 6

1.7. PERVIOUS CONCRETE FOR SUSTAINABLE URBAN DEVELOPMENT.....7

1.8. IMAGE ANALYSIS OF PERVIOUS CONCRETE 7

CHAPTER 2 LITERATURE SURVEY 9

2.1. GENERAL.....9

2.2 SUSTAINABLE URBAN DRAINAGE SYSTEM(SUDS)/ LOW IMPACT DEVELOPMENT (LID).....9

2.3 COMPOSITION AND MECHANICAL PROPERTIES OF PERVIOUS CONCRETE.....11

2.4 HYDRAULIC PROPERTIES OF PERVIOUS CONCRETE 18

2.5 CLOGGING OF PERVIOUS CONCRETE..... 20

2.6 IMAGE ANALYSIS OF PERVIOUS CONCRETE..... 24

2.7 LITERATURE SUMMARY 25

2.8 LITERATURE GAPS..... 26

2.9 RESEARCH OBJECTIVES 26

CHAPTER 3 METHODOLOGY..... 27

3.1 GENERAL 27

3.2 MIX DESIGN AND COMPOSITION 28

3.2.1 Binding material..... 28

3.2.2 Aggregates 29

3.2.3 Mix design 30

3.2.4 Sample Preparation 33

3.3 LABORATORY SET UP FOR PERMEABILITY 34

3.4 SOFTWARE USED 35

3.4.1 ImageJ 35

3.4.2 R..... 36

3.5 CLOGGING OF CONCRETE 36

3.6 IMAGE ANALYSIS OF PERVIOUS CONCRETE..... 39

3.6.1 Use of ImageJ for Pore Analysis of Pervious Concrete..... 39

3.7 STATISTICAL ANALYSIS OF PORE PROPERTIES OF PERVIOUS CONCRETE 42

3.7.1 Violin plot 42

3.7.2 Data analysis through violin plot 43

3.7.3 Split Violin plots..... 44

3.7.4 Use of R for Pore Analysis of Pervious Concrete..... 44

3.8 PROPERTIES OF PERVIOUS CONCRETE 47

3.8.1 Compressive strength test 47

3.8.2 Porosity 47

3.8.3 Permeability test 48

3.8.4 Clogging test 48

CHAPTER 4 RESULTS AND DISCUSSION 51

4.1 INTRODUCTION 51

4.2 INFLUENCE OF AGGREGATE SIZE ON THE COMPRESSIVE STRENGTH OF PERVIOUS CONCRETE 51

4.3 INFLUENCE OF AGGREGATE SIZE ON THE HYDRAULIC PROPERTIES OF PERVIOUS CONCRETE 55

4.4 CLOGGING POTENTIAL OF PERVIOUS CONCRETE 59

4.4.1 Clay clogging 59

4.4.2 Sand clogging 61

4.4.3 Clogging potential 61

4.5 EXFILTRATE QUALITY ANALYSIS 63

4.6 USE OF IMAGE ANALYSIS FOR UNDERSTANDING TOP SURFACE CLOGGING OF PERVIOUS CONCRETE 65

4.7 ANALYIS OF AREA OF THE PORES ON TOP SURFACE OF PERVIOUS CONCRETE 66

4.8 ANALYSIS OF PERIMETER OF THE PORES ON THE TOP SURFACE OF PERVIOUS CONCRETE 70

4.9 ANALYSIS OF ASPECT RATIO OF THE PORES ON THE TOP SURFACE OF PERVIOUS CONCRETE 74

4.10 ANALYIS OF CIRCULARITY OF PORES ON THE TOP SURFACE OF PERVIOUS CONCRETE 88

4.11 ANALYSIS OF ROUNDNESS OF PORES ON THE TOP SURFACE OF PERVIOUS CONCRETE..... 102

4.12 ANALYSIS OF SOLIDITY OF PORES ON THE TOP SURFACE OF PERVIOUS CONCRETE..... 115

4.13 CLOSURE..... 128

CHAPTER 5 CONCLUSIONS..... 129

5.1 CONCLUSIONS 129

5.2 LIMITATIONS 130

5.3 FUTURE WORK 130

REFERENCES 131

LIST OF PUBLICATIONS 141

BIO DATA.....143

LIST OF FIGURES

Figure 1.1 Layers of Pervious Concrete Pavement(Chandrappa and Biligiri 2016) 4

Figure 2.1 Aggregate/ Binder and Water/ Binder ratios as referred from literature 12

Figure 2.2 The experimental set up used in literature 18

Figure 3.1 Micro GGBS(Ground Granulated Blast Slag) 29

Figure 3.2 Aggregate size range of 2.36 - 4.75mm 30

Figure 3.3 Cement paste drain at the bottom of concrete specimen.....31

Figure 3.4 Concrete specimens for compressive strength 34

Figure 3.5 Permeability fabrication for pervious concrete 35

Figure 3.6 Sieve Analysis of Clay and Sand particles 37

Figure 3.7 Clogging of clay and sand on the pervious concrete mix - 2.36 - 4.75mm narrow gradation.....38

Figure 3.8 Clogging of clay and sand on the pervious concrete mix - 4.75 - 6.30mm narrow gradation.....39

Figure 3.9 Flowchart for image analysis in ImageJ 40

Figure 3.10 Comparison of box plot and violin plot(Hintze and Nelson 1998)....43

Figure 3.11 Syntax for plotting violin plot in R 45

Figure 3.12 Syntax for plotting violin plot with box plot in R.....45

Figure 3.13 Syntax for plotting split violin plot in R 46

Figure 3.14 Compressive testing of pervious concrete specimen 47

Figure 3.15 Mixing of clay particles for clogging test 49

Figure 4.1 Comparison of compressive strength from literature with present study 55

Figure 4.2 Comparison of porosity from literature with present study..... 57

Figure 4.3 Comparison of permeability from literature with present study 57

Figure 4.4 Relationship between permeability and porosity 59

Figure 4.5 Box plot of variations of permeability for both aggregate size gradations 58

Figure 4.6 Comparison of permeability due to clay clogging 60

Figure 4.7 Comparison of permeability due to sand clogging..... 61

Figure 4.8 Clogging potential for all case scenarios..... 63

Figure 4.9 Cumulative clay retention..... 64

Figure 4.10 Cumulative sand retention..... 64

Figure 4.11 Split violin plot of area comparing clay and sand clogging – 2.36-4.75mm 69

Figure 4.12 Split violin plot of area comparing clay and sand clogging – 4.75-6.30mm 70

Figure 4.13 Split violin plot of perimeter comparing clay and sand clogging – 2.36 – 4.75mm 73

Figure 4.14 Split violin plot of perimeter comparing clay and sand clogging –4.75 – 6.30mm 74

Figure 4.15 Split violin plot of aspect ratio comparing clay and sand clogging – 2.75 – 4.75mm 78

Figure 4.16 Split violin plot of aspect ratio comparing clay and sand clogging – 4.75 – 6.30mm 79

Figure 4.17 Aspect Ratio Vs Area for 2.36-4.75mm - Clay clogging cycles..... 80

Figure 4.18 Aspect Ratio Vs Perimeter for 2.36-4.75mm - Clay clogging cycles 81

Figure 4.19 Aspect Ratio Vs Area for 2.36-4.75mm - Sand clogging cycles..... 82

Figure 4.20 Aspect Ratio Vs Perimeter for 2.36-4.75mm - Sand clogging cycles83

Figure 4.21 Aspect Ratio Vs Area for 4.75-6.30mm – Clay clogging cycles.....84

Figure 4.22 Aspect Ratio Vs Perimeter for 4.75-6.30mm – Clay clogging cycles 85

Figure 4.23 Aspect Ratio Vs Area for 4.75-6.30mm – Sand clogging cycles 86

Figure 4.24 Aspect Ratio Vs Perimeter for 4.75-6.30mm –Sand clogging cycles87

Figure 4.25 Split violin plot of circularity comparing clay and sand clogging – 2.36-4.75mm.....91

Figure 4.26 Split violin plot of circularity comparing clay and sand clogging – 4.75-6.30mm.....92

Figure 4.27 Circularity Vs Area for 2.36-4.75mm - Clay clogging cycles.....93

Figure 4.28 Circularity Vs Perimeter for 2.36-4.75mm - Clay clogging cycles ...94

Figure 4.29 Circularity Vs Area for 2.36-4.75mm - Sand clogging cycles 95

Figure 4.30 Circularity Vs Perimeter for 2.36-4.75mm - Sand clogging cycles...96

Figure 4.31 Circularity Vs Area for 4.75-6.30mm - Clay clogging cycles.....98

Figure 4.32 Circularity Vs Perimeter for 4.75-6.30mm - Clay clogging cycles ...99

Figure 4.33 Circularity Vs Area for 4.75-6.30mm - Sand clogging cycles 100

Figure 4.34 Circularity Vs Perimeter for 4.75-6.30mm - Sand clogging cycles.101

Figure 4.35 Split violin plot of roundness comparing clay and sand clogging – 2.36-4.75mm.....104

Figure 4.36 Split violin plot of roundness comparing clay and sand clogging – 4.75 – 6.30mm.....105

Figure 4.37 Roundness Vs Area for 2.36 - 4.75mm - Clay clogging cycles.....106

Figure 4.38 Roundness Vs Perimeter for 2.36 - 4.75mm - Clay clogging cycles 107

Figure 4.39 Roundness Vs Area for 2.36 - 4.75mm - Sand clogging cycles 108

Figure 4.40 Roundness Vs Perimeter for 2.36 - 4.75mm - Sand clogging cycles 109

Figure 4.41 Roundness Vs Area for 4.75-6.30mm - Clay clogging cycles 111

Figure 4.42 Roundness Vs Perimeter for 4.75-6.30mm – Clay clogging cycles 112

Figure 4.43 Roundness Vs Area for 4.75-6.30mm - Sand clogging cycles..... 113

Figure 4.44 Roundness Vs Perimeter for 4.75-6.30mm - Sand clogging cycles 114

Figure 4.45 Split violin plot of solidity comparing clay and sand clogging – 2.36 – 4.75mm 117

Figure 4.46 Split violin plot of solidity comparing clay and sand clogging – 4.75 – 6.30mm 118

Figure 4.47 Solidity Vs Area for 2.36 - 4.75mm - Clay clogging cycles 119

Figure 4.48 Solidity Vs Perimeter for 2.36 - 4.75mm - Clay clogging cycles ... 120

Figure 4.49 Solidity Vs Area for 2.36 - 4.75mm - Sand clogging cycles..... 121

Figure 4.50 Solidity Vs Perimeter for 2.36 - 4.75mm - Sand clogging cycles... 122

Figure 4.51 Solidity Vs Area for 4.75-6.30mm - Clay clogging cycles 124

Figure 4.52 Solidity Vs Perimeter for 4.75-6.30mm - Clay clogging cycles 125

Figure 4.53 Solidity Vs Area for 4.75-6.30mm - Sand clogging cycles..... 126

Figure 4.54 Solidity Vs Perimeter for 4.75-6.30mm - Sand clogging cycles..... 127

LIST OF TABLES

Table 2.1 Summary of the mix proportion, specimen size and properties of pervious concrete 13

Table 3.1 Cement paste drain studies of different mix proportions 31

Table 3.2 Mix Proportions for pervious concrete.....33

Table 3.3 Geometric property and its equations.....40

Table 4.1 Compressive strength of the pervious concrete mixes 52

Table 4.2 Compressive strength, porosity and permeability ranges from standards 52

Table 4.3 Reference of mix proportion and properties of pervious concrete.....54

Table 4.4 Porosity and density of the pervious concrete mixes 56

Table 4.5 Clogging potential equation 63

Table 4.6 Pore shape and its geometric properties.....65

Table 4.7 Basic statistics of area(mm^2) for clay and sand clogging cycle – 2.36-4.75mm.....67

Table 4.8 Basic statistics of area(mm^2) for clay and sand clogging cycle – 4.75 – 6.30mm.....68

Table 4.9 Basic statistics of perimeter(mm) for clay and sand clogging cycles – 2.36-4.75mm 71

Table 4.10 Basic statistics of perimeter(mm) for clay and sand clogging cycles – 4.75-6.30mm 72

Table 4.11 Basic statistics of aspect ratio for clay and sand clogging cycles – 2.36-4.75mm.....75

Table 4.12 Basic statistics of aspect ratio for clay and sand clogging cycles –4.75-6.30mm.....77

Table 4.13 Basic statistics of circularity for clay and sand clogging cycles – 2.36 – 4.75mm 89

Table 4.14 Basic statistics of circularity for clay and sand clogging cycles –4.75 – 6.30mm 90

Table 4.15 Basic statistics of roundness for clay and sand clogging cycles – 2.36 – 4.75mm 102

Table 4.16 Basic statistics of roundness for clay and sand clogging cycles – 4.75-6.30mm 103

Table 4.17 Basic statistics of solidity for clay and sand clogging cycles 115

Table 4.18 Basic statistics of solidity for clay and sand clogging cycles 116

LIST OF ABBREVIATIONS

Abbreviation	Meaning
µGGBS	Micro Ground Granulated Blast Furnace Slag
ACI	American Concrete Institute
IQR	Inter Quartile Range
IS	Indian Standards
LID	Low Impact Development
NBR	Norma Brasileira Regulamentadora
OPC	Ordinary Portland Cement
SUDS	Sustainable Urban Drainage Systems
SWMM	Storm Water Management Model
VTT	Valtion Teknillinen Tutkimuskeskus

CHAPTER 1
INTRODUCTION

1.1 GENERAL

Pervious Concrete is a distinct type of concrete in which narrow gradations of aggregates are used to increase the porosity. It contains cement, water, gravel or stone, and little to no sand. It is also called no-fines concrete. It creates an open cell structure that allows water and air to pass through it. (Huang et al. 2010) used latex, natural sand, and fiber to improve pervious concrete's strength and drainage characteristics. It allows storm water to infiltrate through the pavement and reduces or eliminates the need for additional control structures, such as retention ponds. It is one of the Best Management Practices (BMPs) recommended by US Environmental Protection Agency (EPA).

Pervious concrete is a green solution for reducing the impact of high urban runoff. It can minimize the rate of runoff in highly impervious areas by allowing the passage of rainfall through the pervious concrete matrix. Though it has a lot of advantages, clogging of pervious concrete is a concern for making it commercial in developing countries. Clogging of pervious concrete takes place on the top surface of the pavement (Kayhanian et al. 2012). Clay causes more clogging than sand for a given pervious concrete (Coughlin et al. 2012). The recent research involves image analysis to understand the pore structure of pervious concrete. The average planar area fractions obtained from image analysis correlate with the volumetric porosities for pervious concrete mixes (Neithalath et al. 2010). 2D image analysis can be performed on cut sections of pervious concrete to calculate the average pore area in the planar images (Liu et al. 2020). Two-dimensional image analysis and finite element modeling are used to study the impact of void distribution on pervious concrete's strength, stiffness, and permeability (Akand et al. 2016). The vertical porosity profile is understood through image analysis of vertically cut pervious concrete specimens (Martin et al. 2013). Clogging analysis

and prediction on pervious concrete can be studied through image analysis. The ratio of the size of the clogging material with respect to the pore size of the pervious concrete is a critical factor in determining the clogging potential of pervious concrete (Zhou et al. 2019). Onsite monitoring of the surface of permeable concrete through cell phones helps identify the clogging pattern and its restoration methods (Valeo 2018). Image analysis is also used to study the pore properties of rocks to understand the hydrological properties of the same. The pore size and shape factor of the pores of the sandstone sample was calculated using image analysis to understand sandstone's hydrological properties (Gong et al. 2020). The geometric properties of the pore system like area, perimeter, aspect ratio, circularity, roundness, and solidity are analysed for dolomite rocks to understand their hydrological properties (Pavičić et al. 2021). The geometric properties of pores in the pervious concrete can be studied for understanding permeability and clogging. Since most of the clogging takes place on the top surface of the pervious concrete, an analysis of the pore parameters across clogging cycles is helpful for understanding the clogging potential of the concrete mix.

In recent years, pervious or porous concrete pavement is acknowledged as a smart solution for flooding in urban infrastructure. A wide variety of binders, aggregates and admixtures are used for enhancing the mechanical properties of pervious concrete mixes. To make it environmentally friendly, waste and recycled materials are used as replacement for conventional materials. Relationship between mechanical and hydraulic properties are investigated for standardizing the pervious concrete mix design. Understanding the clogging mechanism of these mixes based on material type and size is critical for determining the life of the mix. Prior studies have emphasized on the importance of maintenance for increasing the hydraulic performance of pervious concrete pavements. Studies are reported about the use of concrete as a purification material for surface runoff. To quantify the performance of this material, hydrological model incorporating pervious concrete are evaluated in software environment.

1.2 MIX PROPORTION

The pervious concrete has the same proportion as that of normal concrete but the amount of fine aggregates is reduced to create macro pores which allow the passage of air and water. The cementitious material generally used are Portland cement and pozzolonic cement. Flyash, quarry dust, ground granulated blast furnace slag can be used as additional cementitious materials. It is important to evaluate the critical water cement ratio to prevent flow of cement to lower layers (Nguyen et al. 2014). Admixtures are added to increase workability and setting time of the pervious concrete mix. Rounded aggregates are preferred since they yield higher strength to the concrete. Below the pervious concrete layer, there is a layer of stone aggregates as shown in Fig: 1 which are required for temporary storage of rain water. The depth of the layer depends on the amount of rainfall and the infiltration capacity of the soil.

The mix proportion of pervious concrete has the same proportion as that of normal concrete, but the amount of fine aggregates is reduced to create macropores which allow the passage of air and water. The cementitious material generally used is Portland cement and pozzolanic cement. Flyash, quarry dust and ground granulated blast furnace slag can be used as additional cementitious materials (El-Hassan and Kianmehr 2018a). High strength pervious concrete mixes are developed by using silica fume, polymers and superplasticizers (Zhong and Wille 2015). The coarse aggregates are narrowly graded to increase the porosity of the concrete Click or tap here to enter text.(Zhou et al. 2016). Fine aggregates are added in small amounts to increase the strength of concrete (Bonicelli et al. 2015). It is important to evaluate the critical water-cement ratio to prevent the flow of cement to lower layers (Nguyen et al. 2014). Admixtures are added to increase workability and setting time of the pervious concrete mix (Kia et al. 2018). Rounded aggregates are preferred since they yield higher strength to the concrete (Ong et al. 2016). Below the pervious concrete layer, there is a layer of stone aggregates as shown in Figure 1.1 which are required for temporary storage of rainwater. The depth of the layer depends on the amount of rainfall and the infiltration capacity of the soil.

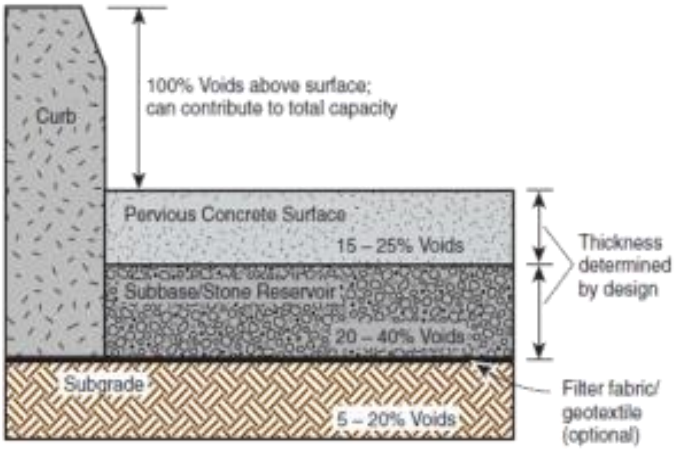

Figure 1.1 Layers of Pervious Concrete Pavement (Chandrappa and Biligiri 2016)

1.3 ENVIRONMENTAL SIGNIFICANCE

Pervious concrete systems provide valuable storm water management tool. (Welker et al. 2013) conducted tests for evaluating the pollutant removal performance of pervious concrete. Groundwater and aquifer recharge are boosted, peak water flow through drainage channels is decreased, and flooding is minimised by collecting rainwater and allowing it to permeate. Heat island effects in metropolitan areas can be reduced thanks to the light colour of concrete pavements. It retains less heat from solar radiation than darker pavements, and the open pore structure of pervious concrete ensures good passage of air (Haselbach et al. 2012).

Yekkalar et al. (2018) evaluated changes in temperature and moisture of clay soils next to an underground aggregate storage bed of a pervious concrete pavement system during the winter using sensors. (Schwartz and Asce 2010) emphasize that by placing pervious concrete far from the main sources of particulate loading, effective site design reduces surface clogging.

During field studies on the turning zone of the pervious concrete pavement, the aggregate layers are under higher stresses and causes more raveling than the other zones of the pavement (Gupta 2014).

1.4 RESEARCH SIGNIFICANCE

The aggregate used in the pervious concrete mix is greater than 6mm size. The large size of aggregates in pervious concrete mixes causes raveling. It is a process of removal of top surface of aggregates due to weak bonding of aggregates. Cement, aggregates with sizes ranging from 2.36 to 4.75 mm, µGGBS as an additive, and superplasticizer are the components of pervious concrete mixes. The aforementioned aggregates were chosen to offer a smoother surface and prevent ravelling of aggregates, a common occurrence in pervious concrete. The smaller aggregates ensure better bonding between the cement paste and the aggregates. The aggregate cement ratio is ranging from 3 to 4 and the water cement ratio is maintained at 0.3. The mixture is compacted but not vibrated. The vibration reduces the permeability of concrete by causing cement near the bottom to settle, resulting in an uneven distribution of cement. It results in uneven distribution of pores and effects its permeability. (Lin et al. 2016a) studied the effect of vehicle vibration on clogging of pervious concrete. The permeability and clogging potential is determined for the mix to study the impact of smaller pore size on the permeability. Though the permeability is reduced, the strength of the concrete increases making it useful for wider applications.

The size of the aggregates is significant for creating the porous nature of pervious concrete (Ćosić et al. 2015). Generally, the aggregate used in the pervious concrete mix is greater than 6mm size. The large size of aggregates in pervious concrete mixes causes raveling (Kevern 2015). It is a process of removal of the top surface of aggregates due to weak bonding of aggregates. (Crouch et al. 2007) stated that smaller aggregates would produce a higher compressive strength than larger aggregates with similar porosities. The smaller aggregates ensure better bonding between the cement paste and the aggregates. (Yang and Jiang 2003) mentioned that the keys to improve the strength of pervious concrete are expanding the cement paste binder area and strengthening the cement binder.

The clogging of pervious concrete is a major disadvantage to this source sustainable urban drainage system. It also reduces the permeability of concrete. The clogging is due to dust particles, soils deposited from wheels of vehicles, sand and clay

suspension in the runoff and polluted runoff (Hasan et al. 2017). (Kia et al. 2018) summarized the result of clogging of pervious concrete due to clay and sand and its mixture. The clogging material used in this study is clay and sand. The permeability and clogging potential **are** determined for the mix comprising the two narrow gradations to study the following phenomena: impact of pore size on the permeability, effect of clogging material gradation on the permeability, the influence of time interval on the permeability of the pervious concrete mix.

1.5 LOW IMPACT DEVELOPMENT(LID)

LID is a sustainable approach for storm water management that seeks to imitate the natural hydrology of a site using decentralized micro to small-scale control measures (Coffman 2002) by achieving pre-development hydrographs. LID adheres to the following principles for sustainable development:

1. Include storm water management techniques in the early planning and design stages of the site.

2. Utilise scattered micro-scale practices to control storm water as near to the source as practicable.

3. Encourage environmentally friendly design.

4. Encourage the development of natural water features and hydrologic processes to develop a hydrologic multifunctional landscape.

5. Place more emphasis on prevention than mitigation and remediation.

6. Lower the expense of building and maintaining drainage infrastructure.

7. Encourage community involvement and education in environmental conservation.

The primary objectives of LID principles and practices are to reduce runoff (peak and volume), boost infiltration, recharge groundwater, protect streams, and improve water quality by removing pollutants through filtration, chemical sorption, and biological processes (Hunt et al. 2010). There are many green technologies which addresses the above problem like detention tanks, rain water harvesting etc,

out of which we have chosen Pervious Concrete as the source control mode of urban flood mitigation.

1.6 PERVIOUS CONCRETE FOR SUSTAINABLE URBAN DEVELOPMENT

Pervious concrete uses identical-sized particles to promote porosity. No-fines concrete is another name for it. It is a mixture of cement, gravel or stone, water and little or no sand which creates an open pore structure that allows water and air to pass through it. It reduces the generation of urban runoff by allowing water to flow through the concrete system. The process also recharges the groundwater reserve. By allowing storm water to permeate through the pavement, it helps to lessen the need for additional control features like retention ponds. In fact, the US Environmental Protection Agency (EPA) recommends it as one of the best management practices(BMPs).

1.7 IMAGE ANALYSIS OF PERVIOUS CONCRETE

Pervious concrete is a green solution for reducing the impact of high urban runoff. It can minimize the rate of runoff in highly impervious areas by allowing the passage of rainfall through the pervious concrete matrix. Though it has a lot of advantages, clogging of pervious concrete is a concern for making it commercial in developing countries. Clogging of pervious concrete takes place on the top surface of the pavement (Kayhanian et al. 2012). Clay causes more clogging than sand for a given pervious concrete (Coughlin et al. 2012). The recent research involves image analysis to understand the pore structure of pervious concrete. The average planar area fractions obtained from image analysis correlate with the volumetric porosities for pervious concrete mixes (Neithalath et al. 2010). 2D image analysis can be performed on cut sections of pervious concrete to calculate the average pore area in the planar images (Liu et al. 2020). 2D image analysis and finite element modeling are used to study the influence of the distribution of voids on the stiffness, strength, and permeability of pervious concrete (Akand et al. 2016). The vertical porosity profile is understood through image analysis of vertically cut pervious concrete specimens (Martin et al. 2013). Clogging analysis and prediction

on pervious concrete can be studied through image analysis. The ratio of the size of the clogging material with respect to the pore size of the pervious concrete is a critical factor in determining the clogging potential of pervious concrete (Zhou et al. 2019). Onsite monitoring of the surface of permeable concrete through cell phones helps identify the clogging pattern and its restoration methods (Valeo 2018). Image analysis is also used to study the pore properties of rocks to understand the hydrological properties of the same. The pore size and shape factor of the pores of the sandstone sample was calculated using image analysis to understand sandstone's hydrological properties (Gong et al. 2020). The geometric properties of the pore system like area, perimeter, aspect ratio, circularity, roundness, and solidity are analysed for dolomite rocks to understand their hydrological properties (Pavičić et al. 2021). The geometric properties of pores in the pervious concrete can be studied for understanding permeability and clogging. Since most of the clogging takes place on the top surface of the pervious concrete, an analysis of the pore parameters across clogging cycles is helpful for understanding the clogging potential of the concrete mix.

CHAPTER 2

LITERATURE SURVEY

2.1 GENERAL

Pervious concrete or permeable concrete is a source sustainable solution to runoff mitigation and ultimately urban flooding. The major disadvantage but its clogging due to dust particles, clay and sand has to be studied to understand the effect of the sediments on the performance of pervious concrete. The literature review presents the various studies taken up for evaluating clogging phenomena and its impact on permeability of pervious concrete.

2.2 SUSTAINABLE URBAN DRAINAGE SYSTEM(SUDS)/ LOW IMPACT DEVELOPMENT (LID)

Chen (2017) proposed an integrated assessment to determine the best drainage system that combines existing conventional grey infrastructure with prospective green infrastructure. According to the integrated evaluation, additional combination of the low impact development practices of rain barrel, pervious concrete and green roof improved the drainage performance at the lowest cost.

Palla and Gnecco (2016) studied the effect of green roofs and permeable pavement in Storm Water Management Model (SWMM). He investigated the various land use change scenarios to assess the effect of low impact development systems at an urban catchment scale.

Liao et al. (2016) studied the cost effectiveness of porous pavement, bio-retention , rain barrels, infiltration trench, grass swale, and its combination on a increasingly urbanized city of Caohejing in Shanghai, China. The life cycle cost method is used to evaluate the cost of these methods. He concluded that rain barrel, infiltration trench and their combination are more suitable for Caohejing area in Shanghai, China.

Page et al. (2015) concluded that retrofitting with innovative stormwater control measures like bio retention cell street retrofit, permeable pavement parking stalls and tree filter installed within the public right-of-way can reduce the hydrologic impacts of existing residential development.

Dierkes et al. (2015) concluded that uncertainty in long-time performance of SUDS and lack of clear guidance make it difficult to implement such systems. Each catchment should therefore be carefully examined to determine whether centralized or decentralized systems would be the most appropriate and feasible option.

Drake et al. (2014) observed that there was no runoff from the permeable pavement during the two year study period in a cold climate over low permeability soil. The pavement was able to attenuate the peak discharge during all seasons and individual precipitation events.

Li et al. (2013) explored the use of permeable/ pervious pavements as a potential practice for heat island mitigation and storm water management. The interlocking concrete pavers have the highest permeability (or infiltration rate, 0.5 cm/s), according to the permeability results. The two permeable asphalt pavements exhibit the lowest permeability, but even so, their infiltration rate of 0.1 cm/s is sufficient to allow rainfall to drain without runoff during the majority of typical rain events in central California.

Chai et al. (2012) conducted hydraulic performance of fully permeable shoulder of highway for understanding storm water runoff management. Simulation investigations conducted on storage reservoir of permeable pavement suggested that for the majority of climate areas and rainfall events in California, full depth permeable pavements can offer enough storm water runoff volume storage.

Burns et al. (2012) proposed a flow regime management approach that aims to maintain the pre-urban frequency of untreated storm flows, reduce the total stormwater runoff volume through evapotranspiration or harvesting, and deliver filtered flow rates to correspond to pre-urban baseflow rates in order to restore and protect the ecological structure and function of urban streams.

(Agudelo-vera et al. 2012) discussed about various options for building linkages between urban infrastructures to create resources for more resilient cities. The urban harvest concept uses resource flow which occurs at spatial and temporal scales.

Ahiablame and Engel (2012) reviewed the existing low impact development practices and suggested that all LID practices could perform proficiently as long as proper design, implementation, and maintenance are followed. SWMM can be used to accurately estimate fundamental processes occurring within the practices. The computational models presented in the review have diverse levels of complexity and use different approaches to represent LID practices.

Fassman and Blackbourn (2010) concluded that permeable pavements can be used to achieve pre-development hydrology. It concluded that porous/ permeable pavements can be used to control small-scale storms (less than 2 cm) and retain first flush runoff during large-scale storm events on clay soils.

Modelling small catchments with SWMM results in an equivalent performance to that for average size and large catchment (Tsihrintzis 1998). He had modelled the catchement areas in the range of 5.95 - 23.59ha. The model works well for frequent and non-frequent events.

2.3 COMPOSITION AND MECHANICAL PROPERTIES OF PERVIOUS CONCRETE

Figure 2.1 shows the various aggregate/ binder ratio and water/ binder ratio available in literature.

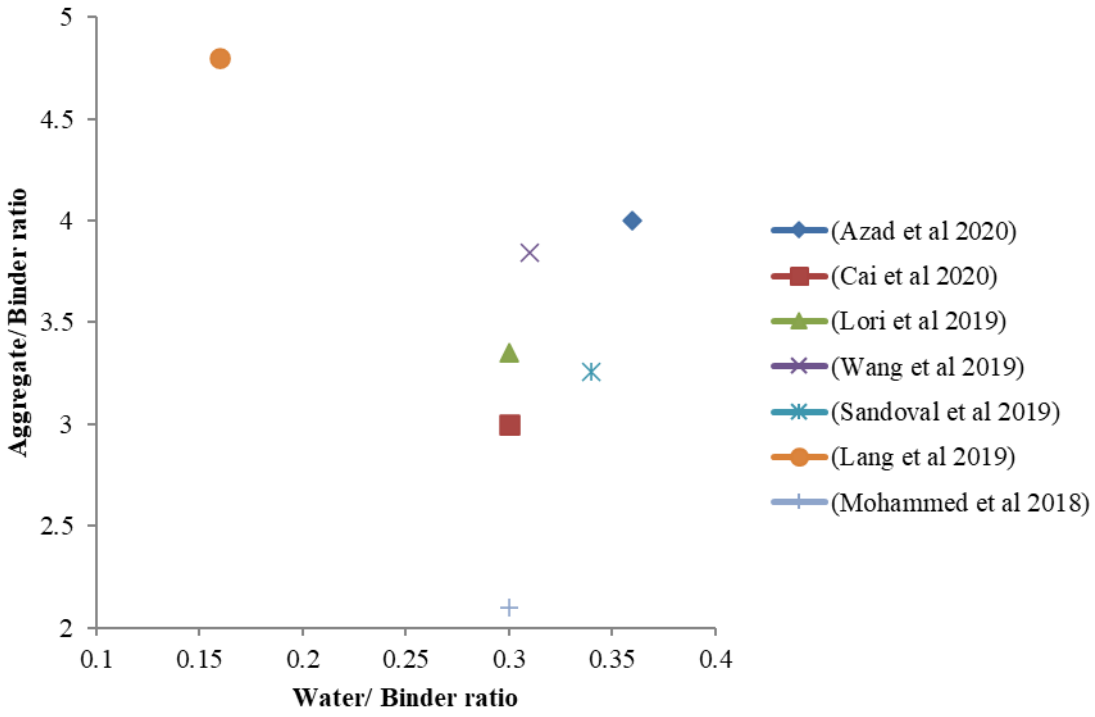

Figure 2.1 Aggregate/ Binder and Water/ Binder ratios as referred from literature

Haselbach et al. (2015) concluded that screening of aggregates appears not to impact the hydraulic functionality of pervious concrete made with the local gravel in the Porto Alegre region.

Table 2.1 tabulates the coarse aggregate, aggregate binder ratio, water binder ratio, compressive strength specimen size, compressive strength, porosity specimen, porosity %, permeability test method, permeability specimen size and permeability. The comparison is done as the values of properties of pervious concrete depends on the specimen size and method of analysis. In some of the mixes, fine aggregate is used to increase the strength of the pervious concrete. The specimen size is also included to understand the variability of the specimen sizes used. Since there is a lack of standardization, there are different sizes used. The specimen's shape is primarily cylindrical, while some are cuboidal or cubical. The method of permeability calculation is either a constant head or falling head.

Table 2.1 Summary of the mix proportion, specimen size and properties of pervious concrete

Reference	CA Size(mm)	A/B by weight	W/B by weight	Compressive strength specimen size(cm)	Compressive Strength (MPa)	Porosity Specimen(cm)	Porosity %/ Voids%	Permeability test method	Permeability specimen size(cm)	Permeability(mm/s)
(Marcaida and Nguyen 2018)	3-5, 5-8 and 8-10	5% binder content	Polyurethane binder	-	-	15 - H, 10 - D	30.7 - 34.3	Constant head	15 - H, 10 - D	5.06 - 7.74
(Huang et al. 2020)	5-10, 10-15	2.41 - 3.65	0.2, 0.25, 0.3	As per CJJ/T135-2009.	7.6 - 56.9	As per CJJ/T135-2009.	12.0 - 21.0	Constant head	As per CJJ/T135-2009.	0.42 - 2.98
(Tan et al. 2020)	4.75 - 9.5	2.107 - 4.988	0.23	10 x 10 x 10	11.0 - 42.0	10 - H, 10 - D	5.2 -27.2	Constant head	10 - H, 10 - D	0.67 - 8.2

(Hatanaka et al. 2019)	5.0-13.0	6.14	0.35	-	-	60x20x20	15 - 35	Constant head, h=5,10,15,20cm	60x20x20	Hydraulic gradient is calculated
(Sandoval et al. 2019)	9.5(max size)	3.26	0.34	20 - H, 10 - D	3.8 - 10.1	20 - H, 10 - D	19.3 - 27.1	Constant head, h=52cm	20 - H, 10 - D	5.0 - 15.1
(Lang et al. 2019)	2.5 - 5, 5 - 10, 10 - 15	4.8	0.16	10x10x10	34.0 - 41.0	10x10x10	24.0 - 27.0	Constant head, head diff - 15cm	20 - H, 10 - D	6.0 - 7.0
(Azad et al. 2020)*	4.75 - 9.5	4 - 4.85	0.36	15x15x15	9.2 - 14.8	10x10x10	30.0 - 36.0	Falling head	10x10x10	6.17 - 5.36
(Lori et al. 2019)*	4.75 and 12.5	3.35	0.3	10x10x10	17.9 - 23.5	10 - H, 10 - D	20.4 - 21.6	Falling head	10 - H, 10 - D	3.05 - 3.33

(Opiso et al. 2019)	10.0 - 14	3.5	0.35	30.48 - H, 15.24 - D	10.1 - 29.1	-	-	Falling head	15.24 - H, 10.16 - D	0.0192 - 0.0264, 5-9 agg size - 0.02450
(Barišić et al. 2020)*	4-8, 8-16		0.33	15 x 15 x 15	8.2 - 21.1	10 - H, 5 - D	18.7 - 32.4	Falling head	10 - H, 5 - D	14.88 - 48.10
(Kia et al. 2019)*	1.24 - 14	Trial and error based on target porosity and	0.35	10 x 10 x 10, 15 - H, 10 - D	6.0 - 59.0	10 x 10 x 10, 10 - D, 15 - H	2.0 - 32.0	Falling head - 100cm - 25cm	15 - H, 9 - D	3.0 - 16.0
(Jagadeesh et al. 2019)	9.5, 12.5(max	4.5	0.29	-	-	25 - H, 15 - D	26	Falling head	25 - H, 15 - D	intrisinic permeabili

	size) and combination							from 22.5cm to 2.5cm		ty was calculated
(Wang et al. 2019)	2.36 - 4.75, 4.75 - 9.5, 9.5 - 13.2	3.84 - 5.55	0.31	15x15x15	12.7 - 34.5	5 - H, 10 - D	18.7 - 25.7	Falling head, not Darcy	5 - H, 10 - D	6.1 - 7.1

CA - Coarse Aggregate
A/B - Aggregate/ Binder ratio
W/B - Water/ Binder ratio
*Fine aggregate used

(Sandoval et al. 2019) used different aggregates namely electric furnace slag, basalt, recycled concrete aggregates and ceramic waste for preparation of pervious concrete specimens. The compressive strength and flexural strength were tested. The compressive strength specimens were 100mm diameter and 200mm height and the flexural specimens were cuboid of size 750mm x 250mm x 50mm. The compressive strength varied from 3.3 to 11 MPa. The flexural strength was around 40% of compressive strength for most of the aggregate cases.

(Ćosić et al. 2015) used the size of the aggregate between 1.24 to 16mm. The size of the aggregates is significant for creating the porous nature of pervious concrete. The large size of aggregates in pervious concrete mixes causes raveling(Kevern 2015). It is a process of removing the top surface of aggregates due to the weak bonding.(Crouch et al. 2007) stated that smaller aggregates produce a higher compressive strength than larger aggregates with similar porosities. A balance must be maintained between paste content, voids, strength, and workability(Kia et al. 2017). (Yang and Jiang 2003) stated that the binder area and quality have to be enhanced to improve the compressive strength. The essential requirement is to provide optimal cement paste to bind aggregates without causing paste drain at the bottom(Xie et al. 2018). Most of the mixes are continuously graded with a wide range of aggregate sizes. The wide range increases the compressive strength but reduces the permeability. The tortuosity of the flow path increases due to the broad gradation of aggregates(Chandrappa and Biligiri 2017). Fine aggregates are added in small amounts to increase the strength of the concrete(Bonicelli et al. 2015). The aggregate binder ratio varies between 2.1 to 6.14. The water binder ratio varies from 0.16 to 0.36. Most of the water binder ratios are around 0.3. The binder material generally used is Portland cement and pozzolanic cement. Flyash, quarry dust, and GGBS can be used as additional binder materials(El-Hassan and Kianmehr 2018a).

The associated compressive strength, porosity, and permeability capture the variability of the strength and hydrological parameters based on the size and mix design of the pervious concrete mixes.(Chai et al. 2012) compared the saturated and unsaturated hydraulic conductivity for its analysis. (Qin et al. 2015) compared

the permeability measured using falling head and constant head permeameter and concluded that permeability estimated using the falling head method is lower than the constant head method.

2.4 HYDRAULIC PROPERTIES OF PERVIOUS CONCRETE

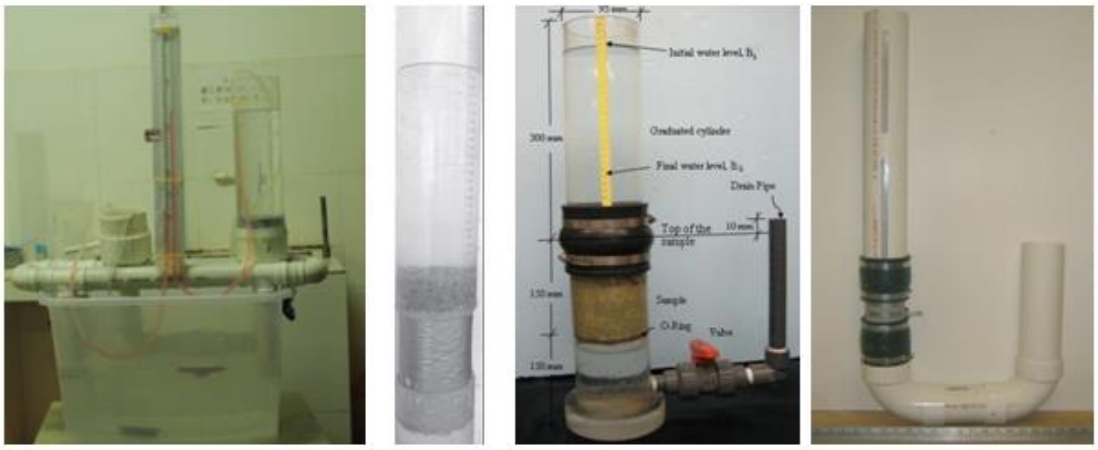

(Qin et al. 2015) (Chandrappa and Biligiri 2016) (Deo et al. 2010) (McCain et al 2010)

Figure 2.2 The experimental set up used in literature

Figure 2.2 shows the experimental set up found in literature from (Deo et al. 2010), (McCain et al. 2010), (Qin et al. 2015) and (Chandrappa and Biligiri 2016)

Hatanaka et al. (2019) concluded that the average flow velocity and hydraulic gradient followed nonlinear relation in pervious concrete. Exponential equation were developed with exponential index set to 0.5 and the permeability coefficient k depended on aggregate size and void ratio. The equations were valid for both vertical and horizontal flow cases. The pervious concrete pavement was effective in delaying peak runoff of rain water when the area of 100m x 100m is paved with pervious concrete.

Sandoval et al. (2019) created a correlation of hydraulic properties that allows to identify the effectiveness of permeability based equation namely Bernoulli's and Darcy's equation on the pervious concrete specimens. A non-linear regression was performed with SPSS software using the experimental results. Through the experiments and calculation, a correlation between porosity and permeability based on Darcy's and Bernoulli's law was performed. The experimental data from the lab

and data from other authors were used to evaluate the suggested equation, which showed high correlation in every case, proving the proposed model's predictability. The correlation was modified considering the theoretical boundary conditions, wherein both permeability and porosity are both variables.

Jagadeesh et al. (2019) analysed the hydraulic, acoustic, and frictional performances of pervious concrete pavement surfaces using X ray computed tomography and digital image processing. The parameters considered were intrinsic permeability, effective porosity, tortuosity, and pore size distribution. The specific discharge at different hydraulic gradients was determined using X-ray CT image-based finite-volume permeability simulations, which led to the development of a new discharge-based segmentation technique capable of predicting non-Darcy permeability of pervious concrete mixtures. The falling head method was used for calibration and validation. The simulation results for permeability from ten alternative global thresholding methods were contrasted with those from the thresholding algorithm that was created. The analyses revealed that the developed discharge-based thresholding method outperforms conventional global thresholding algorithms at predicting non-Darcy permeability features and the effective porosity of pervious concrete mixtures.

Based on the rheological characteristics of cement paste, (Xie et al. 2018) generated empirical functions for permeability. By maximising water cement ratio, superplasticizer dose, and mixture proportion of cementitious materials under the same rheological properties, the empirical functions for the mechanical properties of pervious concretes can be maximised. He also assessed the thickest paste coating that could be applied on aggregates without causing the binder to clog the pores.

After service of three years, the surface infiltration capacity of pervious concrete was very high with a mean and median of 1280 and 1490 cm/h(Crookes et al. 2017). An overall runoff volume reduction of 46% was estimated for four months period. The estimated volume reduction ranged from 21 to 100% on a single event basis.

According to the study by (Shen et al. 2016) , pervious pavement systems have the capacity to recycle stormwater to a quality that satisfies the requirements for use in agricultural irrigation.

Winston et al. (2016) studied the effects of vacuum cleaning, street sweeping, high pressure washing and milling as maintenance measures for permeable pavement surface. He concluded that debris flow in runoff requires more maintenance. Pressure washing was best for porous asphalt. Number of maintenance increases every year to maintain desired threshold surface infiltration rate.

Haselbach et al. (2015) concluded that the pervious concrete made with the local gravel in Porto Alegre region of Brazil will have similar hydraulic functionality regardless of whether or not there is additional screening of the gravel. The most important parameter is the porosity, which if too low (<20%) might have a negative impact. Since strength and durability are also important variables for pervious concrete and typically decrease with porosity, they might be the limiting considerations for the porosity of the mix designs in the higher ranges and the effect of screening on them might be considered for further study. This study indicated that screening appears to not impact the hydraulic functionality of pervious concrete made with the local gravel in the Porto Alegre region.

2.5 CLOGGING OF PERVIOUS CONCRETE

The clogging of pervious concrete is a significant disadvantage to this source sustainable urban drainage system. It reduces the permeability of concrete. (El-Hassan and Kianmehr 2018b) investigated the clogging potential due to dust. (Fwa et al. 2015) used an aqueous solution of fine-grained soil as a clogging material. (Kia et al. 2018) summarized the effect of clogging of pervious concrete due to clay and sand and its mixture. (Marcaida and Nguyen 2018) concluded that graded sand particles cause more clogging than single graded sand particles. (Walsh et al. 2014) developed a laboratory set up to record how sediment accumulation affects the pervious concrete's hydraulic conductivity. (Lin et al. 2016a) studied the effect of vehicle vibration on clogging of pervious concrete. (Cui et al. 2016) measured the electrical conductivity as an indicator of pervious concrete clogging. (Ketcheson and Price 2014) conducted laboratory experiments to study the effect of sand application and temperature on concrete. (Barišić et al. 2020) concluded that pervious concrete made with smaller aggregate fractions is more prone to clogging.

Cui et al. (2016) studied the role of electrical conductivity as an indicator of pervious concrete clogging. Quick clogging, temporary clogging mitigation, and progressive clogging are the three phases that often make up the continuous pore clogging process. While the uniformity of sediment and the porosity of pervious concrete have roughly equal positive influences on the coefficient, the Reynolds number of horizontal runoff has a much smaller negative impact on the coefficient of stable stage, though a higher Reynolds number can delay clogging. The aggregate-sediment size ratio affects coefficient favourably in the study area.

The ability to recycle stormwater into a form that satisfies the requirements for use in agricultural irrigation exists in permeable pavement systems. The study by (Nnadi et al. 2015) goes on to show that the pervious pavement system is highly effective in removing hydrocarbons, metals, and other pollutants, even under the worst-case scenario for pollutant loading.

Lee et al. (2015) analysed clogging process as a function of deposited sediments. Clogging at the bottom of the surface is caused by sediments associated with runoff and also by fine sediments contributed from the applied gravel aggregate.

On several cores for each of the clay kinds and the suspension volumes and concentrations, (Haselbach et al 2012.) conducted clogging cycle tests. The amount of time it took for the suspension water to enter the core was used to calculate the infiltration rate. The suspensions were poured into the core while leaving about 10 mm at the top to reduce head impacts. The sample spent at least 24 hours in a 50°C oven after each "clogging" cycle. The idea was to simulate the aftermath of a major disaster, when the pavement would be exposed to hot, sunny weather. Four to ten clogging cycles were required before the sample ceased to function. Each sample was "maintained" by cleaning the extra clay off the top with a brush once the clogging cycles were finished. The testing for the rinse cycle were made to resemble consecutive downpours. With a 200ml exfiltrate, these experiments were conducted in the same manner as the initial infiltration rate testing. There wasn't much clay in the exfiltrate. Each core was kept in an oven at 50°C for at least 24 hours in between cycles.

As more and more clogging materials were added throughout the clogging test, the coefficient of permeability for both the pervious concrete and the porous asphalt mixtures was repeatedly determined. For this investigation, (Fwa et al. 2015) created a constant-head test apparatus. A test specimen with a 150 mm diameter and a thickness range of 40 to 200 mm can be tested with this arrangement. The increase in permeability coefficient, k with porosity for both pervious concrete and porous asphalt mixtures was explained by an exponential relationship of the form $k = a\ eb^{P}$, where a and b are positive regression coefficients. When combination porosity was raised above 20%, their permeability and clogging resistance both significantly increased. In comparison to the porous asphalt specimens, the pervious concrete specimens contributed higher initial permeability. An exponential relationship of the type $k = a\ e^{bN}$, where a and b are positive regression coefficients, can be used to illustrate the trends in the decline of permeability coefficient k as a function of clogging cycles N.

Walsh et al. (2014) developed a laboratory set-up to study how sediment accumulation affects the hydraulic conductivity of pervious concrete. The aim of the study was to develop a model to forecast the hydraulic conductivity of pervious concrete based on the type of sediment and the amount accumulated in the pervious concrete void matrix. This model was used to determine maintenance schedules for pervious concrete. D_{50} of the sediments were found out to identify the mean size of the particle. Sediment accumulation or loading rate of 0.95 mg(cm^2/day) was used. The study assumed that rainfall occurred every 4 days on average. Sediment load testing - effluent from the hydraulic conductivity test was tested for total suspended solids to quantify the amount of sediment removed. Graph was drawn between hydraulic conductivity and total accumulated sediment using exponential decay equation.

The impact of sand application and temperature (frozen and thawed conditions) on flow dynamics and salt retention/transport was studied by (Ketcheson and Price 2014) in laboratory tests on pervious concrete slabs. In every trial, salt was promptly carried through the permeable concrete. Although there was only a slight amount of salt dispersion in the electric conductivity breakthrough curves, there is

a significant chance that salt will quickly flush through the extremely permeable matrix of pervious concrete structures. Due to the significantly longer flow channels caused by the freezing temperatures and greater sand application, dispersion increased slightly. Sand was sprinkled on the pervious concrete's surface to slow the flow of water through the pores. Peak flow as measured at the base of the slab was delayed as a result of application of sand. These effects are restricted to the concrete's near surface because it is improbable that the sand will enter the pore space further within the structure. The investigation showed that neither sanding nor chilling significantly reduced the slabs' capacity to convey flow. The ability of concrete to drain only marginally diminishes by excessive sand applications and low temperatures.

Welker et al. (2013) conducted tests to assess the efficacy of pervious concrete in removing pollutants. Through both volume control and a reduction in the concentration of metals in the storm water, the use of permeable pavements in parking lots can reduce the metals burden reaching a surface water body. When used in conjunction with an infiltration bed, permeable pavements effectively manage storm water through a variety of means, including volume control through infiltration, pollutant removal through the capture of sediments in the void space of pavements with pollutants sorbing onto these sediments, and adsorption of pollutants onto the rocks in the infiltration bed and the natural soils beneath the infiltration bed.

Deo et al. (2010) used fine (0.1–0.84 mm) and coarse (0.84–1.8 mm) grained river sand as clogging material. 25 g of the sand was spread evenly on the specimen surface for each clogging cycle and permeability of water flow through the specimen was measured. The process was repeated till the flow rate was very slow or further sand additions did not result in visible changes in permeability. Due to pore channel blockage, porosity reduction, and tortuosity rise, permeability dropped as the amount of sand added increased. Because of their bigger pore diameters and greater pore connectivity, samples with higher porosity had higher residual permeability at the end of testing. Large particles are prevented from

entering the sample by coarse sand, hence there were no substantial permeability changes compared to fine sand.

2.6 IMAGE ANALYSIS OF PERVIOUS CONCRETE

Pavičić et al. (2021) used ImageJ for geometric characterization of pores and distribution of pore characteristics in Upper Triassic Dolomites in north west Croatia. The rock strata are important geothermal and groundwater aquifers of that region. The parameters measured were pore area, perimeter, circularity, aspect ratio, roundness, solidity, feret aspect ratio, compactness and fractal dimension. The parameters were represented as frequency diagrams for assessing the distribution of the geometric parameters.

Sai and Kothala (2018) used MATLAB for image processing of various construction materials. The internal structure was evaluated through scanning electron microscope(SEM) and X-ray whereas the infiltration in porous friction course mixtures were evaluated through image analysis.

Buckman et al. (2017) quantified porosity through automated image collection and batch image processing for the carbonates and aragonite cemented sandstone. Backscattered electron images collected from polished sections of the sample were analyzed in ImageJ and MATLAB software. The parameters measured were pore size, shape, grain size/ shape, orientation and mineral distribution.

The mechanical strength properties of pervious concrete depends on the distribution of voids. (Akand et al. 2016) analyzed the influence of pores on the strength, stiffness and permeability of pervious concrete microstructure. ImageJ was used for 2D image analysis and Analysis System, ANSYS was used for finite element modeling. Representative volume element is evaluated for analysis of the above parameters. The results are compared with experiments conducted following American Society for Testing and Materials, ASTM standards. A 99% accuracy was seen between the model and physical experiments.

Martin et al. (2013) used an open source photo editing software called GNU Image Manipulation Program (GIMP) to understand the vertical distribution of porosity through image analysis. The specimen was cut in half through the middle vertically

down and a rectangular area of length of 15.2cm was scanned at high resolution of 600dpi. The ratio of the pore area to the total area for each row of pixels was calculated using MATLAB. The representative elemental area concept was used to understand the porosity distribution. It was compared with two volumetric method and a vacuum sealing device to check the accuracy of the image analysis. The image analysis method yielded a higher porosity values but the average porosity was comparable with other standard methods.

Kytyr and Valach (2010) assessed the pore size distribution of porous material using image analysis. The scanning electron microscopy (SEM) and a high resolution flatbed scanner was used for obtaining 2D and 3D images. The evaluation of pore size was done through association method. It was compared and verified with mercury intrusion porosimetry.

Pervious Concrete is a sustainable solution to urban flooding but its clogging due to dust particles, clay and sand has to be studied to understand the effect of the sediments on the performance of pervious concrete. The literature review presents the various studies taken up for evaluating clogging phenomena and its impact on permeability of pervious concrete.

2.7 LITERATURE SUMMARY

The literature discusses various sustainable urban drainage methods and its impact. It identifies the different mix design and composition of pervious concrete mixes. It discusses the various admixture, aggregate gradation used for improving the strength and performance of pervious concrete. The measurement of compressive strength, porosity and permeability are tabulated for comparison between the different methods. The most common methods for measuring permeability are constant head and falling head method based on Darcy's equation. The literature emphasis on the effect of clogging on the hydraulic performance of pervious concrete. The use of image analysis for understanding the pore structure is also included in the literature survey.

2.8 LITERATURE GAPS

1. Lack of standard method to evaluate permeability of pervious concrete.
2. The use of narrow aggregate size gradation for pervious concrete for improving mechanical properties.
3. The effect of clogging on the hydraulic performance of pervious concrete.
4. Use of 2D images for understanding surface properties of pervious concrete.

2.9 RESEARCH OBJECTIVES

The specific objectives of the research work are:

1. To examine the permeability of pervious concrete based on the narrow size gradation of small aggregates.
2. To construct a mathematical model between permeability and porosity of pervious concrete for small aggregates.
3. To investigate the clogging potential of pervious concrete mixes.
4. To distinguish the clogging pattern on the top surface of pervious concrete based on the particle size of sediment.
5. To analyze the pore properties of pervious concrete subjected to clogging.

CHAPTER 3
METHODOLOGY

3.1 GENERAL

Pervious concrete is a source sustainable concrete which can reduce the impact of urban runoff creation to a large extent. The studies related to pervious concrete comes under structural engineering, geotechnical engineering, transportation engineering and hydraulic engineering. The structural engineering stream deals with the material characterization, use of new materials, reuse of waste materials, use of steel, void ratio, mix design, casting and curing of pervious concrete. The properties of concrete like compressive strength, split tensile strength, flexural strength, fatigue test etc are also experimented in this stream. The geotechnical engineering deals with permeability equations for porous material. The transportation engineering deals with the suitability of pervious concrete as a pavement material and various test conditions to satisfy as a pavement. The hydraulic engineering deals with the calculation of infiltration, use of the concrete as a medium for reducing runoff and case scenarios of retrofitting such concrete in existing pavements. Through the above studies, one major problem of concern was the clogging of the pores due to the sediments present in the runoff. Though the concrete has lot of advantages in terms of sustainable urban drainage management system, the clogging of its pores due to sediment quantity in runoff reduces the life of the concrete. There are few research works related to clogging by different materials in laboratory and in-field, testing of concrete for water purification. The research focuses on studying the clogging potential of pervious concrete and also understand the pore profile of the top surface of pervious concrete due to clogging. The chapter discusses the mix design and composition of pervious concrete, the fabrication of permeability set up, use of ImageJ and R open-source software, clogging of concrete, compressive strength and permeability of pervious concrete, image analysis of pervious concrete, and statistical analysis of pore properties of pervious concrete. The research explores the use of image interpretation to

understand the settlement of particles of the top surface and its impact on the permeability of pervious concrete.

3.2 MIX DESIGN AND COMPOSITION

3.2.1 Binding material

Cement is the main binding substance used. Mineral admixtures are added in addition to the cement. Micro Ground Granulated Blast furnace Slag(µGGBS) is the mineral admixture that are employed.

i Cement

The cement used is Ordinary Portland Cement (OPC) of Grade 53. It has a mixture of chemicals like calcium, silicon, aluminium and other ingredients. The basic properties of cement such as normal consistency, setting time, specific gravity and compressive strength test are conducted to assess the quality of cement procured.

ii Micro Ground Granulated Blast furnace Slag (µGGBS)

There are many admixtures added to the pervious concrete mix to improve its mechanical properties. GGBS is a cementitious material which is manufactured as a by-product of iron industry. It is used widely in conventional concrete. It is obtained by the heating of limestone, iron ore and coke at a temperature about 1500^{0}C in the blast furnace. The process involves quenching of molten iron slag from a blast furnace in water or steam, then drying and grounding into a fine powder. It can be used a partial replacement or as a mineral admixture. Figure 3.1 shows the sample of µGGBS. The GGBS is further powdered to obtain µGGBS. It is ultrafine GGBS where the particle size is in nanometers. It has more surface area to bind with other material in concrete. The chemical composition depends on the composition of the raw materials in the iron production process. It is greyish-white in colour and has a composition of 40% calcium oxide, 35% silica, 13% alumina and 8% magnesia. In combination with cement or other binding materials it can improve the mechanical properties of concrete.

Figure 3.1 µGGBS

3.2.2 Aggregates

The conventional concrete uses well graded fine and coarse aggregate for optimum mechanical properties of the concrete. In contrast, pervious concrete uses narrow graded aggregates to ensure permeability in the concrete matrix. In this research, the aggregates used in the mix have a narrow gradation of 2.36mm to 4.75mm and 4.75mm to 6.30mm. The Indian Standard (IS) sieve size of 4.75mm categorizes the aggregate into fine and coarse aggregates. As per Indian Standards, IS 383 - 1970, the aggregate size range of 2.36mm to 4.75mm is classified as a last fine aggregate range, and the aggregate size range of 4.75mm to 6.30mm is classified as the first coarse aggregate range. Figure 3.2 shows the sample of the narrow gradation of 2.36 - 4.75mm. The narrow gradation is used to increase the number of pores in the concrete and improve permeability. It is also chosen to reduce the effect of raveling and increase the compressive strength of concrete. Raveling is a process of chipping off of aggregates on the top surface due to weak bonding. When large aggregates are used in pervious concrete, the aggregate on the top surface gets chipped off. It happens due to no or little use of fine aggregates like sand in the concrete mixes. Though the smaller size aggregates reduce the average pore size of the concrete, it tends to increase the strength of concrete. The aggregates are mixed in their natural moisture content to avoid the absorption of excess water during mixing. Rounded aggregates are used to increase the compressive strength.

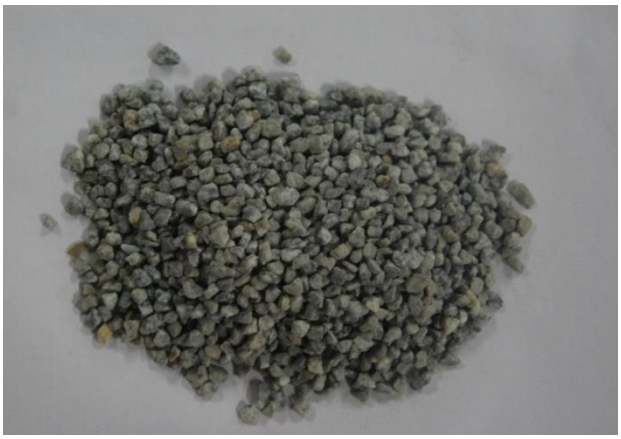

Figure 3.2 Aggregate size range of 2.36 - 4.75mm

3.2.3 Mix design

The mix design for pervious concrete is done based on weigh batching. A number of trial proportions are prepared before the final mix proportions are finalized. The trial batching was done to ensure that the phenomena of cement paste drain at the bottom is not prevalent. Paste drain happens due to the mix proportion itself or due to vibration. Table 3.1 shows the various mix proportion before deciding the final mix proportion for the study.

Table 3.1 Cement paste drain studies of different mix proportions

Aggregate/ cement ratio	Water /cement ratio	Amount of µGGBS	Superplasticizer	Status
3	0.3	$1/5^{th}$ of cement weight	5% of water weight	There was max settlement at the bottom. Permeability was almost zero.
3.5	0.3	$1/5^{th}$ of cement weight	5% of water weight	Less settlement. Permeability can be calculated.
3.7	0.3	$1/5^{th}$ of cement weight	5% of water weight	There was max settlement at the bottom. Permeability was almost zero.
3.7	0.3	No GGBS	5% of water weight	Less settlement. Permeability can be calculated.
4.0	0.3	$1/5^{th}$ of cement weight	5% of water weight	No settlement

Figure 3.3 Cement paste drain at the bottom of concrete specimen

In some of the specimens as shown in Figure 3.3, there was paste drain at the bottom due to fluidity of cement paste. The pervious concrete mix cannot be vibrated since paste drain occurs resulting in non-uniform spread of porosity and decrease the

permeability drastically. The vibration causes the settlement of cement at the bottom creating uneven distribution of cement. The cement settles at the bottom of the concrete making it impermeable.

The aggregate-cement ratio is kept constant at 5.2, and the water-cement ratio is maintained at 0.3. Keeping the water-cement ratio and aggregate-cement ratio as constant, the mix consisted of using two different narrow gradations of aggregates ie as mentioned in 2.36mm to 4.75mm and 4.75mm to 6.3mm. The amount of μGGBS taken is 20% of the weight of cement. Therefore, the aggregate/ binder ratio becomes 3.33, and the water/ binder ratio becomes 0.25. The amount of superplasticizer is taken as 5% by weight of water. The mix is compacted in three layers. Since μGGBS increases the strength of conventional concrete, it is desirable to know the performance of the admixture in pervious concrete specimens. The pervious concrete should be cast in controlled compaction environment to attain near uniform permeability across the vertical profile.

The mix for pervious concrete is made with a composition that has an open pore structure. The fine aggregate is typically lowered in this mixture to produce interconnected voids in the concrete. The main requirement is to supply optimal cement paste to bond the aggregates without allowing any paste to drain at the bottom. The materials used in the pervious concrete mix are cement, aggregates, μGGBS, and superplasticizer. The aggregate-cement ratio is kept constant at 5.2, and the water-cement ratio is maintained at 0.3. The μGGBS is taken as 20% of cement. Therefore, the aggregate/ binder ratio becomes 3.33, and the water/ binder ratio becomes 0.25. The narrow aggregate size gradation used ranges between 2.36mm - 4.75mm and 4.75mm - 6.3 mm in size. Table 3.2 tabulates the mix design used for the study. For each mix, six cubes for compressive strength and six cylinders for permeability was casted. The above aggregates are chosen to provide a smoother surface and avoid raveling aggregates, which is a common phenomenon in pervious concrete. The smaller aggregates ensure better bonding between the cement paste and the aggregates. The mix is compacted, not vibrated. Vibration causes the settlement of cement paste at the bottom.

Table 3.2 Mix Proportions for pervious concrete

Mix proportions	Binder - Cement(%)	Binder - µGGBS%	Aggregate Size	Aggregate / Binder ratio	Water/ Binder ratio	Superplastizier
M1	80	20	2.36 - 4.75mm	3.33	0.25	5% of water
M2	80	20	4.75 - 6.30mm	3.33	0.25	5% of water

3.2.4 Sample Preparation

The concrete was prepared using concrete pan mixer. The cement and µGGBS are mixed well. The aggregates are added to the binder. The naphthalene based superplasticizer was added to the water, and the water was poured slowly to the mix in the concrete pan mixer. The mixing was continued until a uniform mix was achieved. It was cast in cube moulds of 15cm side for compressive strength and cylinder of diameter 15cm and length 15cm for permeability and clogging test. For both, it was compacted in three layers with 25 blows for each layer. Vibration caused the cement paste to settle down. Figure 3.4 shows the concrete specimens in their moulds. It was kept for 48 hours in the cast and then demoulded and cured in a water tank. For each mix, six cubes for compressive strength and six cylinders for permeability were cast. The cylinders used for testing permeability was used for clogging test also. The uniformity of pore structure in a pervious concrete core can be ensured by the uniformity in compaction energy across the vertical layers of the concrete.

Figure 3.4 Concrete specimens for compressive strength

3.3 LABORATORY SET UP FOR PERMEABILITY

The set up for measuring permeability in the study uses the concept of falling head permeability. It allows the free fall of water from the top and the time taken of the falling of water is measured to calculate the permeability. Since there is no standard instrument for measuring permeability, in most of the research an apparatus is fabricated considering either saturated or unsaturated condition. A transparent acrylic pipe of diameter 15 cm as shown in figure 3.5 was fabricated for evaluating the permeability of concrete. It consists of three cylinders from top to bottom for maintaining head, for holding the specimen and for collecting exfiltrate respectively. The length of each is 15cm, 15cm and 10cm respectively. The lower portion of the bottom cylinder is closed on the bottom side. The middle portion and upper portion cylinder are open at both ends. The cylinders are grooved to fit one cylinder over the other. Taps are provided on the top and bottom cylinder. The tap provided on the top cylinder is to maintain the head of water, and the tap provided on the bottom cylinder is to expel out the exfiltrate after the test. The tap can also be used to create a pressured atmosphere beneath the pervious concrete layer which affects the permeability of pervious concrete. Before placing in the setup, the pervious concrete specimen is wrapped with transparent plastic to avoid the leakage of water through the sides of the concrete. During the test, the three cylinders are assembled with clay or any other sealant. Graduated scales are attached on the top

and bottom end of the fabrication. The fabrication can be used for both constant as well as falling head principle. During the test, one liter of water is poured from the top and the time taken for fall of head from 3cm to 1.5cm is noted. For better accuracy, video is taken for accurate measurement of time. The specimen has to be checked for leakage along the circumference of the pervious concrete specimen.

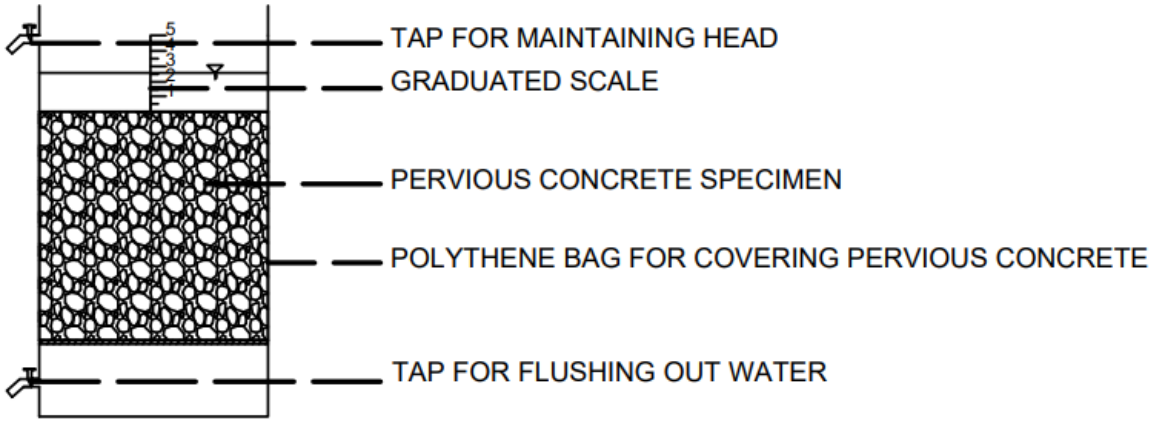

Figure 3.5 Permeability fabrication for pervious concrete

3.4 SOFTWARE USED

3.4.1 ImageJ

ImageJ is an open source image processing program in Java programming language. It is designed with open architecture via Java plugins and recordable macros. It is developed by National Institute of Health and the Laboratory for Optical and Computational Instrumentation, University of Wisconsin. It was basically developed for medical purposes but due to its popularity it has been used in other domains too. Its processing and analysis plugins can be developed using its built in editor and Java compiler. Many image processing and analysing problems can be solved by its user written plugins. It can display, edit, analyze, process, save and print images. Image formats like tiff, gif, jpeg, bmp, dicom and fits can be imported in this software. It supports standard image processing functions such as logical and arithmetical operations between images, contrast

manipulation, convolution, Fourier analysis, sharpening, smoothing, edge detection and median filtering. It does geometric transformation such as scaling, rotation and flips. It also supports image stacking and it can perform parallel functions in multi-CPU hardware. The software can calculate areas and pixel value statistics of user defined selections and intensity-thresholded objects. The statistics data related to areal and perimeter properties can be downloaded as csv files for further analysis. In this study, the ImageJ software is used to analyze the pore structure of the top surface of the pervious concrete specimen. The software is used for image cropping, enhancement, conversion to binary data and extraction of binary data for understanding the areal properties of pore structure.

3.4.2 R

R is a free programming language and software environment used for reporting, graphic representation, and statistical processing and analysis. R was developed by the R Development Core Team at the University of Auckland in New Zealand after it was founded by Ross Ihaka and Robert Gentleman. R is publicly accessible and binary versions that have already been pre-compiled for other operating systems like Linux, Windows, and Mac are also available.

Data analysts, bioinformaticians, and statisticians utilise it to analyse data and create statistical software. In order to extend the capabilities of the R language, users have created packages. It is mostly written in R itself (partially self-hosting), Fortran, and C. There are precompiled executables available for several operating systems. There is a command-line interface for R. There are also numerous third-party graphical user interfaces available, like the integrated development environment RStudio and the notebook interface Jupyter. In this study, R is used to create split violin plots for understanding the distribution of the areal properties of pore structure. The paremeters which are analysed are area, perimeter, aspect ratio, circularity, roundness and solidity.

3.5 CLOGGING OF CONCRETE

In this study, the specimen is exposed to an aqueous solution of clay and sand. A concentration of 5g/l is prepared by mixing 5g of clay or sand with 1 liter of water.

It is mixed at 40 rpm for 1 minute in a motorized mixer. The gradation of the clogging material - clay and sand are tabulated in Figure 3.6. For sand, dry sieve analysis is performed using the sieves 4.75mm, 2.36mm, 1.18mm, 600µm, 300µm, and 150µm. For clay, hydrometric analysis is performed to plot the grain size distribution. This solution is passed through the matrix, and the same principle of calculating permeability is used. This was applicable for both gradations. The experiment is conducted for six cycles. Since the trials cannot be repeated, a video was beneficial for accurately calculating time.

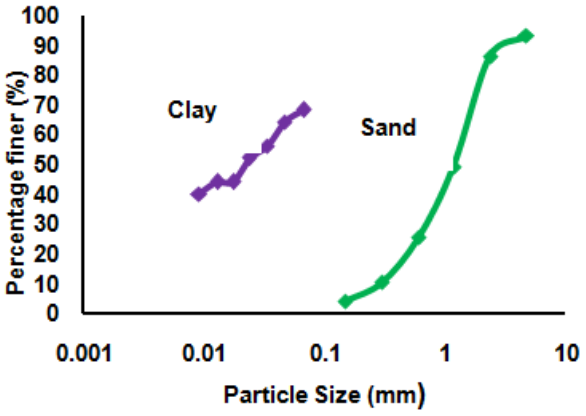

Figure 3.6 Sieve Analysis of Clay and Sand particles

For sand, dry sieve analysis is performed using the sieves 4.75mm, 2.36mm, 1.18mm, 600 µm, 300 µm and 150µm. For clay, hydrometric analysis is performed to plot the grain size distribution.

Figure 3.7 shows the top surface of the pervious concrete containing the narrow gradation of 2.36 - 4.75mm before and after exposure to six clay and sand clogging cycles. Figure 3.8 shows the top surface of the pervious concrete containing the narrow gradation of 4.75 - 6.30mm before and after exposure to six clay and sand clogging cycles. During the experiment's conduction, clay clogging's exfiltrate had clay particles, whereas it was a clear solution for sand clogging. It was also observed that the top surface of the 2.36 - 4.75mm gradation concrete retained a good amount of sand particles during the clogging cycles.

The concentration of the aqueous solution of sand and clay is taken as 5g/l. The concentration of exfiltrate is measured after each cycle.

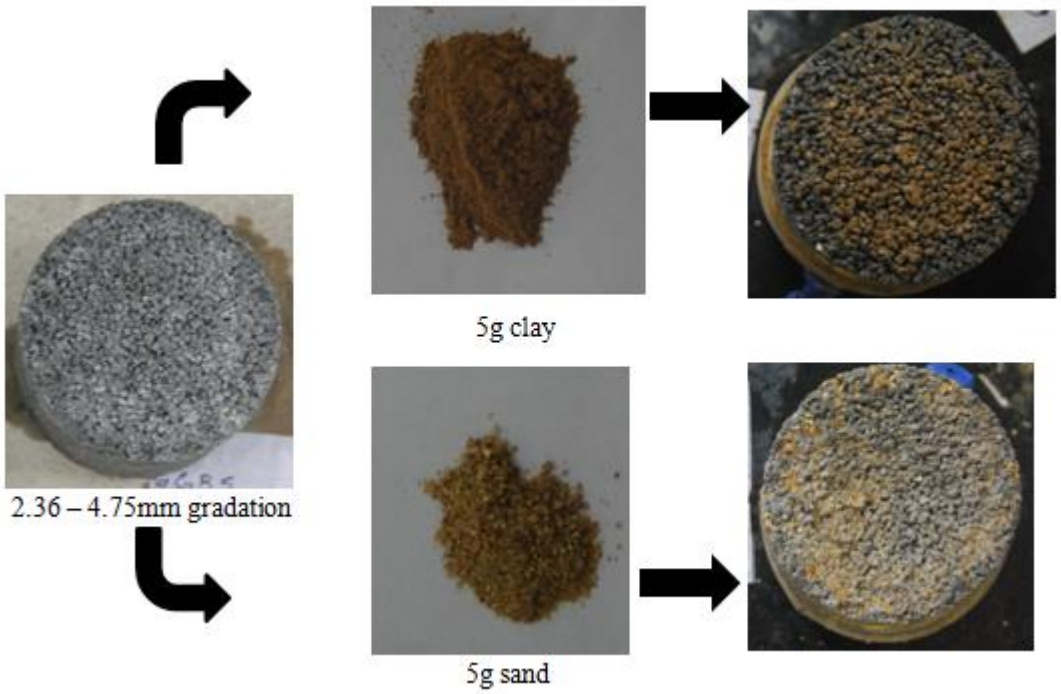

Figure 3.7 Clogging of clay and sand on the pervious concrete mix - 2.36 - 4.75mm narrow gradation

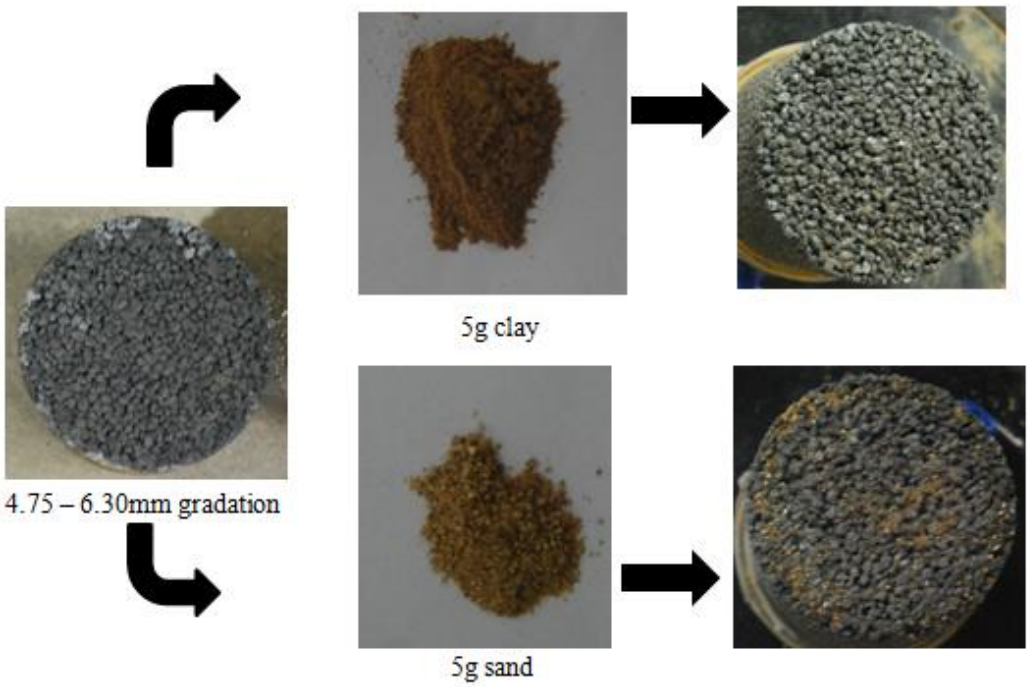

Figure 3.8 Clogging of clay and sand on the pervious concrete mix - 4.75 - 6.30mm narrow gradation

3.6 IMAGE ANALYSIS OF PERVIOUS CONCRETE

3.6.1 Use of ImageJ for Pore Analysis of Pervious Concrete

The images of the top surface of the pervious concrete were taken after every clogging cycle. The photos were taken at a distance of 90cm from the top surface of the concrete. The photos were taken in NIKON D40X. The resolution of photos is 300dpi. The pixels in each photo are 3872(width) x 2592(height). The images captured by the camera are imported in ImageJ to analyze the pore structure of the top surface of the pervious concrete. ImageJ is an open-source image processing software. The JAVA program was developed by the National Institute of Health, University of Wisconsin. The images can be viewed, edited, analyzed, and processed through the software. It was primarily used in the medical field. Due to its popularity, it is being used in other domains also. Figure 3.9 explains the procedure used for the geometric characterization of the pores. A square section of 100mm x 100mm is cropped in the middle of the circular area for analysis. The

image is converted to a gray scale and thresholded to get a binary image. Contrast enhancement is performed for better identification of pores. The average scale used in the analysis is 11 pixel/mm. The area, perimeter, aspect ratio, circularity, roundness, and solidity of the pores can be analyzed through ImageJ after each clogging cycle. The software gives detailed information about each pore on the image in a .csv file.

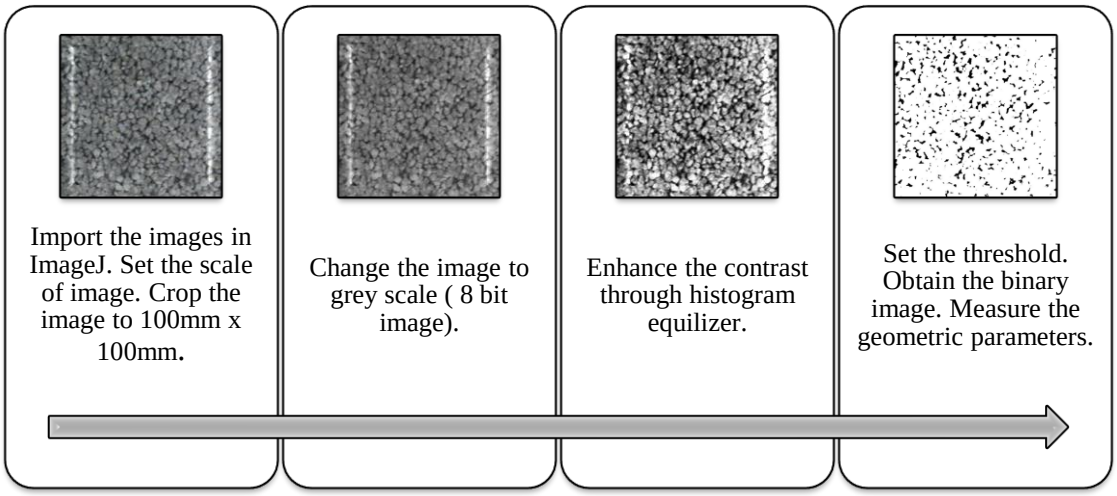

Figure 3.9 Flowchart for image analysis in ImageJ

Table 3.3 shows the formula used for the measurement of the pore parameters. The parameters are extracted from the images in ImageJ. The parameter is measured in units of millimeters(mm).

Table 3.3 Geometric property and its equations

Geometric Property	**Equation**
Area, A(mm^2)	
Perimeter, P(mm)	
Aspect Ratio	$\frac{\text{Major Axis}}{\text{Minor Axis}}$
Circularity	$\frac{4 * \pi * A}{P^2}$

Roundness	$\frac{4 * A}{\pi * d^2}$
Solidity	$\frac{A}{conarea}$

The description of each parameter is shown below:

i Area

The pore area is calculated based on the condition that the minimum area to be analyzed is greater than $0.05mm^2$.

ii Perimeter

The surface of the pore in contact with binding material or aggregate.

iv Aspect Ratio

Aspect ratio of the pores is the height or length of a pore to its diameter or width. It describes the elongation of the pore. It can provide an idea into the flow characteristics and connectivity of pore network. The minimum value of the aspect ratio is one, and as the value increases, it indicates an elongated shape.

iv Circularity

Circularity is a shape descriptor that can mathematically indicate the degree of similarity to a perfect circle. A value of 1.0 designates a perfect circle.

v Roundness

Roundness is similar to circularity but is insensitive to irregular borders along the perimeter of the pore.

vi Solidity

Solidity describes whether the shape is convex or concave. The value of 1 indicates a completely convex shape as the value deviates from 1, greater the extent of concavity.

3.7 STATISTICAL ANALYSIS OF PORE PROPERTIES OF PERVIOUS CONCRETE

The analysis of pore properties can be represented by a number of graphs. The basic graphs are the line graphs, bar graphs, histograms, line plots, frequency tables, circle graphs, stem and leaf plots etc. To get more insight into the data, box plots and violin plots are the most common graphical representations. The violin plots are advanced version of box plots where along with the distribution, the density of each numeric value is represented.

3.7.1 Violin plot

A violin plot depicts distributions of numeric data for one or more groups using density curves. The width of each curve corresponds with the approximate frequency of data points in each region. Densities are frequently accompanied by an overlaid chart type, such as box plot, to provide additional information. Violin plots are useful when distribution comparison is required between multiple groups. It is used to check the similarity between groups based on the peaks, tails and valleys of each group's density curve. In contrast to the more popular histogram, the density curve, kernel density plot, or kernel density estimate are less frequently used ways to represent data distribution.

With a rotated plot on either side that provides more details about the density estimate on the y-axis, it is comparable to a box plot. A violin-like image is produced by mirroring and flipping the density, then filling in the resulting shape. The benefit of a violin plot is that it can reveal subtleties in the distribution that a boxplot cannot. On the other hand, the boxplot makes the outliers in the data more obvious. Box plots are more popular, but violin plots include more information. Since they are uncommon, many readers who are unfamiliar with the violin plot representation may find it challenging to understand their significance.

3.7.2 Data analysis through violin plot

For understanding the data analysis through violin plots, a comparison between box plot and violin plot is shown in Figure 3.10.

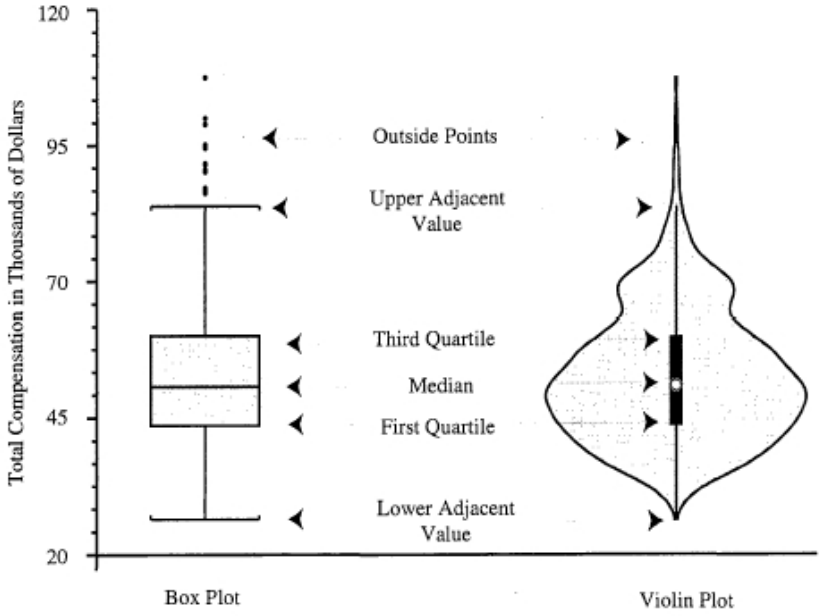

Figure 3.10 Comparison of box plot and violin plot(Hintze and Nelson 1998)

The main features of the plots are:

- Median
- Inter Quartile Range (IQR) defined by Third Quartile – First Quartile
- Lower adjacent value or minimum value defined by First Quartile – 1.5*IQR
- Upper adjacent values or maximum value defined by Third Quartile + 1.5*IQR.
- Outliers defined by values below minimum and above maximum.

The main advantage of the violin plot over the box plot is that it also shows the entire distribution of the data. It becomes useful when the data is multi-modal. Multi modal data are data with more than one peak .

When there is a good amount of data available, kernel density estimation works best since the density estimations are more stable. It is simple to be deceived by the curve's smoothness or the length of the tails past the largest and smallest points when there are few data points available. Individual density curves are constructed around centre lines rather than layered on baselines in a violin plot. The creation and interpretation of curves in a violin plot are identical aside from this variation in display pattern.

3.7.3 Split Violin plots

Violin plot are generally mirrored. It is drawn symmetrical to the axis of the distribution of data point. A split violin plot is represented when a comparison is required between two groups of data. It removes the redundany of mirrored violin plots and make it easier to compare the distributions between multiple conditions. In the present work, the split violin plots are drawn for comparing clay and sand clogging based on the pore parameters.

3.7.4 Use of R for Pore Analysis of Pervious Concrete

The statistical analysis of the geometric properties of the pores was done in R software. Violin plots are created for the statistical analysis of data in the R environment. Violin plots are a method of plotting the entire distribution of data along with the box plot. It is similar to box plot with kernel density. The plots become helpful when the data is multimodal, i.e., containing more than one peak. Split violin plots are created to compare the performance of pervious concrete due to clay and sand. Figure 3.11 shows the syntax for plotting violin plot in R, Figure 3.12 shows the syntax for plotting violin plot with box plot in R and Figure 3.13 shows the syntax of plotting split violin plot in R.

```
library(ggplot2)
library(dplyr)
library(data.table)
library(RColorBrewer)
TheData=read.csv("A:/IMG/R_1.csv")
TheData$Cycle=as.factor(TheData$Cycle)
TheData_Clay<- filter(TheData, Clog=="Clay")
head(TheData)
p<-ggplot(TheData_Clay, aes(x=Cycle, y=Circ))+geom_violin(trim=FALSE,fill='#6699FF')
p+labs(x ="Clay Clogging Cycle", y="Circularity")+ theme_classic()
```

Figure 3.11 Syntax for plotting violin plot in R

```
library(ggplot2)
library(dplyr)
library(data.table)
library(RColorBrewer)
TheData=read.csv("A:/IMG/R_1.csv")
TheData$Cycle=as.factor(TheData$Cycle)
TheData_Clay<- filter(TheData, Clog=="Clay")
head(TheData)
p<-ggplot(TheData_Clay,aes(x=Cycle, y=Circ))+geom_violin(trim=FALSE,fill='#6699FF')
p+geom_boxplot(width=0.1)+labs(x ="Clay Clogging Cycle", y="Circularity")+ theme_classic()
```

Figure 3.12 Syntax for plotting violin plot with box plot in R

```
library(ggplot2)
library(dplyr)
library(data.table)
library(RColorBrewer)
TheData=read.csv("A:/IMG/R_1.csv")
TheData$Cycle=as.factor(TheData$Cycle)
head(TheData)
GeomSplitViolin <- ggproto("GeomSplitViolin", GeomViolin,
                           draw_group = function(self, data, ..., draw_quantiles = NULL) {
  data <- transform(data, xminv = x - violinwidth * (x - xmin), xmaxv = x + violinwidth     *
(xmax - x))
  grp <- data[1, "group"]
  newdata <- plyr::arrange(transform(data, x = if (grp %% 2 == 1) xminv else xmaxv), if (grp
%% 2 == 1) y else -y)
  newdata <- rbind(newdata[1, ], newdata, newdata[nrow(newdata), ], newdata[1, ])
  newdata[c(1, nrow(newdata) - 1, nrow(newdata)), "x"] <- round(newdata[1, "x"])

  if (length(draw_quantiles) > 0 & !scales::zero_range(range(data$y))) {
    stopifnot(all(draw_quantiles >= 0), all(draw_quantiles <=
      1))
    quantiles <- ggplot2:::create_quantile_segment_frame(data, draw_quantiles)
          aesthetics <- data[rep(1, nrow(quantiles)), setdiff(names(data), c("x", "y")), drop =
        FALSE]
    aesthetics$alpha <- rep(1, nrow(quantiles))
    both <- cbind(quantiles, aesthetics)
    quantile_grob <- GeomPath$draw_panel(both, ...)
    ggplot2:::ggname("geom_split_violin",
grid::grobTree(GeomPolygon$draw_panel(newdata, ...), quantile_grob))
  }
  else {
    ggplot2:::ggname("geom_split_violin", GeomPolygon$draw_panel(newdata, ...))
  }
})

geom_split_violin <- function(mapping = NULL, data = NULL, stat = "ydensity", position
= "identity", ...,
                      draw_quantiles = NULL, trim = TRUE, scale = "area", na.rm = FALSE,
                        show.legend = NA, inherit.aes = TRUE) {
  layer(data = data, mapping = mapping, stat = stat, geom = GeomSplitViolin,
        position = position, show.legend = show.legend, inherit.aes = inherit.aes,
        params = list(trim = trim, scale = scale, draw_quantiles = draw_quantiles, na.rm =
na.rm, ...))
}
p<-ggplot(TheData, aes(x=Cycle, y=Circ, fill=Clog))+geom_split_violin(trim = FALSE )
p+scale_fill_manual(values=c("#6699FF",     "#330066"))+labs(x     ="Clogging     Cycle",
y="Circularity")+ theme_classic()
```

Figure 3.13 Syntax for plotting split violin plot in R

3.8 PROPERTIES OF PERVIOUS CONCRETE

3.8.1 Compressive strength test

Compression test is the most common test conducted on hardened concrete for finding out the strength of concrete. The IS standard compression test as per IS 516: 2004(Methods of Tests for Strength of Concrete) is carried out on cubes of size 150x150x150 mm. Figure 3.14 shows the compressive testing machine used for the study. The cast iron moulds are used to prevent distortion of specimen. The test is carried out on 7th, 14th and 28th from the date of curing. The specimens were cured for 48 hours as after 24 hours, the concrete was not set properly.

Figure 3.14 Compressive testing of pervious concrete specimen

3.8.2 Porosity

The porosity or void ratio of the concrete is the amount of voids present in the concrete. It is calculated by the method adopted by Haselbach which is given by the formula(Description 1997).

$$P = \left[1 - \left\{\frac{(W_D - W_S)}{\rho_w * V_T}\right\}\right] * 100$$

where:

P = porosity, %, W_D = oven dry weight, g, W_S = submerged weight, ρ_w = density of water, g/cm^3, V_T = Volume of the specimen

$$V_T = \frac{\pi D_{avg}^2 H_{avg}}{4}$$

The pervious concrete mixes are designed for target porosity. Though there is relationship between porosity and permeability, it can be weakly correlated as interconnected pores change depending on the amount of compaction, size of the aggregates etc.

3.8.3 Permeability test

Permeability (or hydraulic conductivity) refers to the ease with which water can flow through a concrete. It is the intrinsic property of the porous material to transmit liquid under a hydraulic gradient. It is found by the principle of constant head or falling head. A fabricated unit made of transparent acrylic is used to measure the permeability.

The principle of falling head permeameter is used. A volume of 1 liter of water is used consistently for both permeability and clogging test. At the beginning of the test, when the water is poured, the level is around 5.5cm. The time taken is calculated when the water level reaches 3cm. A falling head of 1.5cm from 3cm to 1.5cm from the top surface of the specimen is maintained for the test. The time taken for 1.5cm fall is measured via video for accurate calculation of time. Since the flow takes place very quickly due to its porous nature, a video graphic aid for calculation of time reduces the number of repetitions and also increases the accuracy of the measurement.

A direct relation is difficult to obtain between permeability and porosity as permeability depends on other factors like tortuosity.

3.8.4 Clogging test

Since pervious concrete allows the passage of air and water through its surface, there are chances that dust particles, soil from nearby areas or clayey water can clog the pervious concrete matrix. In this study, the specimen is exposed to clay and sand slurry respectively to understand the effect of clogging. A concentration of 5g/l is prepared by mixing 5g of clay or sand with 1 liter of water. It is mixed at 40 rpm for 1 minute in a motorized mixer as shown in Figure 3.15. This solution is

passed through the matrix, and the same principle of calculating permeability is used. There are two types of exposure conditions which are followed. In the first type, the suspension is passed successively in six cycles whereas the second type has three cycles where after each cycle, the specimen is kept in the oven to simulate the climatic condition of the surrounding area and then proceeded to the next cycle. The change in the permeability pattern is tabulated in the results. Since the trials cannot be repeated, the use of video was extremely useful for accurate calculation of time.

Figure 3.15 Mixing of clay particles for clogging test

Since pervious concrete allows the passage of air and water through its surface, there are chances that dust particles, soil from nearby areas or clayey water can clog the pervious concrete matrix. Clogging causes the decrease of infiltration and permeability over time as particles gets embedded in the concrete matrix. To understand the effect of clogging, it is exposed to six soil condition. The first two samples are clay and sand. A concentration of 10g/l is prepared by mixing 30g of soil sample with 3 litres of water. It mixed at 40 rpm for 1 minute in a motorized

mixer. This solution is passed through the matrix and the same principle of calculating permeability is used. It is repeated for three cycles to evaluate the decrease of permeability.

CHAPTER 4

RESULTS AND DISCUSSION

4.1 INTRODUCTION

The chapter discusses the performance of pervious concrete with respect to its basic mechanical and hydraulic properties. The response of pervious concrete when narrow size gradation is incorporated is analysed for its compressive strength and permeability. The properties are highly dependent on the pore structure of the concrete. The pore structure of pervious concrete specimen contains air voids, capillary pores and gel pores. These pores have random distribution across horizontal and vertical profiles. Though pervious concrete has a lot of advantages as a source sustainable urban management system, the clogging of its pores due to the presence of sediments in the runoff has impacted the life of the green concrete. Clogging studies are conducted to assess the impact of clogging on the pervious concrete. Clay and sand are used separately to understand the clogging pattern on the concrete mixes. Since top surface clogging impacts the hydraulic performance of the concrete, the top surface is analysed using image analysis in ImageJ environment. The software analyses the geometric properties of pore parameters like area, perimeter, aspect ratio, circularity, roundness and solidity on its top surface. The above properties are analysed through violin and box plots in R software environment. Since pervious concrete specimens has high randomness in pore structure, it becomes essential to understand the distribution of its pore parameters as the clogging progresses on the top surface.

4.2 INFLUENCE OF AGGREGATE SIZE ON THE COMPRESSIVE STRENGTH OF PERVIOUS CONCRETE

The compressive strength of pervious concrete is comparatively lower than that of conventional concrete due to presence of pores. It is intentional designed to promote the permeability and drainage capabilities. Compressive strength is the primary property to assess the ability of concrete to resist loads. It depends on mix design, aggregate properties, water-to-cement ratio, curing conditions, and specific

application requirements. In conventional concrete, the porosity is significantly less, and the concrete's strength is not dependent on the porosity. Whereas in pervious concrete, the compressive strength is dependent on the number and size of the pores. The compressive strength is calculated following the similar procedure adopted for conventional concrete. The strength is calculated for 7th, 14th and 28th day to understand the pattern of increase of compressive strength

The compressive strength is calculated on the 28th day for the narrow gradation. Table 4.1 shows the average, maximum, and minimum compressive strength for 2.36mm - 4.75mm and 4.75mm - 6.30mm gradation, respectively. For the same mix design, the 2.36 - 4.75mm aggregate gradation has higher compressive strength than 4.75 - 6.30mm. (Chindaprasirt 2008) concluded that compressive strength in the range of 22 - 39MPa is achieved with porosity in 15 - 25% by maintaining a low water-cement ratio of 0.25.

Table 4.1 Compressive strength of the pervious concrete mixes

Size Gradation	2.36 - 4.75mm	4.75 - 6.3mm
Average Compressive Strength	24MPa	20MPa
Maximum Compressive Strength	27MPa	21MPa
Minimum Compressive Strength	22MPa	16.2MPa

Table 4.2 tabulates the compressive strength, porosity, and permeability values from the American guidelines American Concrete Institute ACI 522R-10, guidelines by Finland Technical Research Centre Valtion Teknillinen Tutkimuskeskus VTT-R-080225-13, and the Brazilian - standards Norma Brasileira Regulamentadora NBR 16416:2015. The average compressive strength is within limits for all the cases except for VTT-R-080225-13, where the max compressive strength is 20MPa. The 2.36 - 4.75mm gradation has a higher compressive strength than the standard.

Table 4.2 Compressive strength, porosity and permeability ranges from standards

Standards	Compressive Strength(MPa)	Porosity(%)	Permeability(mm/s)
ACI 5228-10	6.8 - 37.9	10 - 35	> 1
NBR 16416:2015	20 - 35	15 - 30	> 1
VTT-R-080225-13	10 - 20	20 - 35	> 1.5

Table 4.3 shows the summary of literature relating to mix proportion, compressive strength, porosity, and permeability in comparison with the current study. The Figure 4.1 shows the compressive strength's pictorial representation tabulated in Table 4.3. The literature shows variations in the compressive strength of the specimen. The compressive strength values used in the present study have higher range compared to reported works with similar mix proportions. One of the prime reasons for the same is small aggregates. Small aggregates create small voids and interconnection between them is narrow.

Table 4.3 Reference of mix proportion and properties of pervious concrete

Reference	Aggregate /Binder Ratio	Water /Binder Ratio	Compressive Strength, N/mm^2	Porosity, %	Permeability, mm/s
(Azad et al. 2020)	4 - 4.85	0.36	9.2 - 14.8	30 - 36	5.36 - 6.17
(Cai et al. 2020)	3 - 4.2	0.3	4 - 12	24.8 - 26.1	1.8 - 6.9
(Lori et al. 2019)	3.35	0.3	17.93 - 23.5	20.44 - 21.67	3.05 - 3.33
(Zhu et al. 2020)	3.84 - 5.55	0.31	12.7 - 34.5	18.7 - 25.7	6.1 - 7.1
(Sandoval et al. 2019)	3.26	0.34	3.83 - 10.1	19.26 - 27.06	4.97 - 15.08
(Mohammed et al. 2018)	2.1, 2.61,3.36	0.3	2.5 - 19.9	14.3 - 28.75	3.44 - 9.82
Present study	3.33	0.25	16.2 - 27	15.2 - 23.3	4.34- 6.61

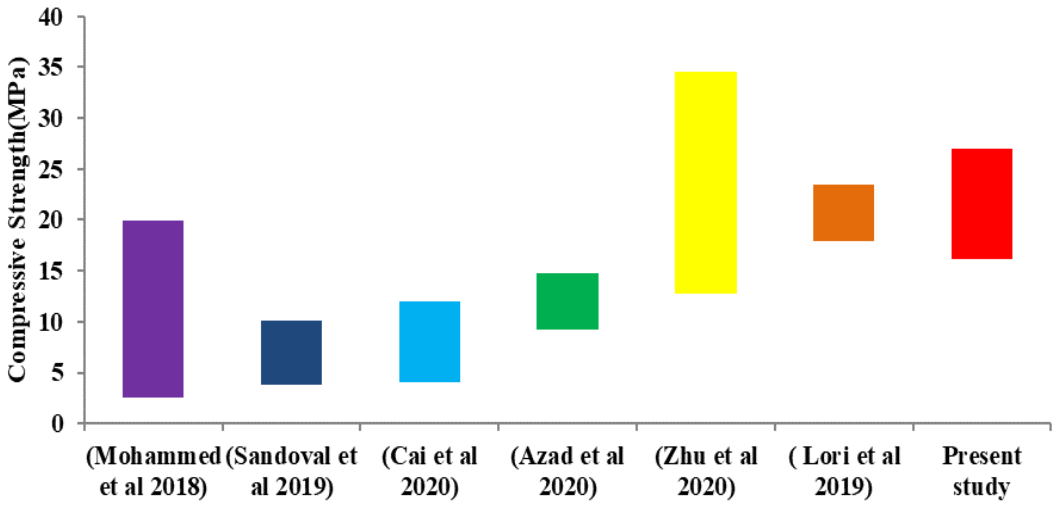

Figure 4.1 Comparison of compressive strength from literature with present study

The compressive strength is compared to literatures with similar aggregate binder ratios. (Mohammed et al and Zhu et al 2018) shows high variation in compressive strength in comparison to (Sandoval et al 2019), (Azad et al 2020) and (Lori et al 2019). Generally, in literature with more than one aggregate size gradation, the variation of compressive strength is high. In conclusion, this section compares the basic statistics of average, maximum and minimum of compressive strength between the two narrow gradations. The values are checked against three standards for its compressive strength. Also, the compressive test results are compared to existing literature for understanding the deviation of the results from the literature.

4.3 INFLUENCE OF AGGREGATE SIZE ON THE HYDRAULIC PROPERTIES OF PERVIOUS CONCRETE

The concrete is compacted in three layers instead of vibration. The uniform degree of compaction ensures uniformity in the engineering properties of the concrete. The calculated porosity and density are tabulated in Table 4.4. Since narrow gradation of aggregate is used, the porosity has increased with the increase in aggregate size. The porosity calculated above is the total porosity. It is essential to calculate the interconnected pores to correlate with permeability strongly. The above results are on par with (Fu et al. 2014), where porosity increases with aggregate size. (Ibrahim et al. 2014) calculated the density for aggregate cement ratio of 8, water-cement

ratio of 0.35 with an aggregate size of 4.5mm as 1780.31 kg/m^3. The porosity values are within the range when compared to the standards in Table 4.2. The concrete mix has porosity values in tandem with the literature as shown in Figure 4.2. Since smaller aggregates are used, the maximum value of permeability is less in comparison with the literature. The creation of large pores are limited and since one of the gradation ie 2.36mm - 4.75mm falls under fine aggregate size, most of the pores are filled by the aggregates itself. From literature tabulated in Table 4.3, it is observed that lower binder aggregate ratio also causes lower porosity.

Table 4.4 Porosity and density of the pervious concrete mixes

Size Gradation	2.36 - 4.75mm	4.75 - 6.3mm
Total Porosity Range	15.2 to 17.6%	21.9 to 23.3%
Total Porosity - Average	16.38%	22.61%
Density - Average	1567.4 kg/m^3	1514 kg/m^3
Density - Standard Deviation	67 kg/m^3	37.7 kg/m^3

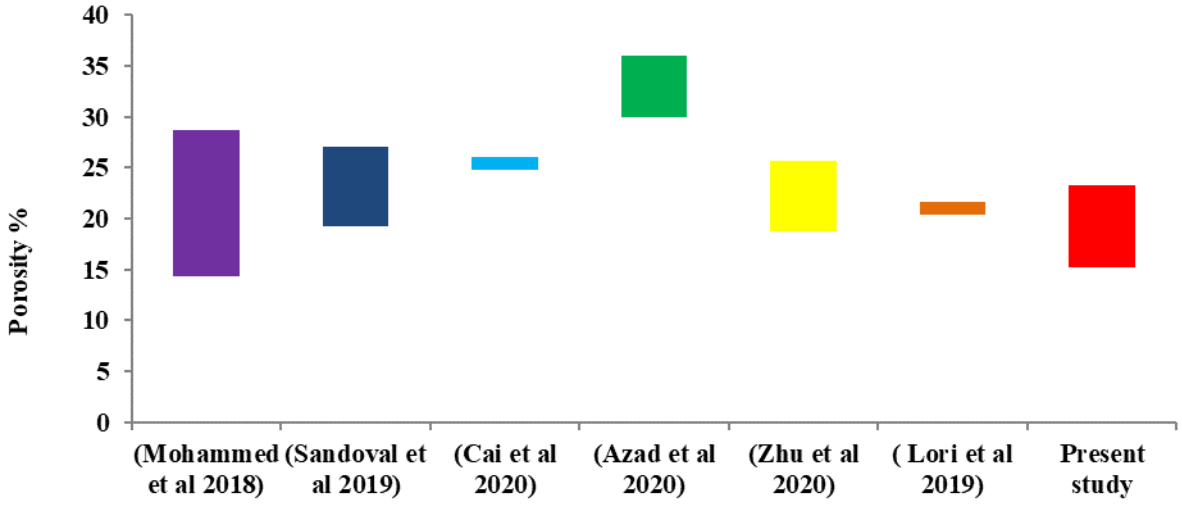

Figure 4.2 Comparison of porosity from literature with present study

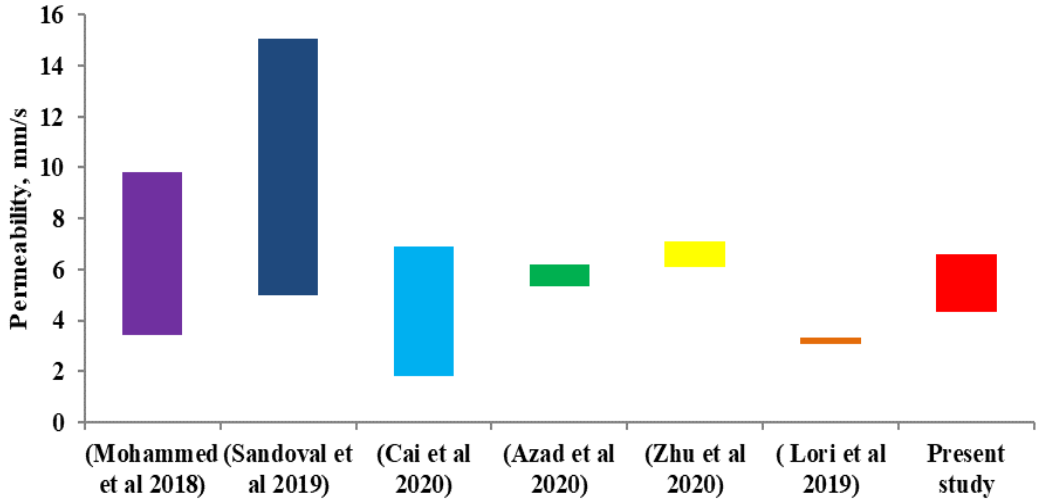

Figure 4.3 Comparison of permeability from literature with present study

Figure 4.3 compares the permeability from literature with the present study. The variation of permeability is less compared to the literature. The permeability values are in tandem with the literature. The motorized vibration method is not done since it causes the settlement of cement slurry at the bottom and makes the concrete impermeable. A lower aggregate cement ratio also causes the bottom layer of the concrete to become impermeable due to the cement paste drain at the bottom. The permeability was analyzed for both the narrow gradation of aggregates. Though the compressive strength is higher for the narrow gradation of 2.36mm - 4.75mm, there is a substantial reduction in the permeability due to lesser interconnected pores in the concrete matrix. The smaller pores due to the presence of smaller aggregates decrease the porosity and ultimately the permeability of the specimen.

Since the gradation is narrow, the size of the aggregates decides the size of the pores. Figure 4.4 shows the comparison of the variation of permeability between the gradation of 2.36 – 4.75mm and 4.75-6.30mm in the form of box plot. There is an average difference of 0.00337m/s between the two gradations. Due to the pores' large size, the larger aggregate size gradation of 4.75mm - 6.3mm shows higher permeability than the smaller size gradation of 2.36mm - 4.75mm. The permeability of the larger size gradation has more variation in permeability with a standard

deviation of 0.00124m/s. Since the compaction is manual, there is variability in the permeability of the specimens. The manual compaction has resulted in uneven distribution of pores within the concrete matrix. The lack of vibration of the concrete specimen has affected the uniformity in the internal structure of the concrete. The variation in the permeability of the larger gradation indicates the presence of numerous interconnected pores resulting in varying flow paths.

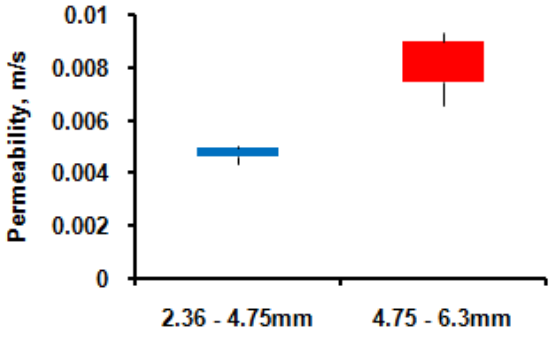

Figure 4.4 Box plot of variations of permeability for both aggregate size gradations

In contrast, the smaller aggregate gradation has a standard deviation of 0.00032m/s, indicating a more uniform permeability. The permeability variation is less for the smaller aggregates, suggesting that manual compaction does not affect the pore structure. Since the aggregate size is small, the pore size is also small. It has resulted in the reduction of the interconnected pores in the specimen. Comparing the two gradations, as shown in Figure 4.4, the size of the aggregate and narrow gradation has a significant role in the permeability of the concrete specimen. Since high permeability is not desired for all use cases of pervious concrete, a curve between permeability and compressive strength effectively classifies the concrete based on the particular use. The permeability values are greater than the values prescribed in the standards, as tabulated in Table 4.2. The current study has comparable permeability with the literature, as shown in Figure 4.5. The maximum values are lower compared to the prior studies. The permeability exhibits an exponential relationship with porosity. The equation is $y=0.934e^{9.622x}$ where y is the permeability in mm/s and x is the porosity as ratio. The equation has an R^2 value of 0.927. In conclusion, this section compares the basic statistics of average, maximum and minimum of porosity and permeability between the two narrow

gradations. The values are checked against three standards for porosity and permeability. Also, the compressive test results are compared to existing literature for understanding the deviation of the results from the literature. The variation of permeability between the two gradations is observed through the box plot. An exponential relation is derived between permeability and porosity.

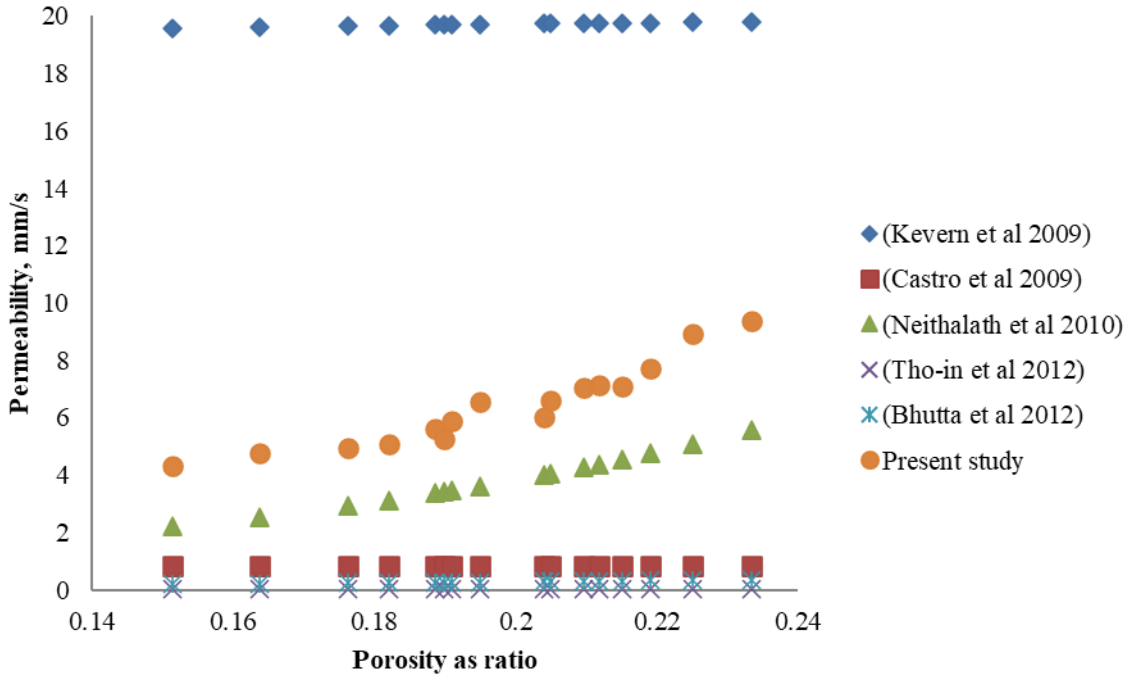

Figure 4.5 Relationship between permeability and porosity

4.4 CLOGGING POTENTIAL OF PERVIOUS CONCRETE

4.4.1 Clay clogging

Though the use of pervious concrete is gaining immense popularity, the clogging caused due to particles on the roadways and the nearby areas is a cause of concern to the life of the concrete and its maintenance requirements. The research on clogging is essential to understand the behavior of concrete in terms of its permeability. Clay is a very fine particle and can easily escape through most porous media. Since it is smaller and cohesive in nature, it can easily pass into the voids or pores of the concrete and cause clogging. It is necessary to know the interaction

between the clay particles and pore structure to assess the type of maintenance required for the concrete. Figure 4.6 shows the trend and the comparison of the clogging due to the two gradations of aggregates for clay clogging. The curve is exponential, and the inflection point is the first clogging cycle. The introduction of clay slurry of 5g/l concentration causes a substantial decrease in permeability. There was a 69.8% and 74.9% reduction in permeability in the first cycle of clogging for a narrow gradation of 2.36 - 4.75mm and 4.75 - 6.30mm, respectively. The initial value of permeability is measured using plain water. The percentage reduction is calculated with respect to the initial permeability value. The clogging of pores in this magnitude limits the use of pervious concrete to places where the stormwater is almost free from solid particles.

The 2.36 - 4.75mm gradation concrete shows a further decrease in permeability after the first cycle. The small pores and interconnections are getting clogged due to exposure to an aqueous clay solution. Whereas for 4.75 - 6.30mm gradation, the permeability is almost constant after the first clogging cycle. The comparatively larger pores allow excess clay particles to pass through their pores. There was accumulation and flushing of clay particles in both cases on the specimen's top surface. The exfiltrate also contained clay particles indicating the movement of clay through the permeable matrix.

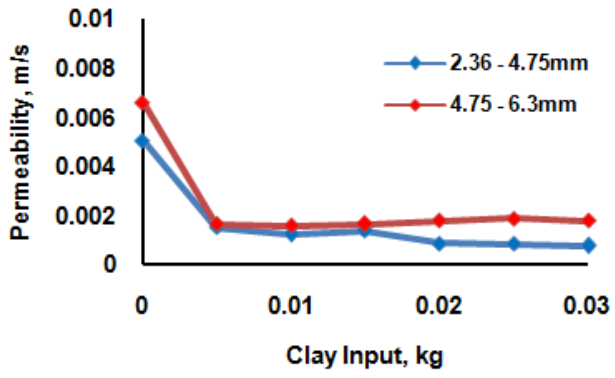

Figure 4.6 Comparison of permeability due to clay clogging

4.4.2 Sand clogging

Sand particles are larger in size and tend to cause more clogging than clay. The trend and the comparison of the clogging due to the two gradations of aggregates are shown in Figure 4.7. The curve is exponential, and the inflection point is the first clogging cycle. It also shows a substantial decrease in permeability due to the introduction of the sand slurry of a 5g/l concentration. There was a 74.7% and 71.7% reduction in permeability in the first cycle of clogging for a narrow gradation of 2.36mm - 4.75mm and 4.75mm - 6.30mm. It also shows that the change in permeability is very minimal after the initial decrease in permeability. Though clay and sand behave differently as a clogging materials, the percentage reduction of permeability is almost the same as clay clogging. The sand particles are retained fully in the concrete matrix for all the cycles. The exfiltrate did not contain sand particles, indicating the accumulation of sand particles in the concrete matrix for the six cycles.

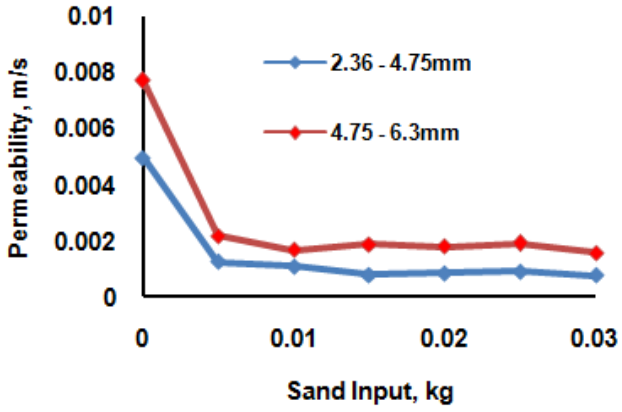

Figure 4.7 Comparison of permeability due to sand clogging

4.4.3 Clogging potential

Clogging potential is the likelihood of a pervious concrete system to experience blockages or reduced permeability due to the accumulation of debris, particles like dust and other materials. It is calculated as a ratio of difference of permeability due to clogging to initial permeability. The clogging material and size of the aggregates in the pervious concrete play an essential role in determining the pervious concrete

mix's clogging potential. The clogging material depends on traffic load carrying the mud, debris or dirt, surrounding environment consisting of organic matter from trees and vegetation and construction debris from construction sites. The clogging potential is plotted when the clogging material is introduced to the concrete matrix. The clogging material is clay and sand. The change in permeability from the first cycle to the sixth cycle and its linearity are shown in Figure 4.8. The slope of the clogging cycles shows decreasing permeability except for the clay clogging of 4.75 - 6.30mm. The regression equations and their R^2 values are tabulated in Table 4.5. The x values are the sediment input in kg, and y is the permeability in m/s. The clogging pattern for clay in the gradation of 2.36 - 4.75mm has the maximum negative slope indicating the maximum permeability decrease. All the equations' slope is approximately zero, indicating that the permeability does not change significantly as the clogging cycle progresses. The least coefficient for determination R^2 is for sand clogging in the gradation of 4.75 - 6.3mm, indicating the mean value's deviation. The clogging material and size of the aggregates play an essential role in determining the pervious concrete mix's clogging potential.

Comparing the permeability due to clogging with the standards tabulated in Table 4.2, the clogging of clay and sand on the pervious concrete with the narrow gradation of 2.36 - 4.75mm causes the permeability value to go below the minimum value of 1mm/s as per American guidelines ACI 522R-10 and the Brazilian standards NBR 16416:2015. In addition, after the first clogging cycle on the above mix, the observed value is below the minimum threshold of 1.5m/s in accordance with the guidelines by Finland Technical Research Centre VTT-R-080225-13. Such low permeability values will not serve the purpose of the pervious concrete. It is recommended not to use small aggregates when there is a chance of high siltation.

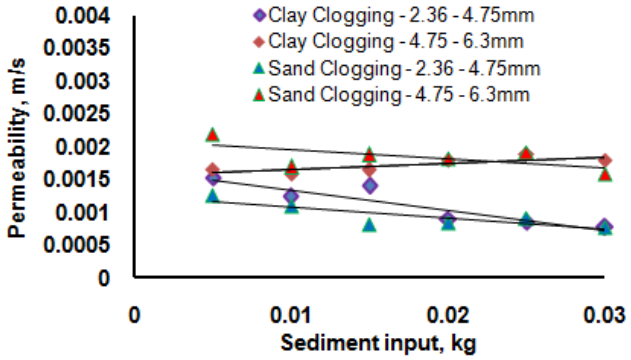

Figure 4.8 Clogging potential for all case scenarios

Table 4.5 Clogging potential equation

S. No	Aggregate Gradation	Clogging material	Equation	R^2
1	2.36 - 4.75mm	Clay	y= -0.031x+0.001	0.84
2	2.36 - 4.75mm	Sand	y= -0.017x+0.001	0.695
3	4.75 - 6.3mm	Clay	y= 0.009x+0.001	0.627
4	4.75 - 6.3mm	Sand	y= -0.014x+0.002	0.394

In this section, the clogging of pervious concrete under the application of aqueous solution of clay and sand separately is studied. A regression equation is framed with respect to changes in permeability under the influence of increasing clogging cycles.

4.5 EXFILTRATE QUALITY ANALYSIS

The concentration of exfiltrate is calculated for understanding the retention of sediment particles in the pervious concrete matrix. Figure 4.9 shows the graph between cumulative clay retention and cumulative clay input. It indicates retention of clay particles in the pervious concrete matrix. The retention is more in the 2.36 – 4.75mm gradation. The small pores due to small aggregates results in better retention of clay particles. Figure 4.10 shows the graph between cumulative sand

retention and cumulative sand input. The sand particles are retained almost fully by the pervious concrete by the six clogging cycles of 5g/l aqueous solution. In both the gradations, the retention is approximately same.

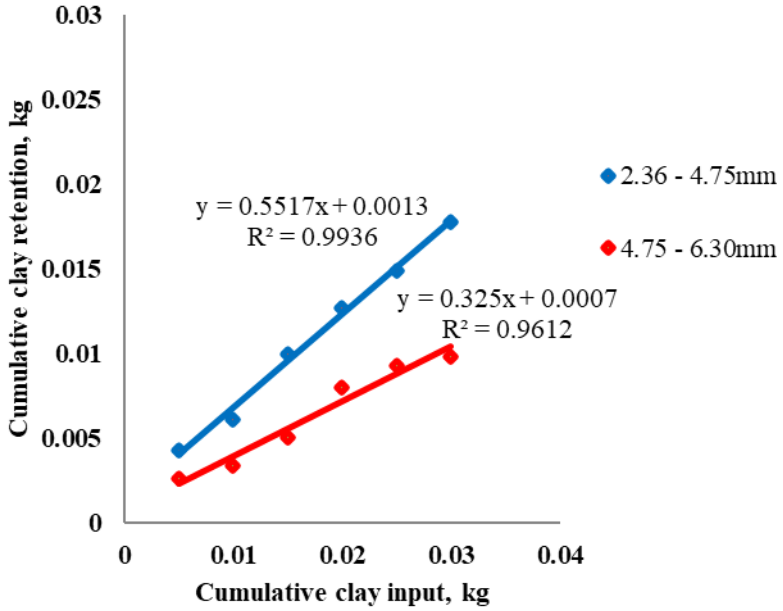

Figure 4.9 Cumulative clay retention

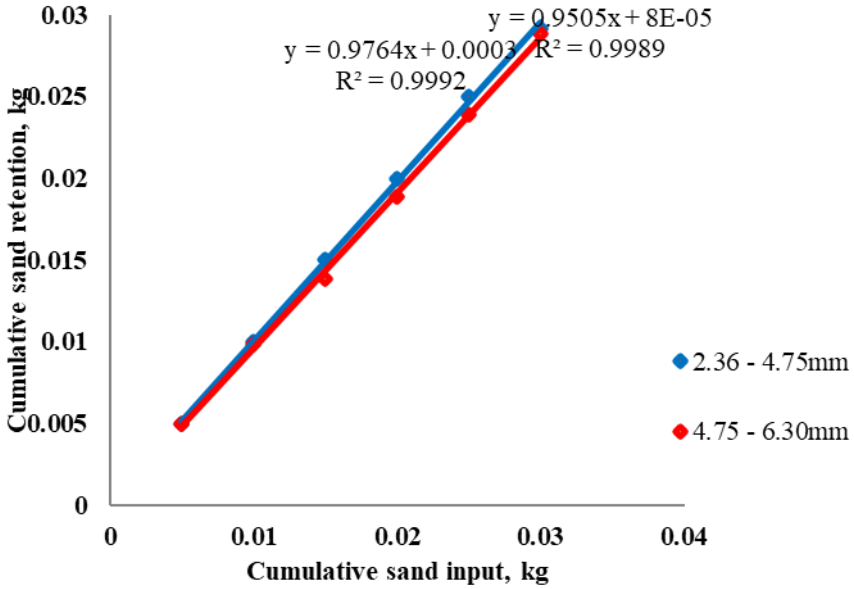

Figure 4.10 Cumulative sand retention

4.6 USE OF IMAGE ANALYSIS FOR UNDERSTANDING TOP SURFACE CLOGGING OF PERVIOUS CONCRETE

The geometric properties of pores on the top surface of the pervious concrete are studied through image analysis. Twenty-eight images were analysed for understanding the pore properties of the top surface of the pervious concrete. The images were divided equally based on the aggregate size used in the concrete namely 2.36 – 4.76mm and 4.76 – 6.30mm. Each aggregate size was further divided equally into clay and sand clogging. A set of seven images were studied for understanding the type of clogging based on the size of the aggregate used. The seven images range from the unclogged top surface to six cycles of clogging by the clogging material. The top surface analysis is significant since the reduction in the pore spaces on the top surface affects the overall permeability of the pervious concrete mix. The parameters are area, perimeter, aspect ratio, circularity, roundness, and solidity. Table 4.6 shows some of the pores extracted and its geometric parameter. It shows the variation of the parameter as the pores taken up different shapes based on the concrete mix design and amount of compaction.

Table 4.6 Pore shape and its geometric properties

Image			
S. No	108	202	356
Label	DSC_4767.JPG		
Area	0.206m^2	4.291m^2	2.93m^2
X	87.59m	99.676m	52.39m
Y	14.646m	32.104m	60.542m
Perimeter	2.486m	10.821m	14.54m
Aspect Ratio	4.047	2.685	4.66

Circularity	0.419	0.461	0.174
Roundness	0.247	0.372	0.215
Solidity	0.636	0.808	0.498

4.7 ANALYIS OF AREA OF THE PORES ON TOP SURFACE OF PERVIOUS CONCRETE

Table 4.7 and Table 4.8 tabulates the count, sum, percentage pores, maximum, minimum, average, and standard deviation of the area for six clay and sand clogging cycles for 2.36 – 4.75mm and 4.75 – 6.30mm aggregate size respectively. The parameters are measured from the area of 100mm x 100mm taken for the analysis. The minimum area of the pore for analysis is taken as 0.05mm^2. Comparing the two aggregate gradations, the maximum value of pore area decreases substantially after the first clogging cycle. For the aggregate size gradation of 2.36 – 4.75mm, in the six clogging cycles of clay, the total percentage area reduced from 14.02% to 8.68%, whereas for sand, the total percentage area reduced from 13.16% to 4.11%. The values indicate that sand clogs the pervious concrete matrix more than clay particles. For the aggregate size gradation of 4.75 – 6.30mm, in the six clogging cycles of clay, the total percentage area reduced from 9.54 % to 6.90%, whereas for sand, the total percentage area reduced from 8.89% to 5.50%. There is a reduction in the max pore area for clay and sand clogging. The decline is evident in sand clogging. The average pore area shows a sinusoidal pattern indicating deposition of the clogging particles to deeper layers of the pervious concrete. Due to its smaller size, the clay particles pass through the concrete matrix, whereas the sand particles are retained in the top layers of the pervious concrete matrix. There is substantial decrease in the total pore area also. The standard deviation of the area is greater than the average value of the area indicating a high variation in the pore area.

Table 4.7 Basic statistics of area(mm^2) for clay and sand clogging cycle – 2.36-4.75mm

S. No	Cycle	Clogging Material	Count	Sum	%	Max	Min	Average	Std. Dev.
1	0	Clay	530	1412.44	14.02	43.29	0.05	2.66	4.48
2	1	Clay	588	914.36	9.09	23.08	0.06	1.56	3.06
3	2	Clay	369	912.66	9.66	32.20	0.05	2.47	4.67
4	3	Clay	511	1269.47	12.60	27.66	0.06	2.48	3.85
5	4	Clay	362	654.44	6.53	32.36	0.06	1.81	3.41
6	5	Clay	478	662.83	6.63	14.87	0.06	1.39	2.11
7	6	Clay	474	875.72	8.68	24.07	0.06	1.85	3.17
8	0	Sand	525	1322.76	13.17	37.26	0.05	2.52	3.75
9	1	Sand	409	858.62	8.53	17.95	0.06	2.10	2.83
10	2	Sand	342	437.33	4.37	11.46	0.06	1.28	1.90
11	3	Sand	196	426.06	4.23	18.70	0.06	1.99	3.02
12	4	Sand	301	406.91	4.03	13.15	0.05	1.35	2.07
13	5	Sand	623	611.15	6.07	11.63	0.05	0.98	1.55
14	6	Sand	406	414.08	4.11	7.73	0.06	1.02	1.42

Table 4.8 Basic statistics of area(mm^2) for clay and sand clogging cycle – 4.75 – 6.30mm

S. No	Cycle	Clogging Material	Count	Sum	%	Max	Min	Average	Std. Dev.
1	0	Clay	375	970.18	9.54	35.26	0.05	1.47	2.41
2	1	Clay	277	731.40	7.29	16.96	0.05	1.77	2.70
3	2	Clay	346	719.98	7.12	26.05	0.06	1.88	3.05
4	3	Clay	275	777.67	7.67	25.30	0.05	1.76	3.53
5	4	Clay	350	730.56	7.2	32.26	0.05	1.62	3.13
6	5	Clay	302	724.67	7.1	32.20	0.05	2.52	4.35
7	6	Clay	355	700.40	6.9	26.20	0.05	1.69	2.77
8	0	Sand	379	901.45	8.89	39.70	0.05	1.29	2.68
9	1	Sand	260	718.20	7.09	15.30	0.06	1.50	2.48
10	2	Sand	334	680.37	6.70	22.54	0.05	1.79	3.03
11	3	Sand	325	664.56	6.51	21.41	0.05	1.57	2.96
12	4	Sand	331	631.85	6.2	14.91	0.06	1.64	2.68
13	5	Sand	385	601.34	5.9	15.07	0.05	1.34	2.33
14	6	Sand	336	561.64	5.5	18.77	0.05	1.33	2.54

Figure 4.11 shows the split violin plot of area of the pores for 2.36 – 4.75mm gradation. It compares the clogging due to clay and sand for six cycles of clogging. The max area of the pore is in the unclogged portion. The bell curve of both the clogging cycles is unimodal. The increase of the width of the bell shape curve indicates the increase in the number of pores. The number of pores are not constant through the cycle. The decrease in the pore number indicates the presence of

temporary or permanent clogging of pores during the particular cycle. There is occurrences of partial clogging of the pores. At the fourth cycle, there is unclogging of large pores indicated by the increase in the area of pores. The phenomena is more evident in clay clogging as the smaller clogging particles flush down the pervious concrete matrix.

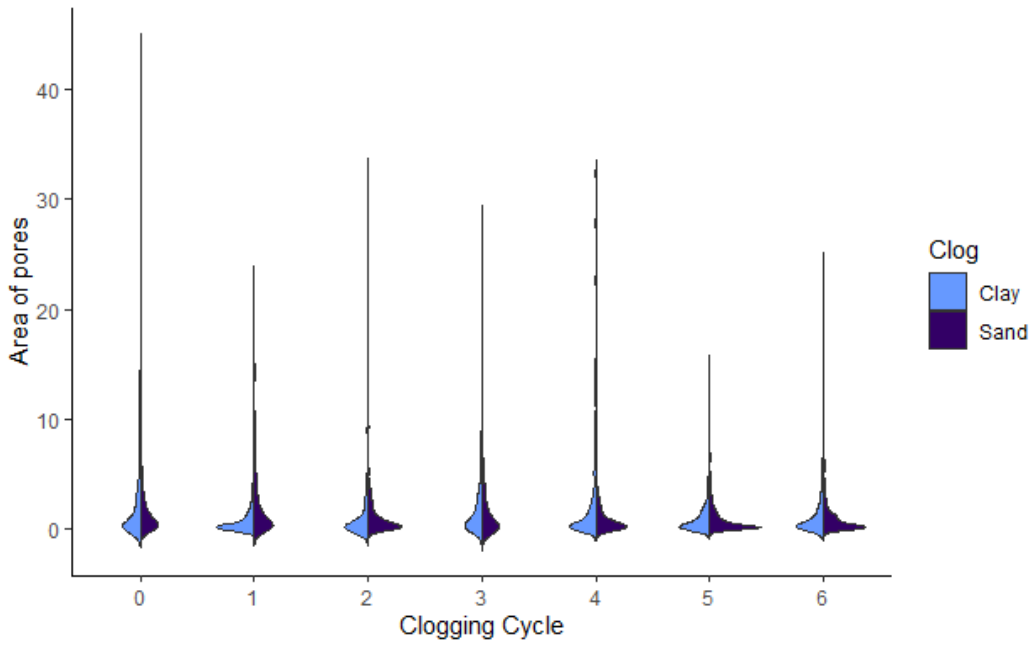

Figure 4.11 Split violin plot of area comparing clay and sand clogging – 2.36-4.75mm

Figure 4.12 shows the split violin plot of area of the pores for 4.75 – 6.30mm gradation. It compares the clogging due to clay and sand for six cycles of clogging. The max area of the pore is in the unclogged portion. The bell curve of both the clogging cycles is unimodal. The increase of the width of the bell shape curve indicates the increase in the number of pores. The number of pores are not constant through the cycle. The decrease in the pore number indicates the presence of temporary or permanent clogging of pores during the particular cycle. The third and fourth cycle shows very similar distribution of area of pores. Sand clogging is more prominent as the pore area is nearing zero as the clogging cycle continues.

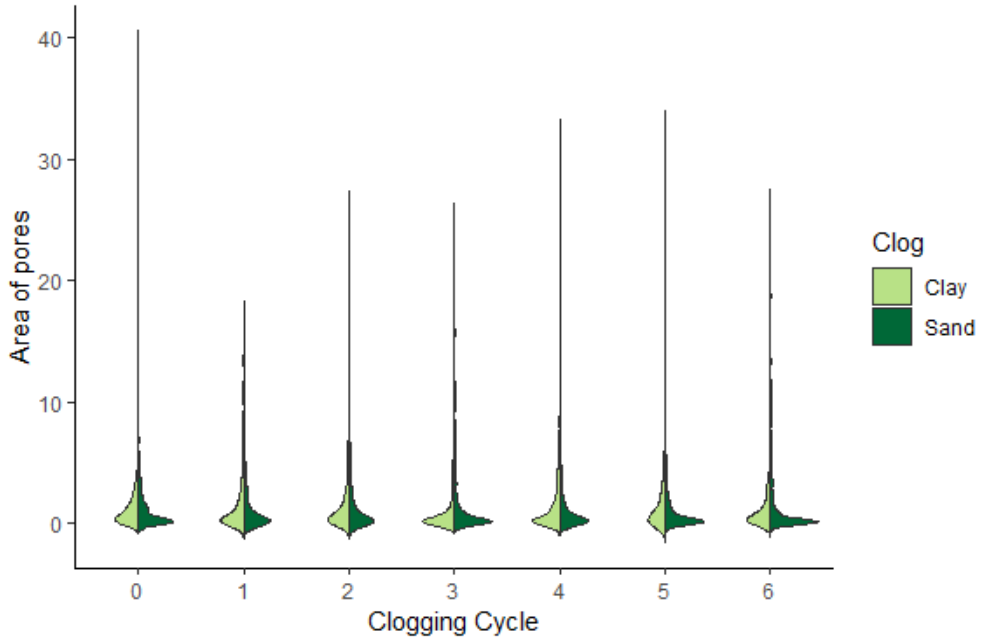

Figure 4.12 Split violin plot of area comparing clay and sand clogging – 4.75-6.30mm

4.8 ANALYSIS OF PERIMETER OF THE PORES ON THE TOP SURFACE OF PERVIOUS CONCRETE

Perimeter is an important 2D property for pore space analysis. The surface length of each pore in contact with cement and aggregate is computed through the images. Table 4.9 tabulates the maximum, minimum, average and standard deviation of the perimeter for six cycles of clay and sand clogging for the gradation of 2.36 – 4.75mm. The standard deviation of the perimeter is almost the same as the average value. High standard deviation indicates that the perimeter has high variation. Generally in exponential and Poisson distribution, the average and standard deviation are almost equivalent. In clay and sand clogging, there is decrease of the maximum and average value of the perimeter after the first cycle.

Table 4.9 Basic statistics of perimeter(mm) for clay and sand clogging cycles – 2.36-4.75mm

S. No	Cycle	Clogging Material	Max	Min	Average	Std. Dev.
1	0	Clay	79.66	0.70	8.30	9.81
2	1	Clay	64.03	0.76	6.91	8.55
3	2	Clay	54.91	0.74	8.22	9.92
4	3	Clay	61.16	0.88	8.56	8.93
5	4	Clay	60.97	0.76	6.61	7.37
6	5	Clay	33.16	0.76	5.86	5.67
7	6	Clay	54.30	0.75	6.68	7.23
8	0	Sand	80.18	0.78	8.05	8.60
9	1	Sand	34.53	0.77	6.45	5.88
10	2	Sand	25.80	0.76	5.20	4.67
11	3	Sand	47.18	0.75	7.08	7.31
12	4	Sand	27.25	0.72	5.22	4.98
13	5	Sand	32.99	0.71	4.39	4.36
14	6	Sand	21.97	0.73	4.36	3.82

Table 4.10 tabulates the maximum, minimum, average and standard deviation of the perimeter for six cycles of clay and sand clogging for the gradation of 4.75 – 6.30mm. It shows a very similar trend to the previous analysis but the decrease in maximum perimeter in the first clogging is substantial for the said gradation.

Table 4.10 Basic statistics of perimeter(mm) for clay and sand clogging cycles – 4.75-6.30mm

S. No	Cycle	Clogging Material	Max	Min	Average	Std. Dev.
1	0	Clay	84.81	0.76	6.01	6.06
2	1	Clay	35.23	0.77	6.65	6.56
3	2	Clay	49.99	0.82	6.81	6.97
4	3	Clay	42.25	0.73	6.32	7.75
5	4	Clay	67.78	0.72	6.44	7.53
6	5	Clay	53.86	0.82	8.23	9.05
7	6	Clay	48.59	0.71	6.35	6.60
8	0	Sand	83.53	0.70	5.70	6.83
9	1	Sand	35.34	0.77	6.07	6.57
10	2	Sand	55.82	0.72	7.15	8.08
11	3	Sand	55.12	0.74	6.19	7.84
12	4	Sand	43.41	0.78	6.02	6.41
13	5	Sand	36.35	0.72	5.49	6.12
14	6	Sand	34.71	0.64	4.74	6.00

Figure 4.13 shows the split violin plot of perimeter of the pores for the gradation of 2.36 – 4.75mm. It compares the clogging due to clay and sand for six cycles of clogging. In the absence of the dimensions of the pores, the calculation of area and perimeter gives a good knowledge about the shape of the pores. The bell curve of both the clogging cycles is unimodal. The graphs of the area and perimeter show similar pattern. In the analysis, for a given perimeter, there is only one value of area

whereas for a given area, there are varying values of perimeter. The largest perimeter is observed in the unclogged pervious concrete specimen. The largest area does not correspond to the largest perimeter. The top surface of the sand clogged surface shows gradual shift of pore perimeter being close to zero as the clogging cycle continues whereas for clay clogging the variation is not very evident.

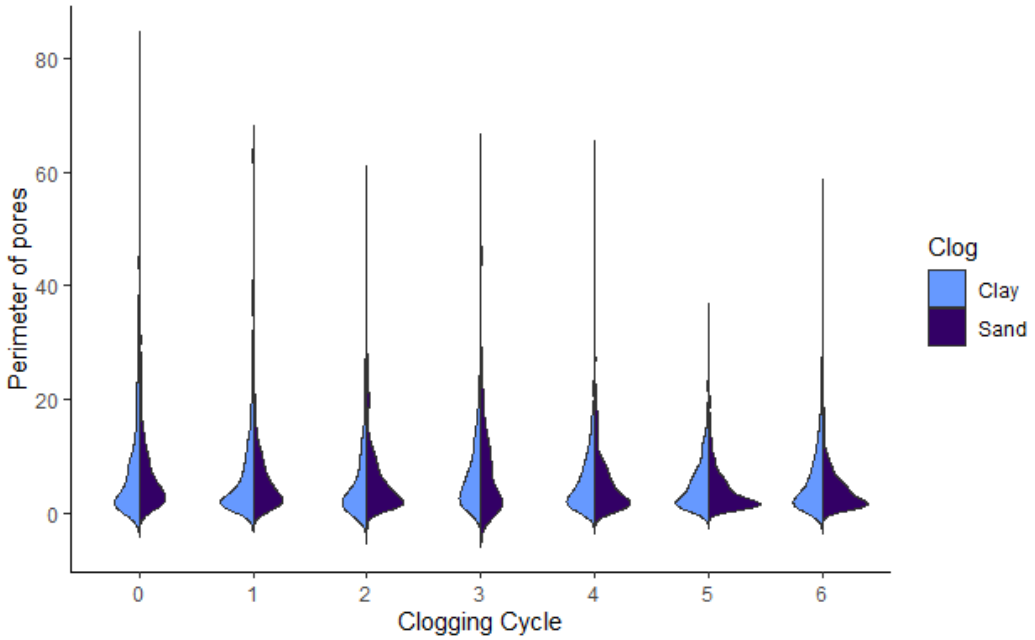

Figure 4.13 Split violin plot of perimeter comparing clay and sand clogging – 2.36 – 4.75mm

Figure 4.14 shows the split violin plot of perimeter of the pores for the gradation of 4.75 – 6.30mm. It compares the clogging due to clay and sand for six cycles of clogging. In the absence of the dimensions of the pores, the calculation of area and perimeter gives a good knowledge about the shape of the pores. The bell curve of both the clogging cycles is unimodal. The largest perimeter is observed in the unclogged pervious concrete specimen. The largest area does not correspond to the largest perimeter. The top surface of the sand clogged surface shows variation in pore perimeter distribution and gradual shift of pore perimeter being close to zero as the clogging cycle continues whereas clay clogging maintains a similar distribution of pore perimeter.

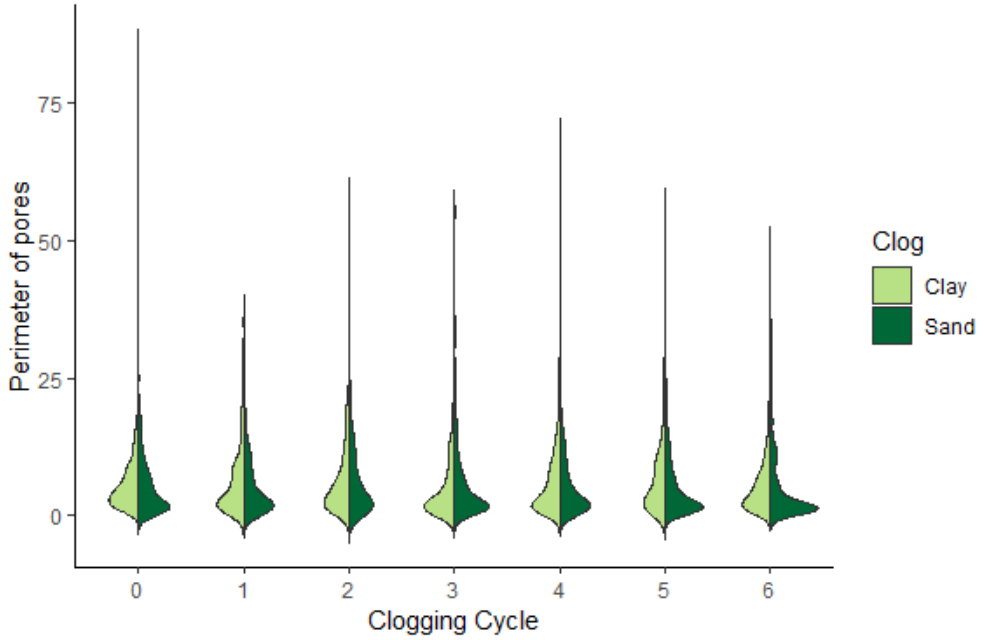

Figure 4.14 Split violin plot of perimeter comparing clay and sand clogging –4.75 – 6.30mm

4.9 ANALYSIS OF ASPECT RATIO OF THE PORES ON THE TOP SURFACE OF PERVIOUS CONCRETE

Aspect ratio can provide information about connectivity and flow characteristics. The higher value of aspect ratio indicates an elongated shape. This type of shape exhibits good connectivity allowing water to flow easily through the pervious concrete matrix. As aspect ratio increases, the permeability of pervious concrete increases. Whereas low aspect ratio resembles more of a spherical or rounded shape. Such pores have limited connectivity and slow down the flow of fluid through the concrete. High percentage of low aspect ratio reduces the drainage efficiency of the concrete.

Table 4.11 tabulates the maximum, minimum, average and standard deviation of the aspect ratio for six cycles of clay and sand clogging for the aggregate gradation of 2.36 – 4.75mm. The minimum value is 1 and the maximum value is 10. There is high variation of maximum value of aspect ratio for clay clogging cycle. The average value varies from 1.98 to 2.15 for clay clogging and varies from 1.92 to

2.30 for sand clogging respectively. The above values indicate that the pores are more elongated. The standard deviation is less than the average value for both the clogging cycles. Pervious concrete with higher percentage of pores with high aspect ratio enhances the connectivity and improves the drainage efficiency. The aspect ratio of pores is influenced by the arrangement and shape of the aggregates within the concrete matrix. Irregular shaped aggregates with different sizes create a complex network with varying aspect ratios.

Table 4.11 Basic statistics of aspect ratio for clay and sand clogging cycles – 2.36-4.75mm

S. No	Cycle	Clogging Material	Max	Min	Average	Std. Dev.
1	0	Clay	7.11	1.04	2.15	0.91
2	1	Clay	6.89	1.00	2.03	0.76
3	2	Clay	10.00	1.09	1.98	0.85
4	3	Clay	5.72	1.03	2.09	0.76
5	4	Clay	4.91	1.04	2.01	0.74
6	5	Clay	5.11	1.01	1.98	0.70
7	6	Clay	7.28	1.04	2.09	0.83
8	0	Sand	6.29	1.03	2.09	0.79
9	1	Sand	6.92	1.00	2.30	0.98
10	2	Sand	7.00	1.06	2.15	0.86
11	3	Sand	7.25	1.02	1.92	0.80
12	4	Sand	6.00	1.00	2.15	0.87
13	5	Sand	5.37	1.00	1.99	0.69
14	6	Sand	6.94	1.05	1.98	0.72

Table 4.12 tabulates the maximum, minimum, average and standard deviation of the aspect ratio for six cycles of clay and sand clogging for aggregate size gradation of 4.75 – 6.30mm. The minimum value is 1 and the maximum value is 8. Compared to the previous case, the maximum value of aspect ratio is less. The average value varies from 1.94 to 2.26 for clay clogging and varies from 1.84 to 2.05 for sand clogging respectively. The above values indicate that the pores are more elongated for clay clogging. The standard deviation is less than the average value for both the clogging cycles. Pervious concrete with higher percentage of pores with high aspect ratio enhances the connectivity and improves the drainage efficiency. The aspect ratio of pores is influenced by the arrangement and shape of the aggregates within the concrete matrix.

Table 4.12 Basic statistics of aspect ratio for clay and sand clogging cycles –4.75-6.30mm

S. No	Cycle	Clogging Material	Max	Min	Average	Std. Dev.
1	0	Clay	6.25	1.04	2.14	0.89
2	1	Clay	7.15	1.04	2.26	1.03
3	2	Clay	8.00	1.04	1.97	0.74
4	3	Clay	5.54	1.03	1.94	0.72
5	4	Clay	6.68	1.02	2.03	0.72
6	5	Clay	7.63	1.03	2.10	0.92
7	6	Clay	7.00	1.03	1.96	0.78
8	0	Sand	5.64	1.05	2.05	0.75
9	1	Sand	8.37	1.00	2.05	0.82
10	2	Sand	5.83	1.01	1.99	0.75
11	3	Sand	4.81	1.03	1.99	0.69
12	4	Sand	4.09	1.00	1.96	0.63
13	5	Sand	6.00	1.04	2.03	0.73
14	6	Sand	4.34	1.00	1.84	0.63

Figure 4.15 shows the split violin plot of aspect ratio of the pores for 2.36 – 4.75mm. It compares the clogging due to clay and sand for six cycles of clogging. The bell curve of both the clogging cycles is unimodal. The bell curve for clay clogging shows similar pattern across all the clogging cycles whereas there is

variation of the shape of the curve for sand clogging cycles. In third and fifth cycle of sand clogging, there is change in the shape of the bell curve. The aspect ratio becomes insignificant when the shape is very elongated.

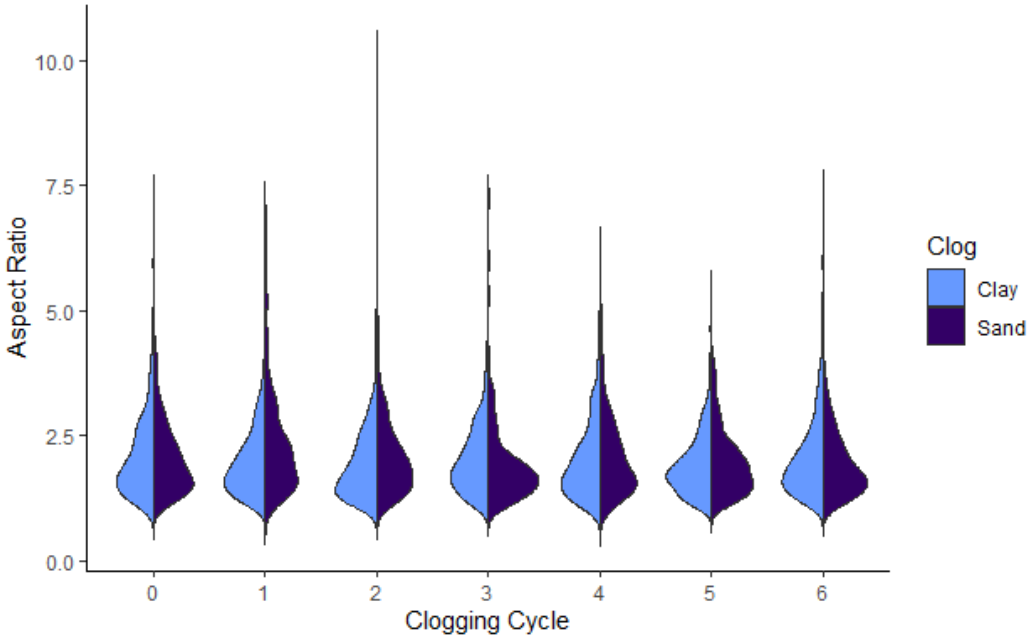

Figure 4.15 Split violin plot of aspect ratio comparing clay and sand clogging – 2.75 – 4.75mm

Figure 4.16 shows the split violin plot of aspect ratio of the pores for 4.75 – 6.30mm. It compares the clogging due to clay and sand for six cycles of clogging. The bell curve of both the clogging cycles is unimodal. The bell curve for clay clogging shows similar pattern across all the clogging cycles except for the third clogging cycle whereas there is variation of the shape of the curve for sand clogging cycles. In the sixth cycle of sand clogging, there is change in the shape of the bell curve indicating weak multi-modality.

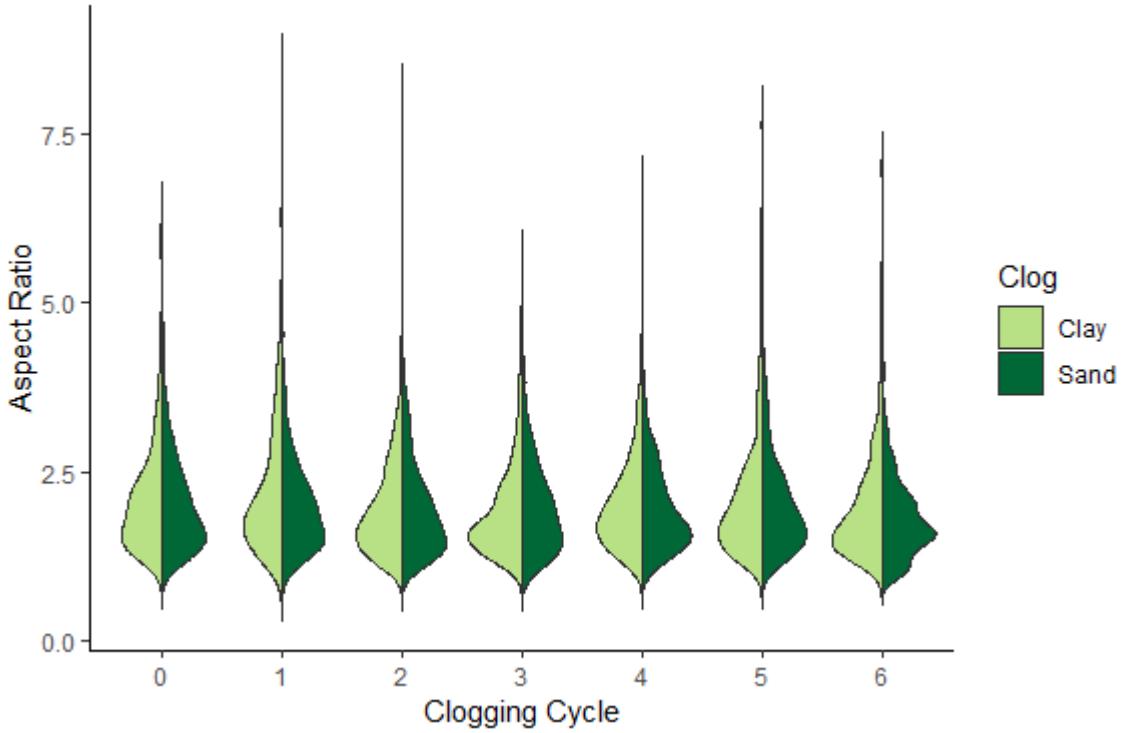

Figure 4.16 Split violin plot of aspect ratio comparing clay and sand clogging – 4.75 – 6.30mm

The below figures gives the distribution of the aspect ratios based on the area and perimeter under the conditions of clay and sand clogging for the aggregate size gradations of 2.36 – 4.75mm and 4.75 – 6.30mm. It is colour coded as per the split violin plots. The graphs provide an insight into the clustering of aspect ratio as progression function of clogging cycles. The outliers can be computed easily through the below scatter plots.

The Figure 4.17 shows the relation between aspect ratio and area for clay clogging for 2.36 – 4.75mm. The aspect ratio shows a random variation along the six clay clogging cycles. The larger area pores are mostly having low aspect ratio. Analysing the region outside the cluster, there is fluctuations in the number of pores and its sizes.

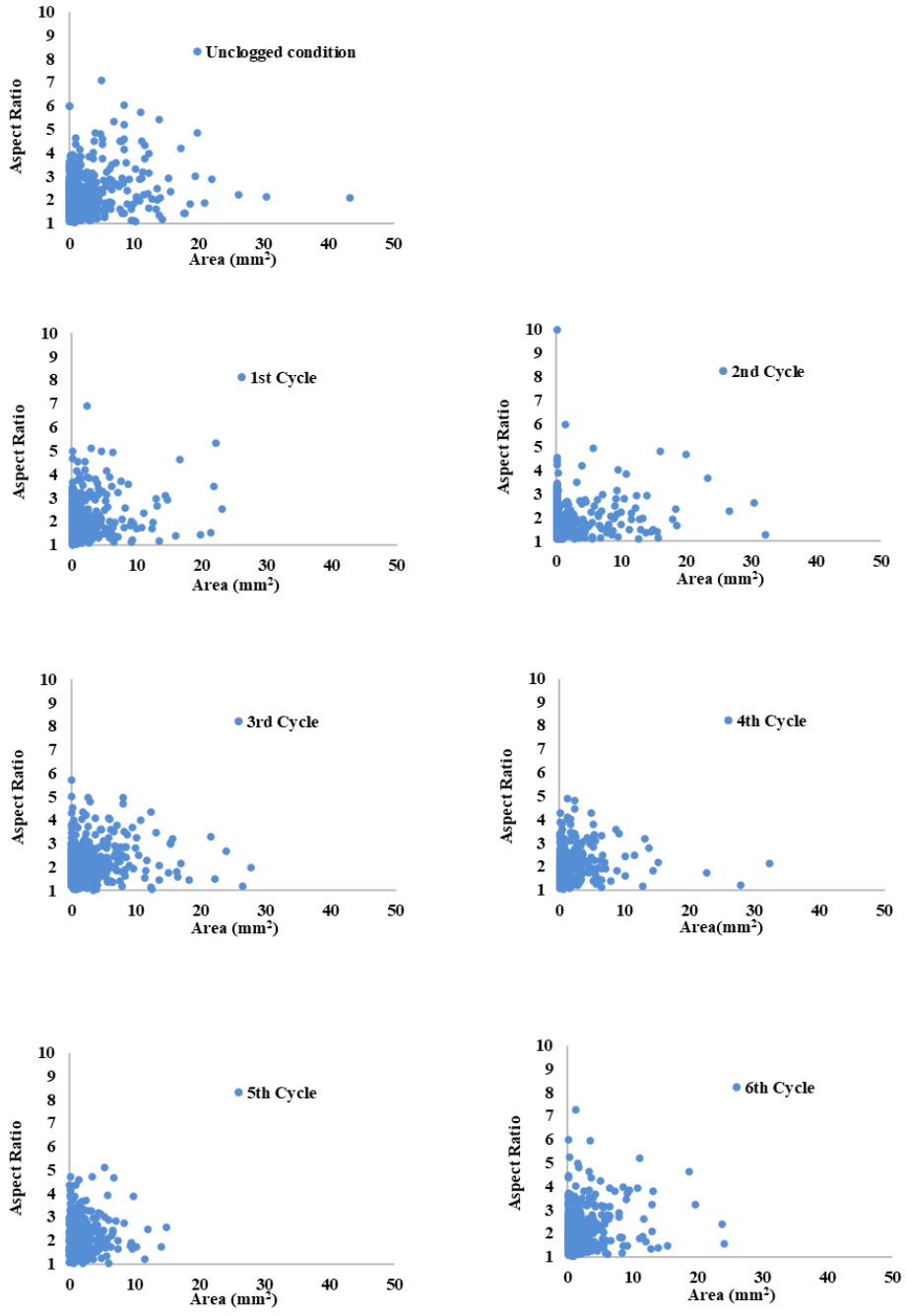

Figure 4.17 Aspect Ratio Vs Area for 2.36-4.75mm - Clay clogging cycles

Figure 4.18 shows the relation between aspect ratio and perimeter for clay clogging for 2.36 – 4.75mm. The aspect ratio is decreasing along the clay clogging cycles with an increase in the sixth clogging cycle. The decrease in aspect ratio is causing an increase in perimeter as per the scatter plot.

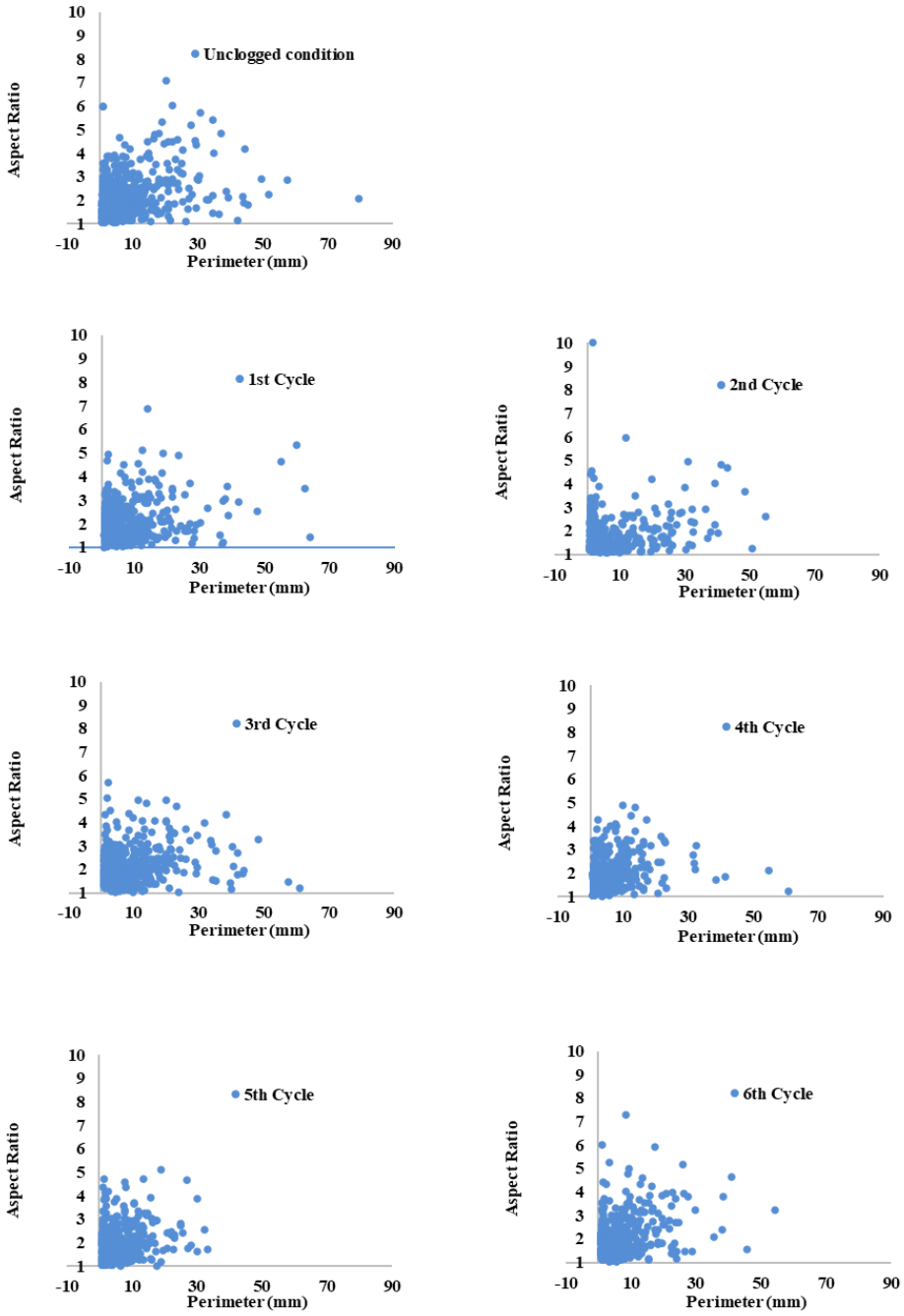

Figure 4.18 Aspect Ratio Vs Perimeter for 2.36-4.75mm - Clay clogging cycles

Figure 4.19 shows the relation between aspect ratio and area for sand clogging for 2.36 – 4.75mm. The third clogging sand cycle shows the max decrease in aspect ratio and area. There is decrease in the value of aspect ratio as the clogging cycle progresses.

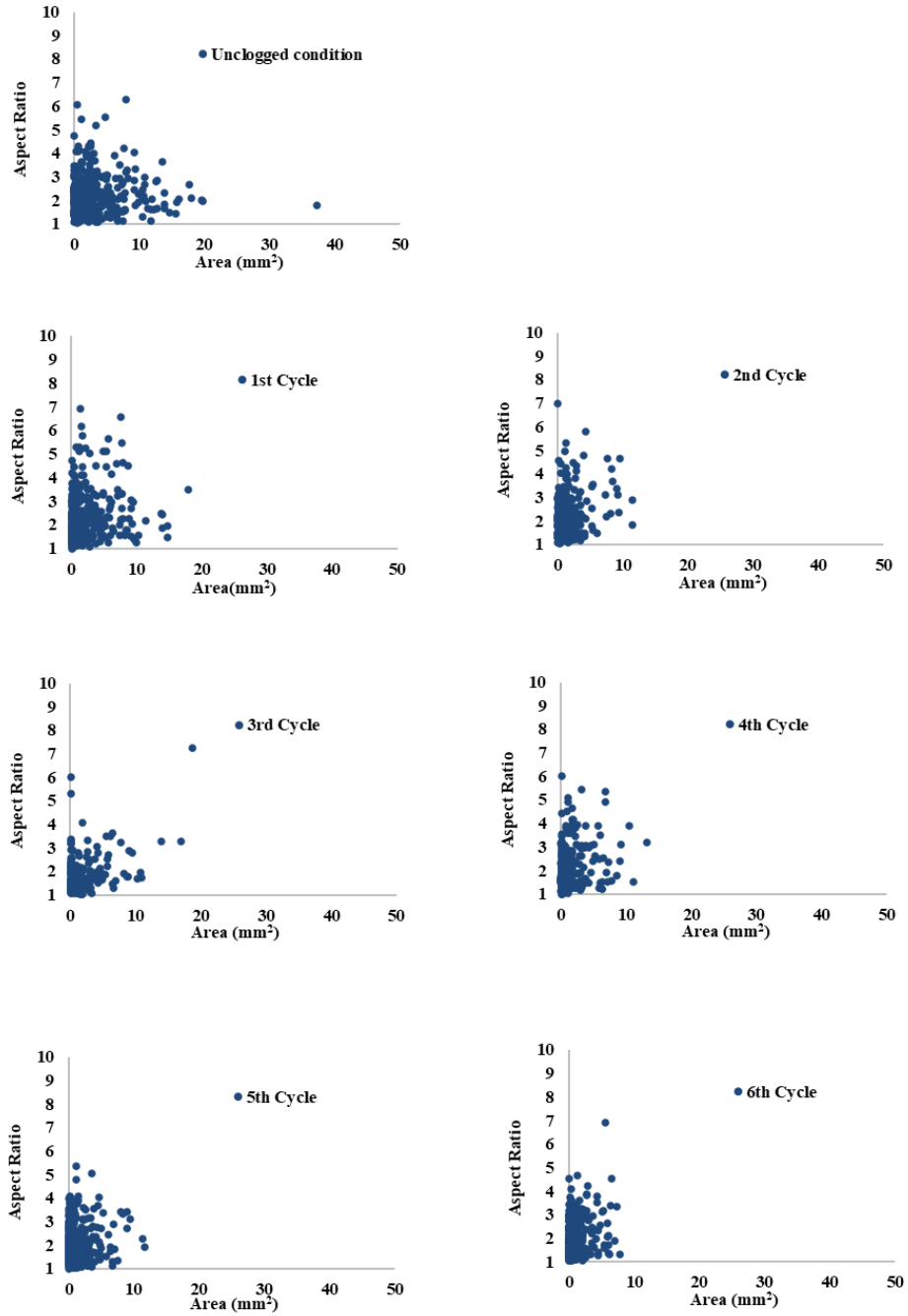

Figure 4.19 Aspect Ratio Vs Area for 2.36-4.75mm - Sand clogging cycles

Figure 4.20 shows the relation between aspect ratio and perimeter for sand clogging for 2.36 – 4.75mm. The perimeter is in the range of 0-10mm^2. In the third clogging cycle, there is lot of pores with similar aspect ratio and perimeter and the pores are not elongated.

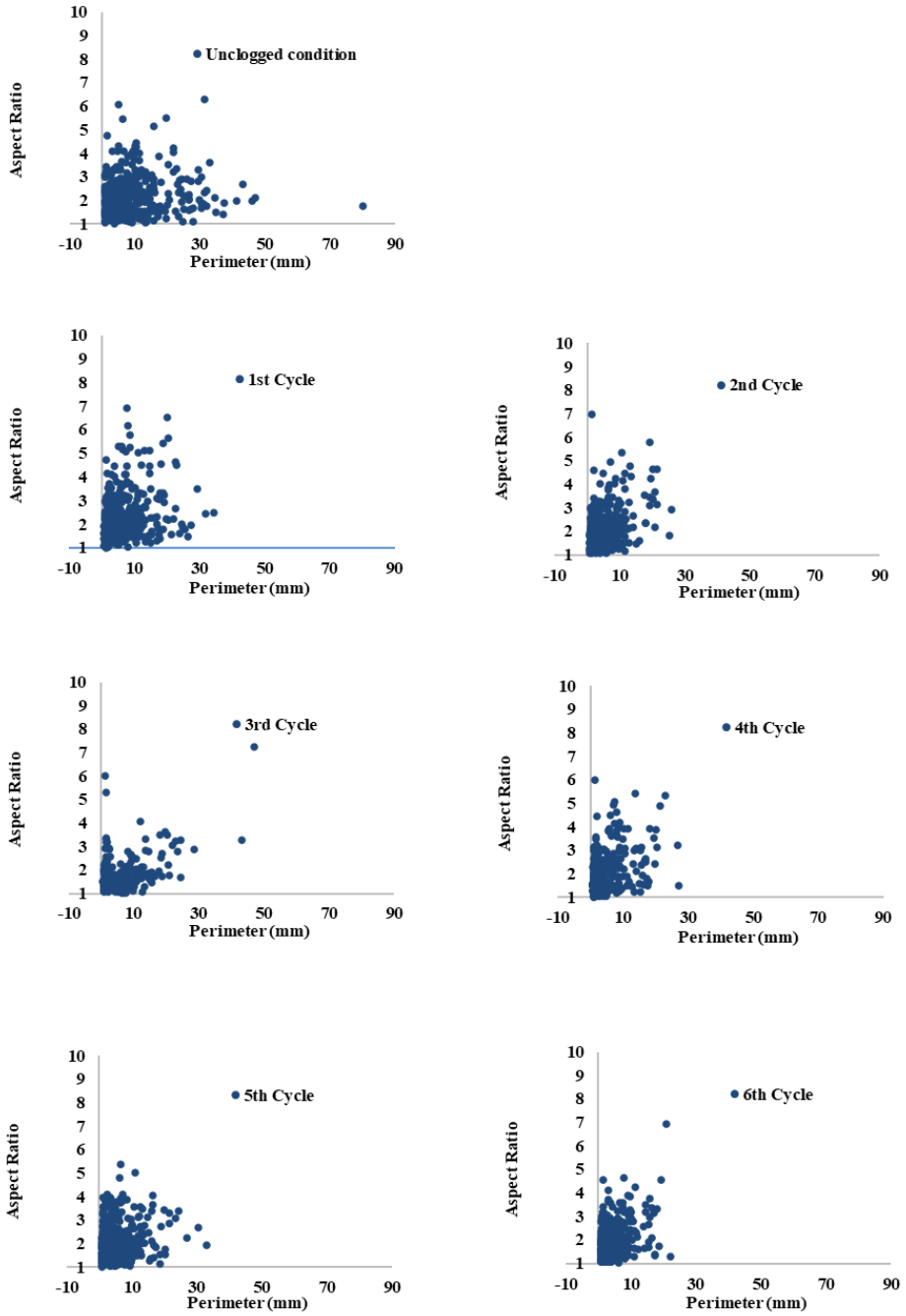

Figure 4.20 Aspect Ratio Vs Perimeter for 2.36-4.75mm - Sand clogging cycles

The Figure 4.21 shows the relation between aspect ratio and area for clay clogging for 4.75 – 6.30mm. In the second, fourth and sixth cycle, there are more number of pores with similar aspect ratio and area with few outliers.

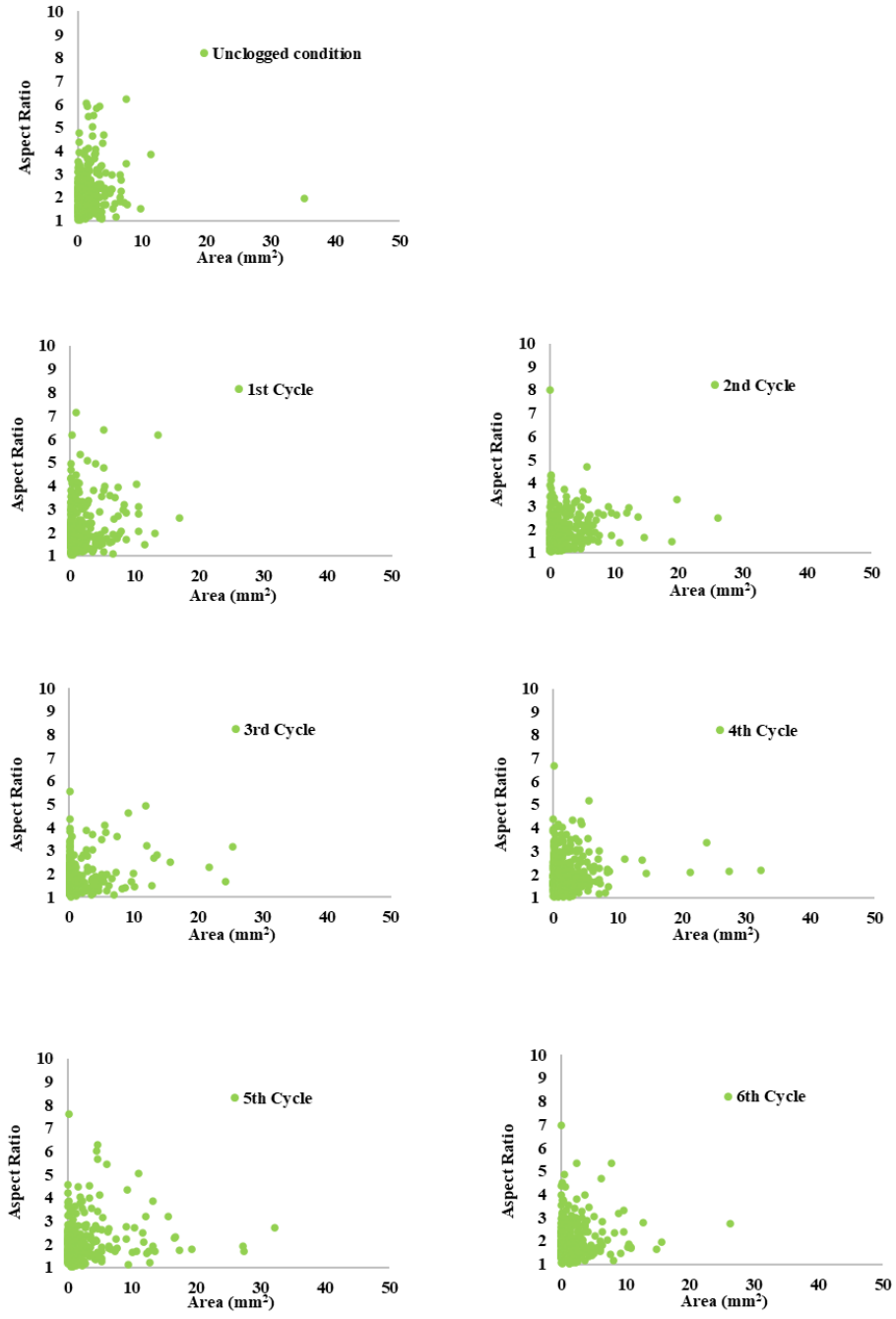

Figure 4.21 Aspect Ratio Vs Area for 4.75-6.30mm – Clay clogging cycles

Figure 4.22 shows the relation between aspect ratio and perimeter for clay clogging for 4.75 – 6.30mm. In the fifth cycle, there is increase in the aspect ratio as well as perimeter which is getting affected by subsequent clogging cycle.

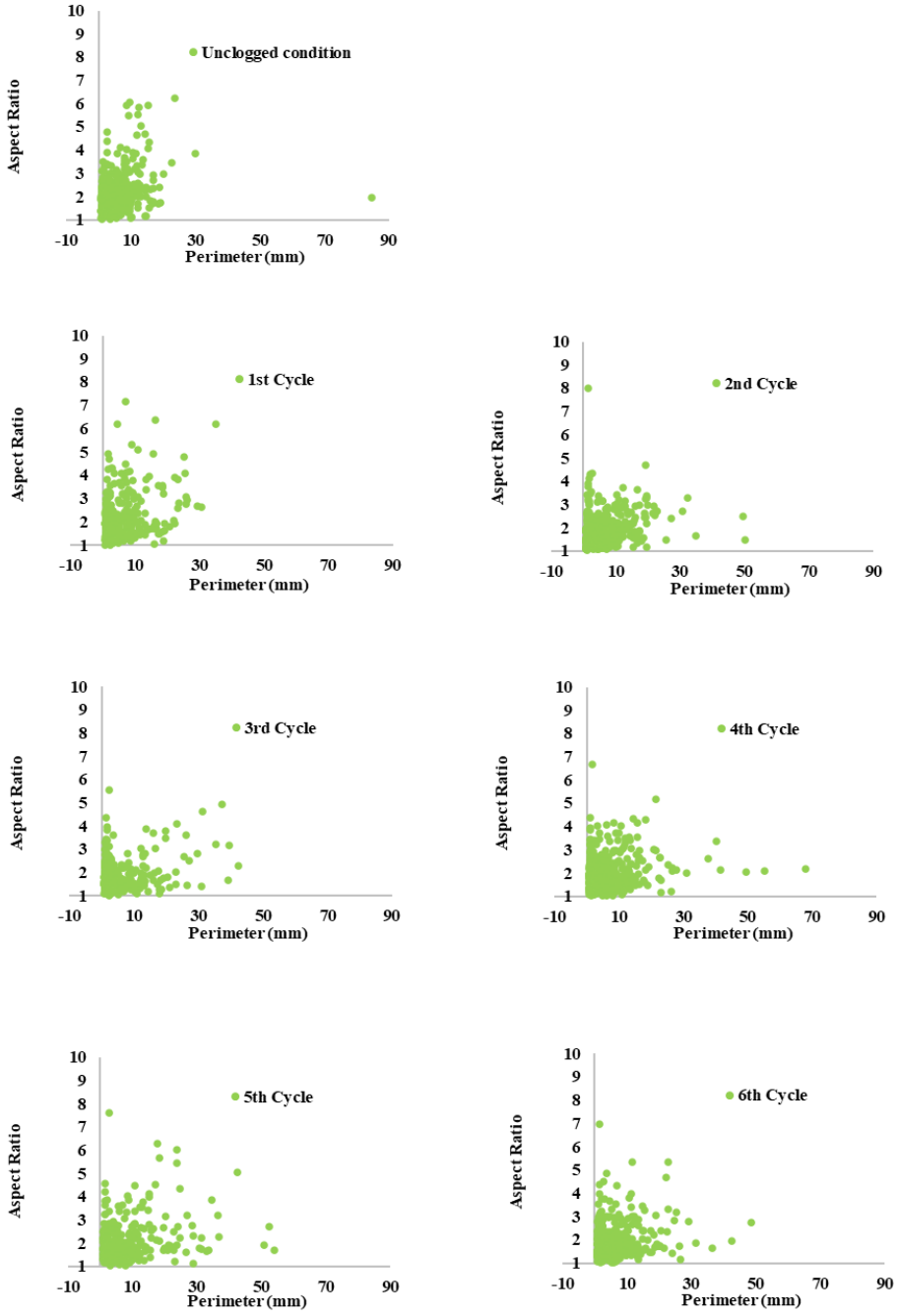

Figure 4.22 Aspect Ratio Vs Perimeter for 4.75-6.30mm – Clay clogging cycles

Figure 4.23 shows the relation between aspect ratio and area for sand clogging for 4.75 – 6.30mm. Sand causes clogging in the first cycle reducing the area and aspect ratio. In the fourth and fifth cycle, there is clogging of large pores.

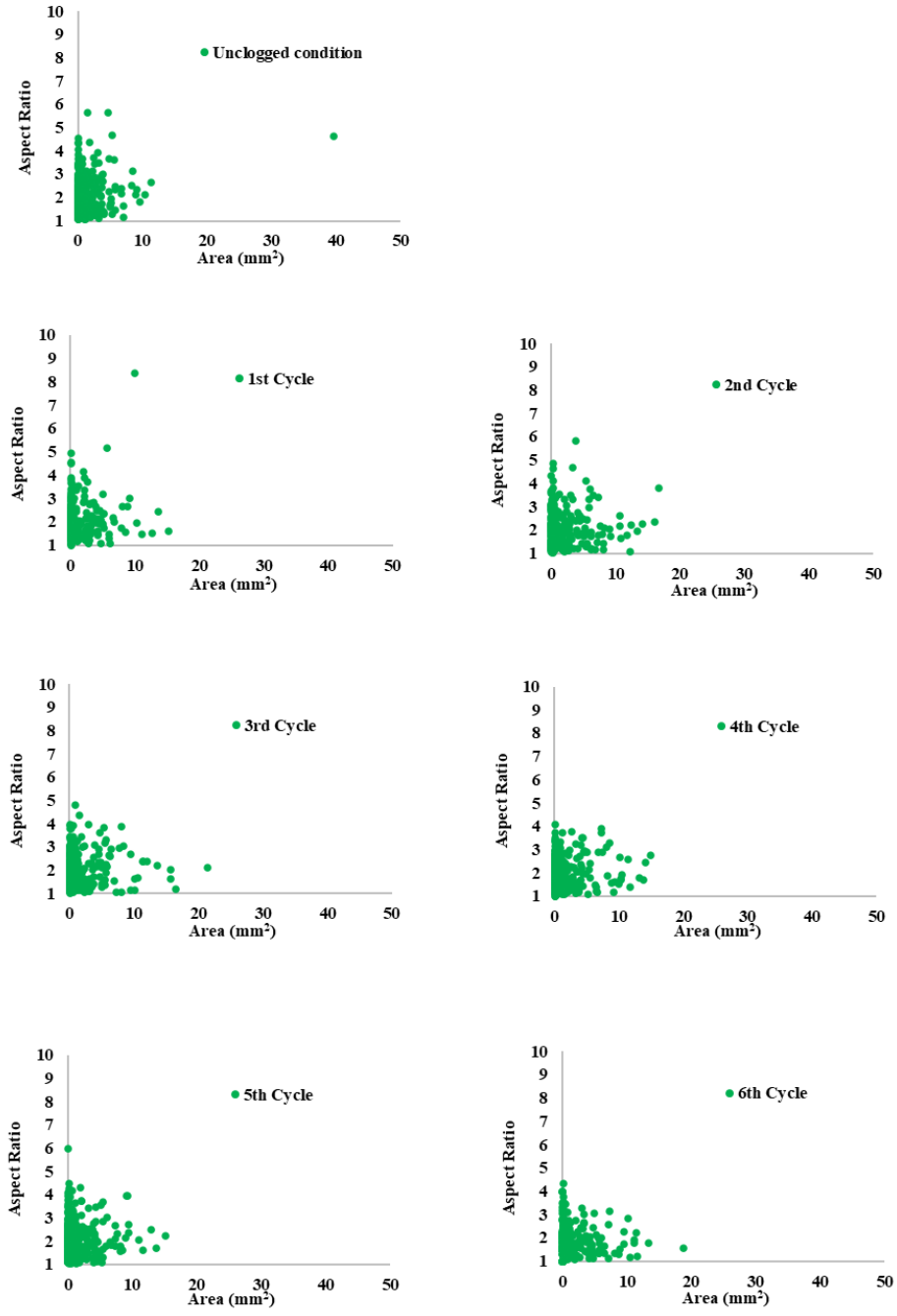

Figure 4.23 Aspect Ratio Vs Area for 4.75-6.30mm – Sand clogging cycles

Figure 4.24 shows the relation between aspect ratio and perimeter for sand clogging for 4.75 – 6.30mm. Similar to the previous series of graphs, sand clogs the pervious concrete in the first cycle itself but in the second cycle unclogs the larger pores. By the sixth cycle, the aspect ratios are less than five creating a less elongated pore.

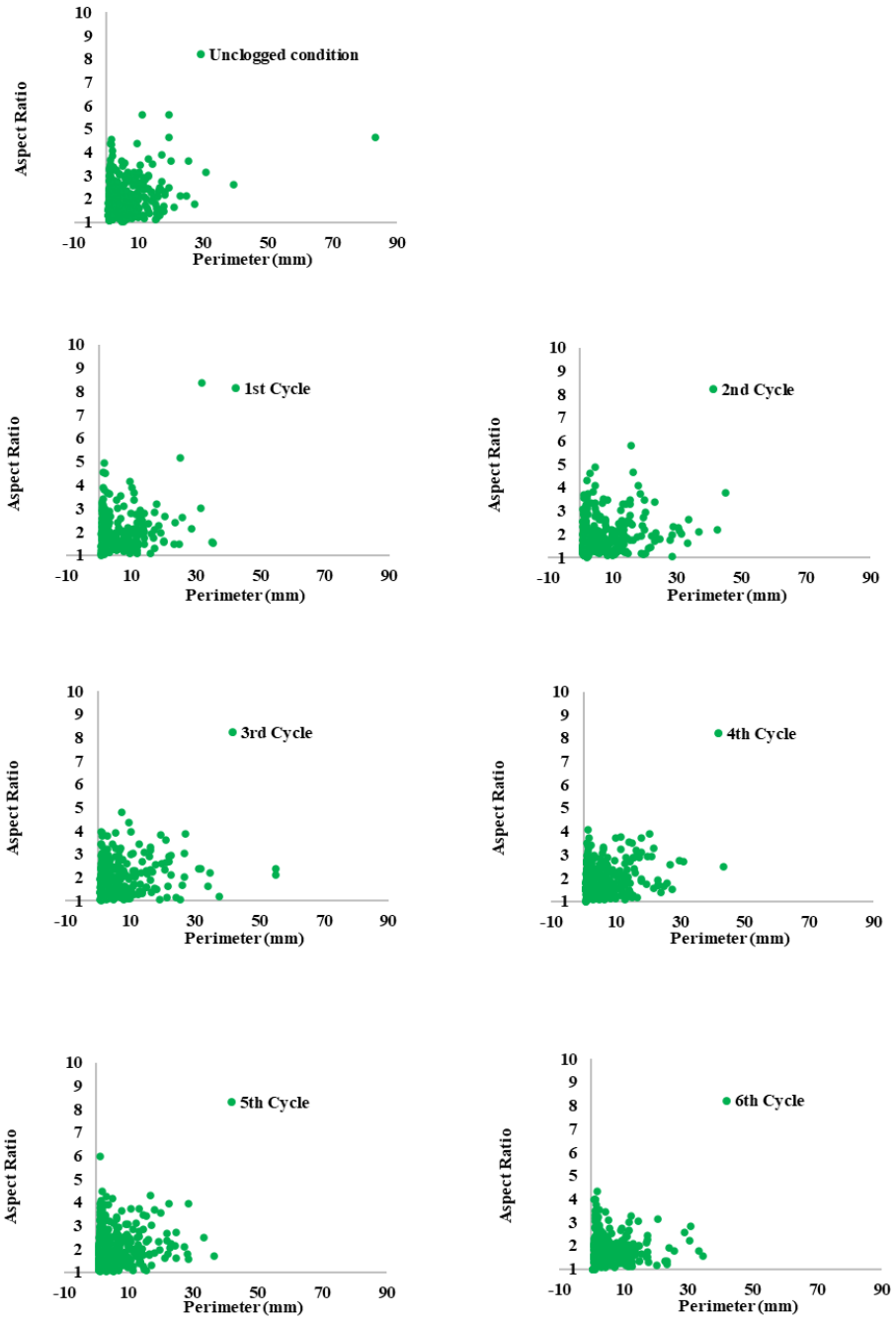

Figure 4.24 Aspect Ratio Vs Perimeter for 4.75-6.30mm – Sand clogging cycles

4.10 ANALYIS OF CIRCULARITY OF PORES ON THE TOP SURFACE OF PERVIOUS CONCRETE

The value of 1 for circularity indicates a perfect circular pore. Circular pore indicates a symmetrical surface and encourages uniform flow. Circular pores have higher permeability and drainage properties. Circularity considers both the particle form and roughness. Non-circular pores cause variation in flow pattern and reduces the permeability of pervious concrete.

Table 4.13 tabulates the maximum, minimum, average and standard deviation of the circularity for six cycles of clay and sand clogging for the aggregate gradation of 2.36 – 4.75mm. The minimum value is 0.06 and the maximum value is 1. The maximum value of all the clogging cycle is 1. The average value of circularity of pores is higher in sand clogging compared to clay clogging. Overall the pores are non circular and reduces the permeability of the top surface.

Table 4.13 Basic statistics of circularity for clay and sand clogging cycles – 2.36 – 4.75mm

S. No	Cycle	Clogging Material	Max	Min	Average	Std. Dev.
1	0	Clay	1.00	0.08	0.48	0.23
2	1	Clay	1.00	0.06	0.40	0.21
3	2	Clay	1.00	0.07	0.41	0.23
4	3	Clay	1.00	0.07	0.40	0.19
5	4	Clay	1.00	0.09	0.47	0.22
6	5	Clay	1.00	0.12	0.47	0.21
7	6	Clay	1.00	0.08	0.48	0.23
8	0	Sand	1.00	0.07	0.48	0.20
9	1	Sand	1.00	0.15	0.58	0.21
10	2	Sand	1.00	0.15	0.53	0.21
11	3	Sand	1.00	0.10	0.49	0.26
12	4	Sand	1.00	0.14	0.55	0.22
13	5	Sand	1.00	0.12	0.57	0.22
14	6	Sand	1.00	0.16	0.58	0.20

Table 4.14 tabulates the maximum, minimum, average and standard deviation of the circularity for six cycles of clay and sand clogging for the aggregate gradation of 4.75 – 6.30mm. The minimum value is 0.06 and the maximum value is 1. The maximum value of all the clogging cycle is 1. The average value of circularity of pores is almost same for all sand clogging and clay clogging cycles. Overall the pores are non-circular and reduces the permeability of the top surface.

Table 4.14 Basic statistics of circularity for clay and sand clogging cycles –4.75 – 6.30mm

S. No	Cycle	Clogging Material	Max	Min	Average	Std. Dev.
1	0	Clay	1.00	0.06	0.48	0.18
2	1	Clay	1.00	0.10	0.45	0.21
3	2	Clay	1.00	0.10	0.47	0.22
4	3	Clay	1.00	0.11	0.50	0.26
5	4	Clay	1.00	0.06	0.46	0.22
6	5	Clay	1.00	0.08	0.42	0.19
7	6	Clay	1.00	0.11	0.48	0.22
8	0	Sand	1.00	0.07	0.48	0.23
9	1	Sand	1.00	0.10	0.46	0.21
10	2	Sand	1.00	0.08	0.41	0.22
11	3	Sand	1.00	0.05	0.47	0.23
12	4	Sand	1.00	0.09	0.52	0.24
13	5	Sand	1.00	0.08	0.51	0.24
14	6	Sand	1.00	0.11	0.64	0.27

Figure 4.25 shows the split violin plot of circularity of the pores for aggregate gradation of 2.36 – 4.75mm. It compares the clogging due to clay and sand for six cycles of clogging. The bell curves show a distinctive peak for clay clogging whereas for sand clogging the values are more distributed and not unimodal. More circular pores are observed in sand clogging. The pattern of circularity is different for clay and sand clogging across all cycles. The higher values of circularity is observed in smaller areas of the pores.

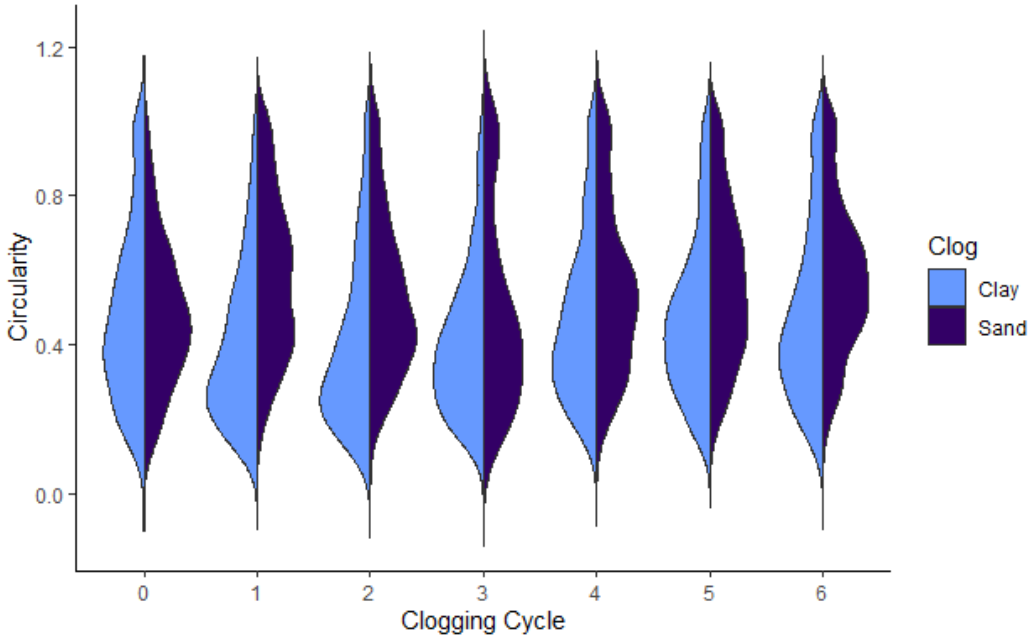

Figure 4.25 Split violin plot of circularity comparing clay and sand clogging – 2.36-4.75mm

Figure 4.26 shows the split violin plot of circularity of the pores for aggregate gradation of 4.75 – 6.30mm. It compares the clogging due to clay and sand for six cycles of clogging. The bell curve comparison shows difference in the distribution of circularity for both the cases. In the sixth clogging cycle of sand, there is increase in circular pores. It also shows multi-modality. The pattern of circularity is different for clay and sand clogging across all cycles.

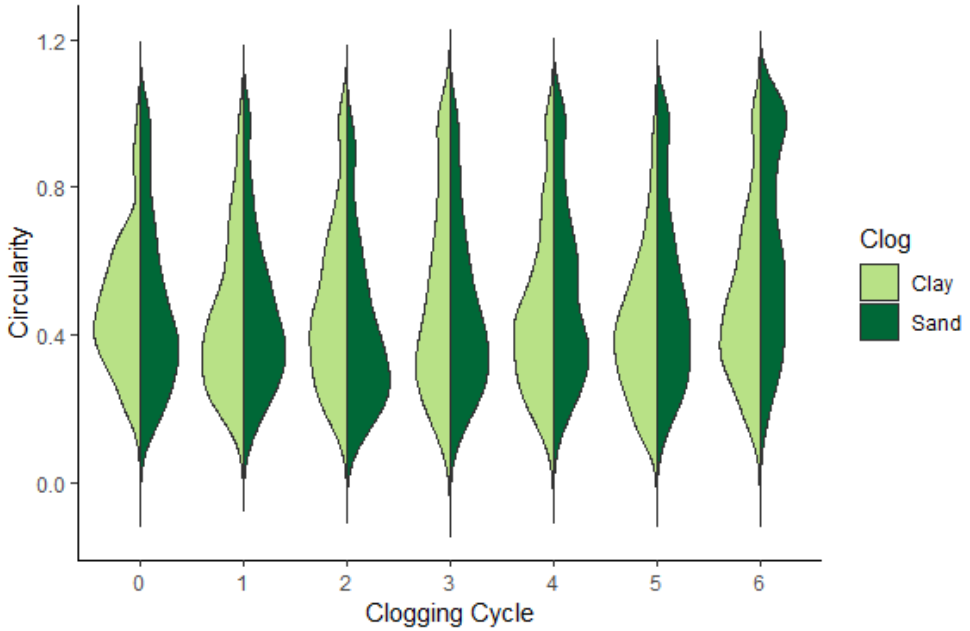

Figure 4.26 Split violin plot of circularity comparing clay and sand clogging – 4.75-6.30mm

The below figures give the distribution of the circularity based on the area and perimeter under the conditions of clay and sand clogging for the aggregate size gradations of 2.36 – 4.75mm and 4.75 – 6.30mm. It is colour coded as per the split violin plots. The graphs give an insight into the clustering of circularity through the progression of clogging cycles. The outliers can be computed easily through the below scatter plots.

The Figure 4.27 shows the relation between circularity and area for clay clogging for 2.36 – 4.75mm, Figure 4.28 shows the relation between circularity and perimeter for clay clogging for 2.36 – 4.75mm, Figure 4.29 shows the relation between circularity and area for sand clogging for 2.36 – 4.75mm, Figure 4.30 shows the relation between circularity and perimeter for sand clogging for 2.36 – 4.75mm. The below four figures are graph showing the change of circularity as the clogging cycle progresses. The circularity has an exponential **trend** with both area and perimeter. In the second clay clogging cycle, the circularity values are reduced indicating the deviation from circular shapes.

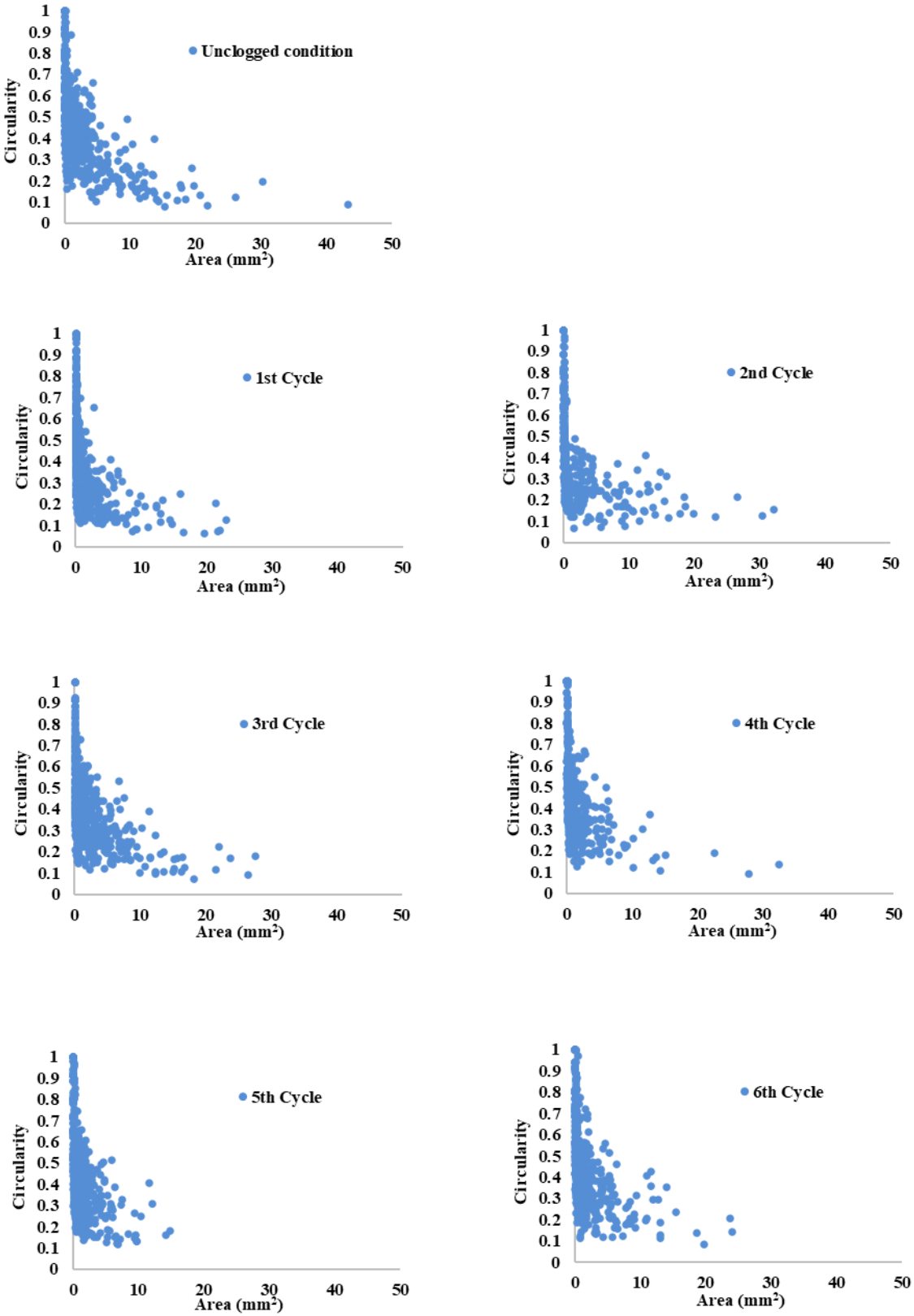

Figure 4.27 Circularity Vs Area for 2.36-4.75mm - Clay clogging cycles

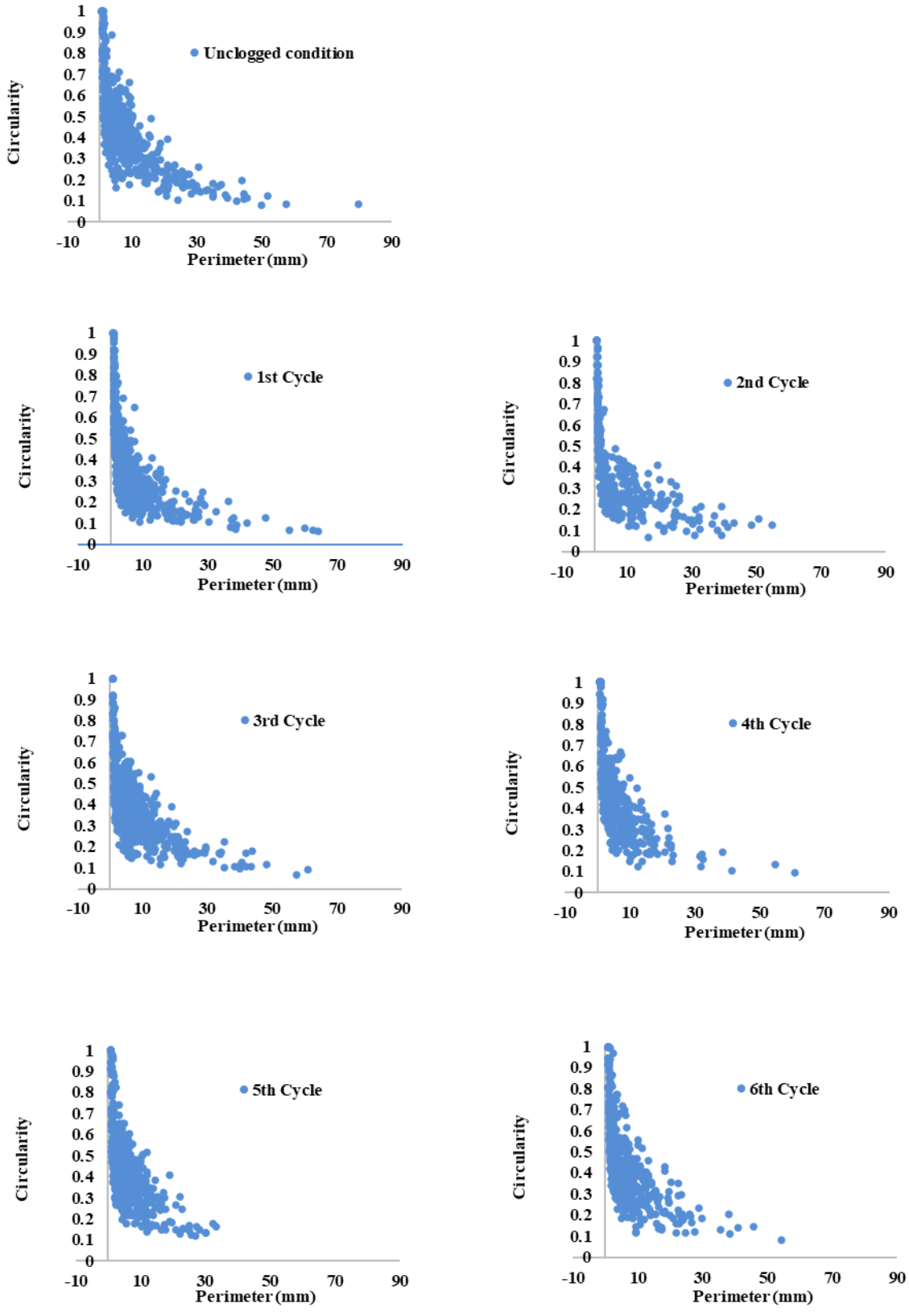

Figure 4.28 Circularity Vs Perimeter for 2.36-4.75mm - Clay clogging cycles

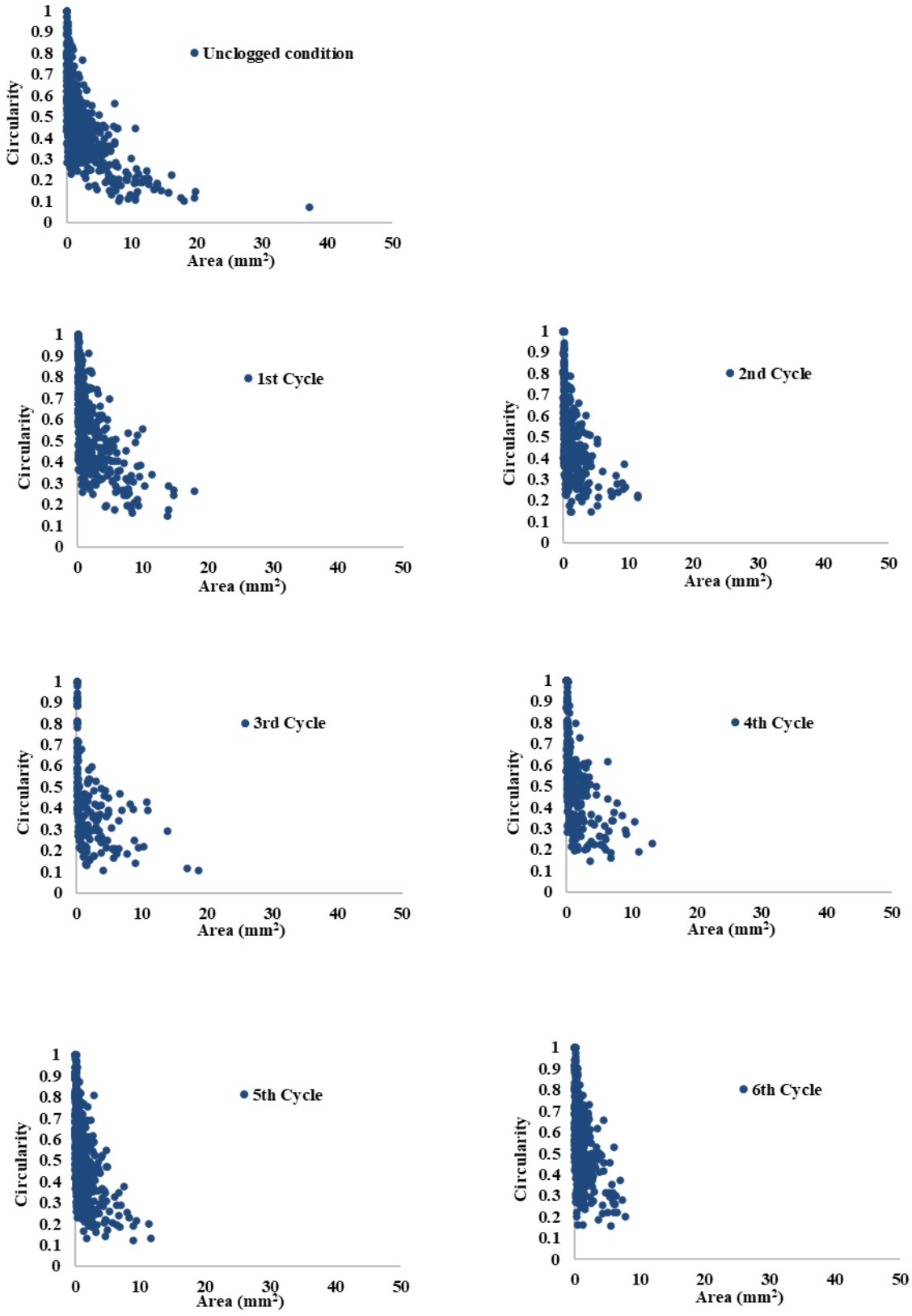

Figure 4.29 Circularity Vs Area for 2.36-4.75mm - Sand clogging cycles

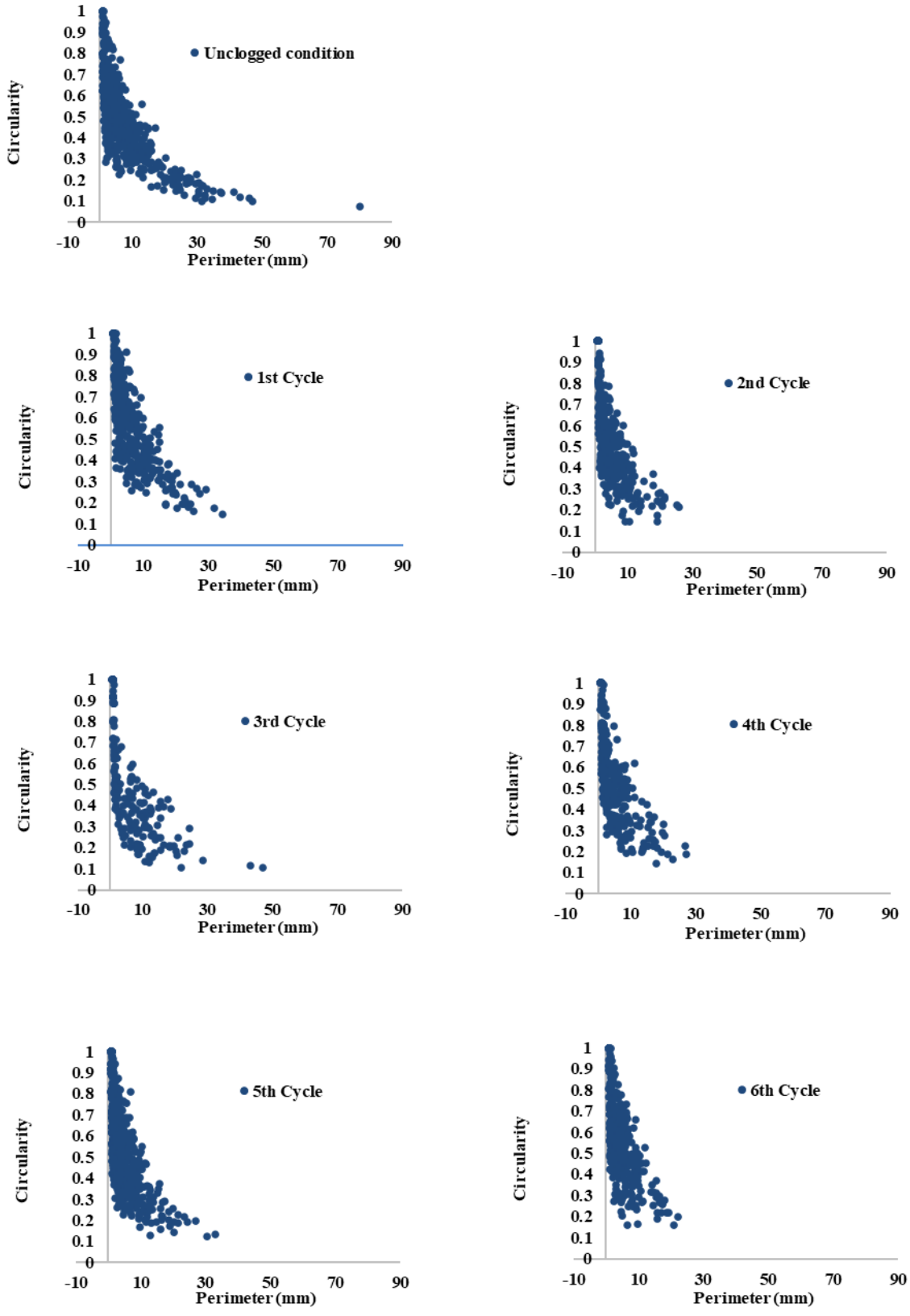

Figure 4.30 Circularity Vs Perimeter for 2.36-4.75mm - Sand clogging cycles

The Figure 4.31 shows the relation between circularity and area for clay clogging for 4.75 – 6.30mm, Figure 4.32 shows the relation between circularity and perimeter for clay clogging for 4.75 – 6.30mm, Figure 4.33 shows the relation between circularity and area for sand clogging for 4.75 – 6.30mm, Figure 4.34 shows the relation between circularity and perimeter for sand clogging for 4.75 – 6.30mm. The series of graph shows an exponential **trend** with area and perimeter. It is asymptotic to y-axis confirming that lot of pores have area and perimeter close to zero with varying circularity. There is dispersion in the area and perimeter as the clogging cycle progresses for both clay and sand clogging.

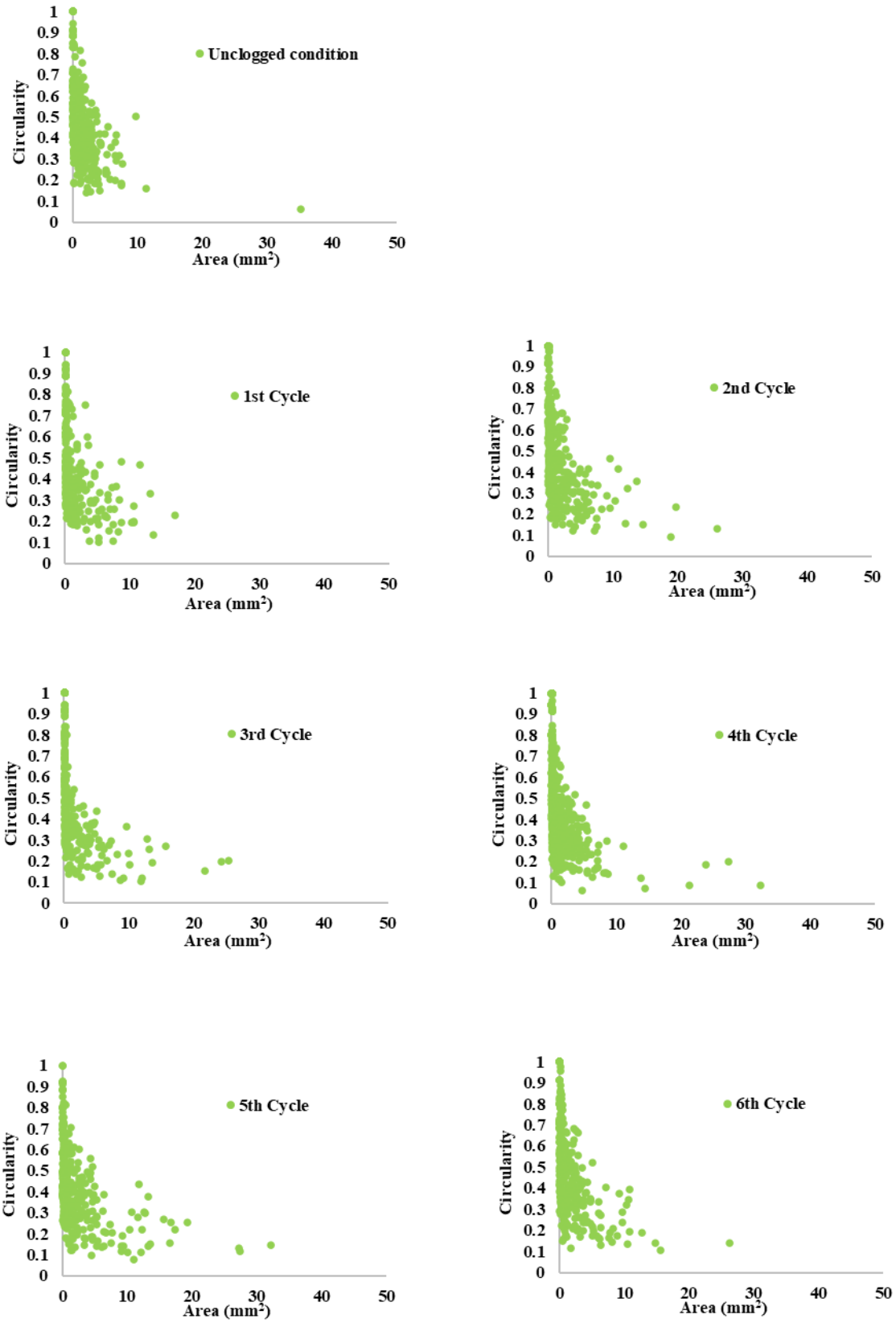

Figure 4.31 Circularity Vs Area for 4.75-6.30mm - Clay clogging cycles

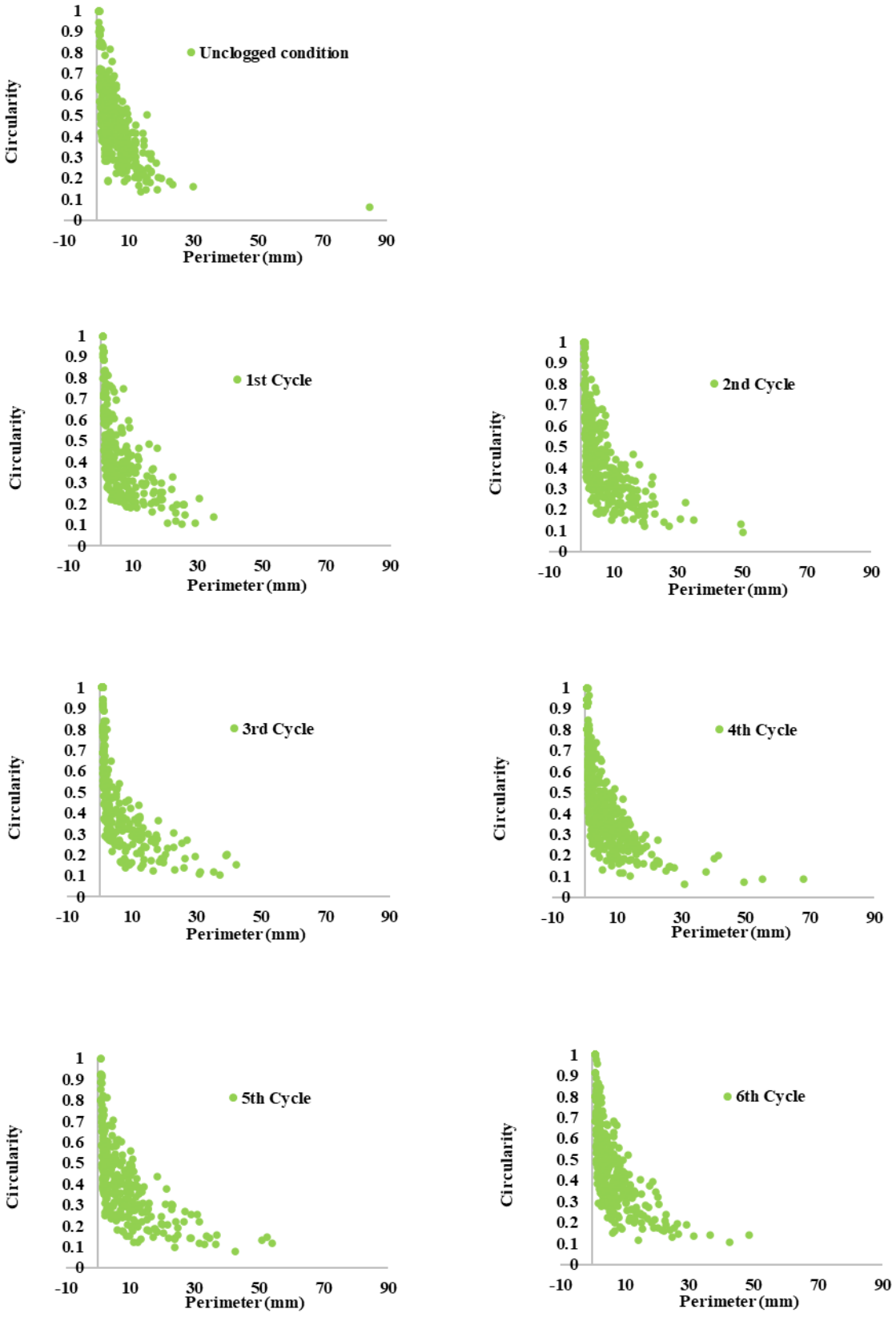

Figure 4.32 Circularity Vs Perimeter for 4.75-6.30mm - Clay clogging cycles

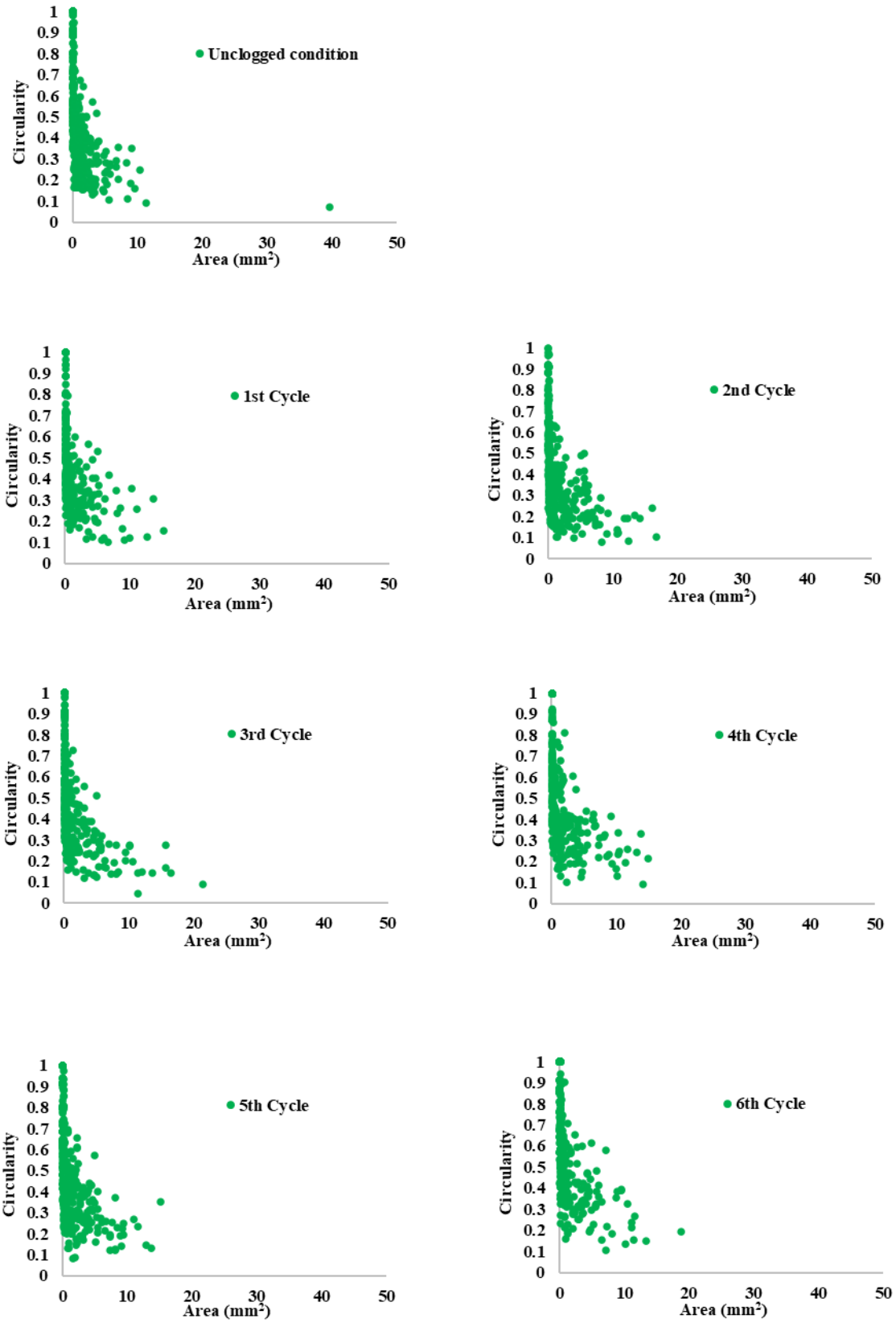

Figure 4.33 Circularity Vs Area for 4.75-6.30mm - Sand clogging cycles

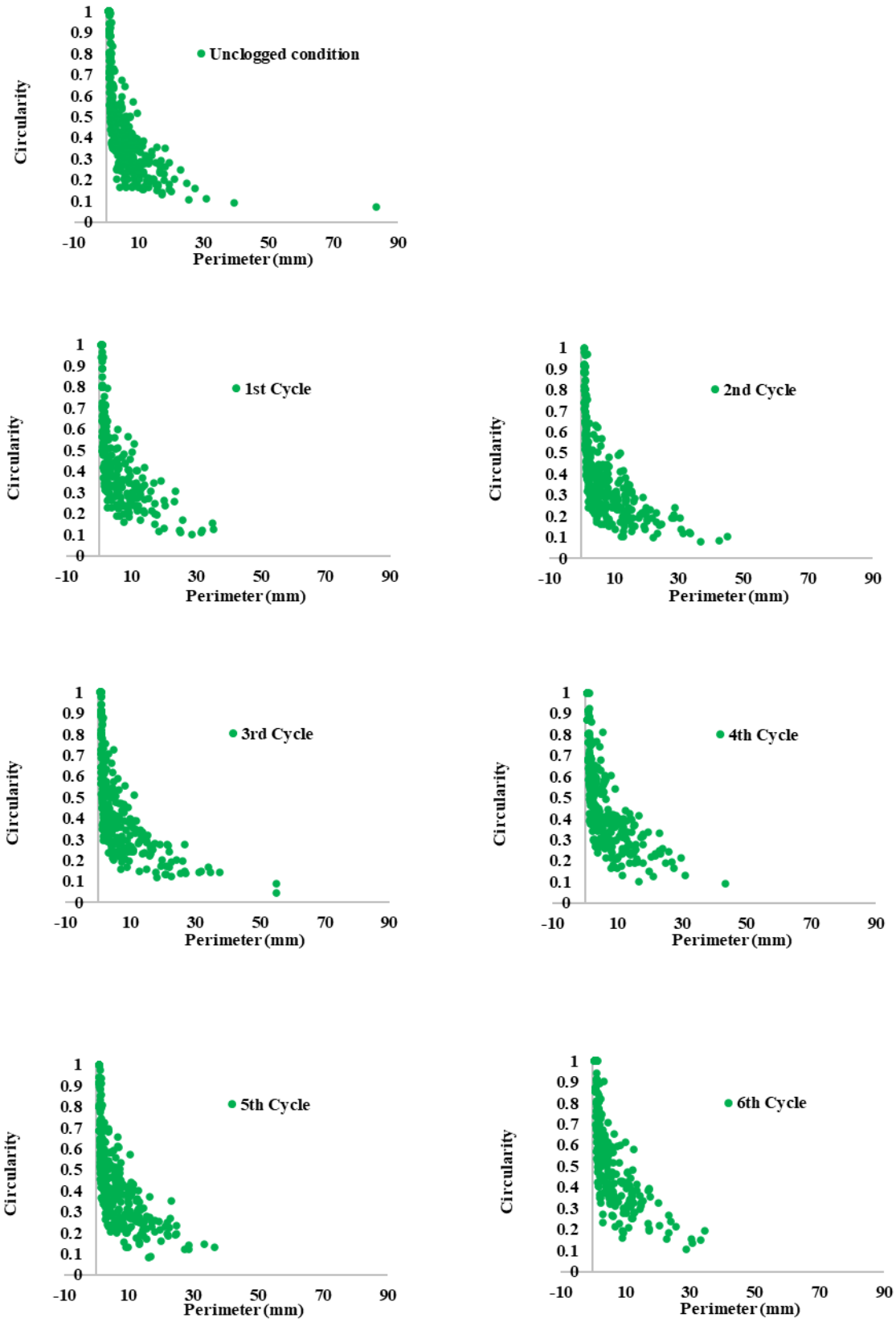

Figure 4.34 Circularity Vs Perimeter for 4.75-6.30mm - Sand clogging cycles

4.11 ANALYSIS OF ROUNDNESS OF PORES ON THE TOP SURFACE OF PERVIOUS CONCRETE

Roundness is similar to circularity, however it does not consider undulations of the pore perimeter. The major axis of best fit ellipse is considered for calculating roundness. Table 4.15 tabulates the maximum, minimum, average and standard deviation of the roundness for six cycles of clay and sand clogging for the aggregate gradation of 2.36 – 4.75mm. The minimum value is 0.1 and the maximum value is 1. The average value and standard deviation of roundness is approximately equal to 0.53 and 0.17 respectively across all the clogging cycles.

Table 4.15 Basic statistics of roundness for clay and sand clogging cycles – 2.36 – 4.75mm

S. No	Cycle	Clogging Material	Max	Min	Average	Std. Dev.
1	0	Clay	0.96	0.14	0.53	0.18
2	1	Clay	1.00	0.15	0.55	0.17
3	2	Clay	0.92	0.10	0.57	0.18
4	3	Clay	0.97	0.18	0.54	0.17
5	4	Clay	0.96	0.20	0.56	0.18
6	5	Clay	0.99	0.20	0.56	0.17
7	6	Clay	0.96	0.14	0.54	0.17
8	0	Sand	0.97	0.16	0.54	0.17
9	1	Sand	1.00	0.15	0.50	0.18
10	2	Sand	0.95	0.14	0.53	0.17
11	3	Sand	0.98	0.14	0.58	0.17
12	4	Sand	1.00	0.17	0.53	0.18
13	5	Sand	1.00	0.19	0.56	0.17

14	6	Sand	0.95	0.14	0.56	0.17

Table 4.16 tabulates the maximum, minimum, average and standard deviation of the roundness for six cycles of clay and sand clogging for the aggregate gradation of 4.75 – 6.30mm. The minimum value is 0.12 and the maximum value is 1. The average value and standard deviation of roundness across the clogging cycles show less deviation.

Table 4.16 Basic statistics of roundness for clay and sand clogging cycles – 4.75-6.30mm

S. No	Cycle	Clogging Material	Max	Min	Average	Std. Dev.
1	0	Clay	0.96	0.16	0.53	0.17
2	1	Clay	0.97	0.14	0.52	0.18
3	2	Clay	0.97	0.13	0.57	0.17
4	3	Clay	0.97	0.18	0.57	0.17
5	4	Clay	0.98	0.15	0.54	0.16
6	5	Clay	0.97	0.13	0.54	0.17
7	6	Clay	0.97	0.14	0.57	0.17
8	0	Sand	0.95	0.18	0.54	0.17
9	1	Sand	1.00	0.12	0.55	0.17
10	2	Sand	0.99	0.17	0.56	0.18
11	3	Sand	0.97	0.21	0.56	0.18
12	4	Sand	1.00	0.25	0.56	0.16
13	5	Sand	0.97	0.17	0.55	0.17
14	6	Sand	1.00	0.23	0.60	0.19

Figure 4.35 and Figure 4.36 shows the split violin plot of roundness of the pores for the aggregate gradation of 2.36 - 4.75mm and 4.75 – 6.30mm respectively. It compares the clogging due to clay and sand for six cycles of clogging. Similar to circularity, the roundness value indicates that the pores are not circular. The difference in pattern of circularity and roundness indicates that there are undulations along the perimeter of the pores. The pattern of roundness shows variation for sand clogging cycles for both aggregate gradations.

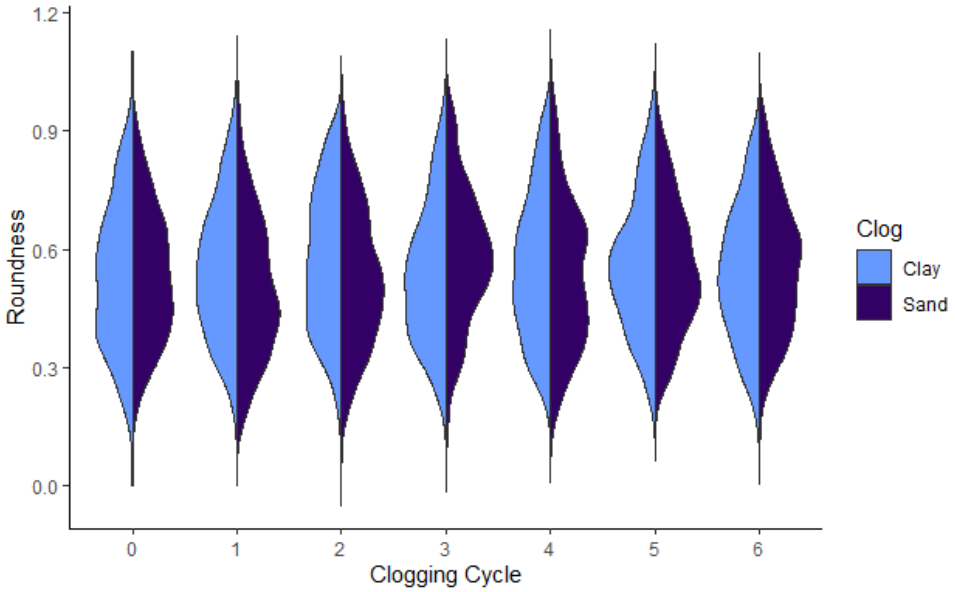

Figure 4.35 Split violin plot of roundness comparing clay and sand clogging – 2.36-4.75mm

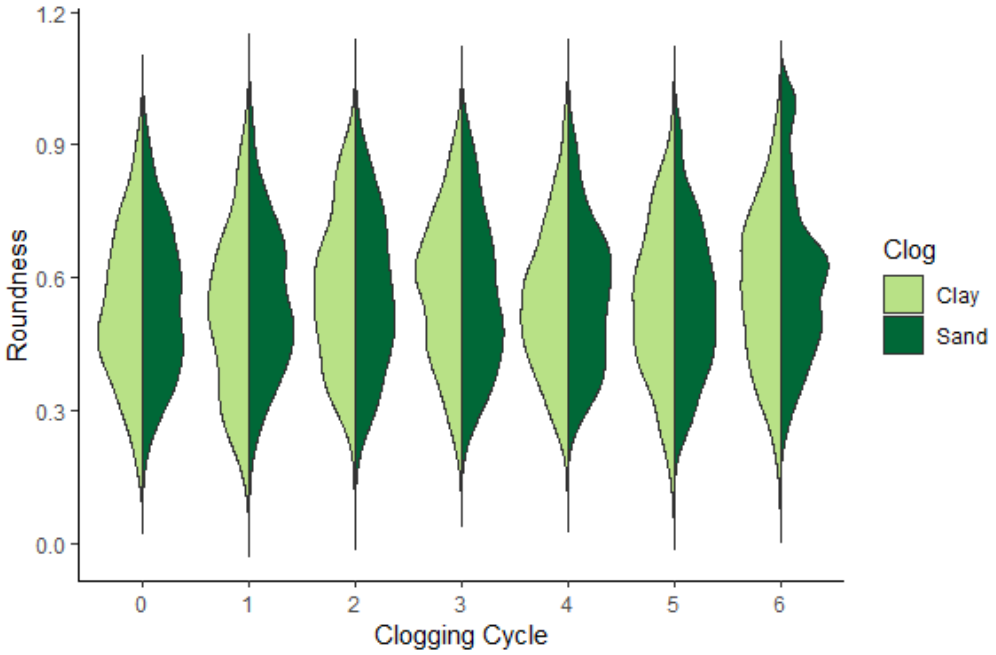

Figure 4.36 Split violin plot of roundness comparing clay and sand clogging – 4.75 – 6.30mm

The below figures give the distribution of the roundness based on the area and perimeter under the conditions of clay and sand clogging for the aggregate size gradations of 2.36 – 4.75mm and 4.75 – 6.30mm. It is colour coded as per the split violin plots. The graphs give an insight into the clustering of roundness through the progression of clogging cycles. The outliers can be computed easily through the below scatter plots.

The Figure 4.37 shows the relation between roundness and area for clay clogging for 2.36 – 4.75mm, Figure 4.38 shows the relation between roundness and perimeter for clay clogging for 2.36 – 4.75mm, Figure 4.39 shows the relation between roundness and area for sand clogging for 2.36 – 4.75mm, Figure 4.40 shows the relation between roundness and perimeter for sand clogging for 2.36 – 4.75mm. The values of roundness ranges from 0.2 to 1. There is more dispersion or scattering of roundness values with perimeter compared to area. The second and sixth sand clogging cycle shows lesser scattering. The top surface has clogged maximum at these two cycles.

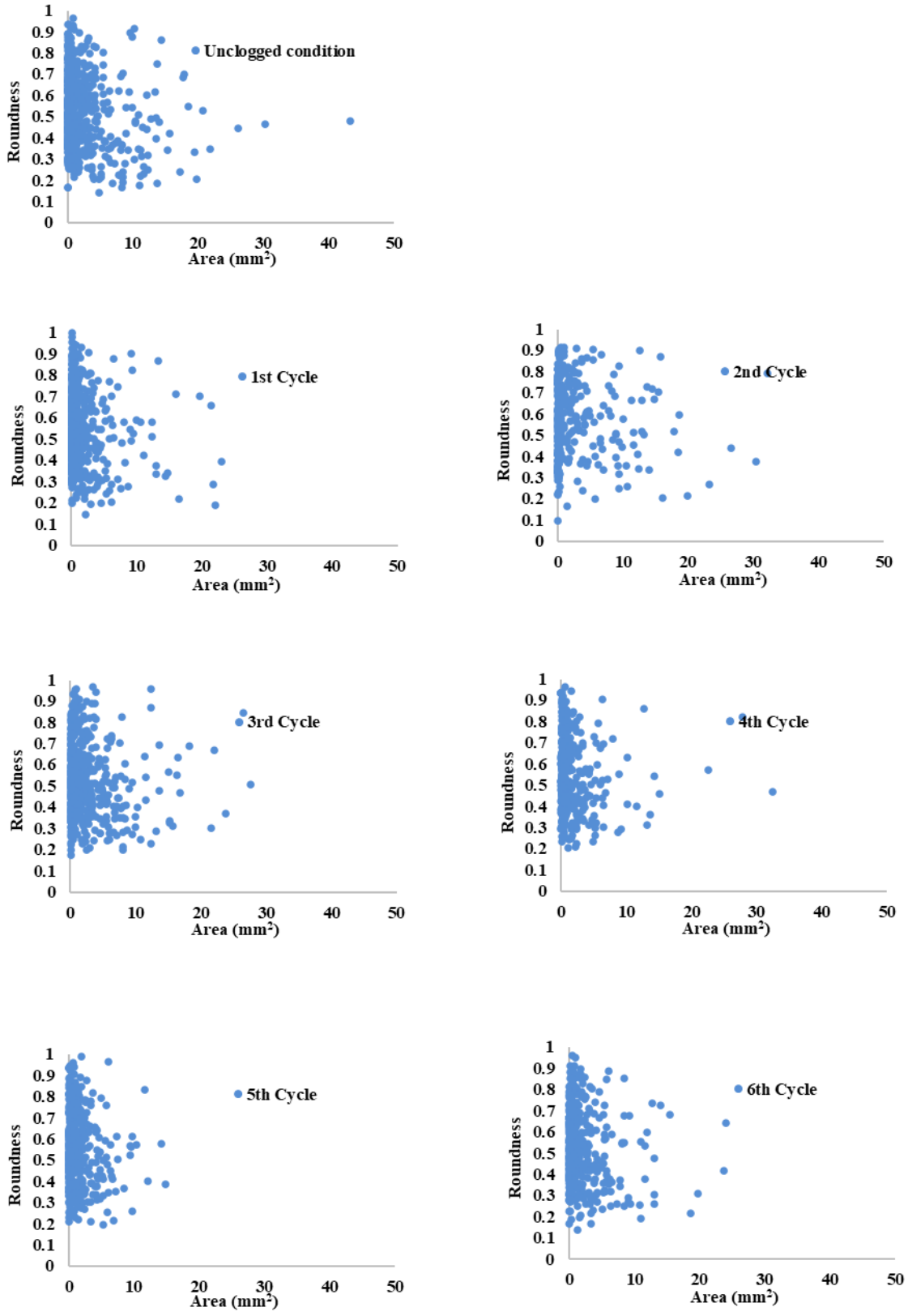

Figure 4.37 Roundness Vs Area for 2.36 - 4.75mm - Clay clogging cycles

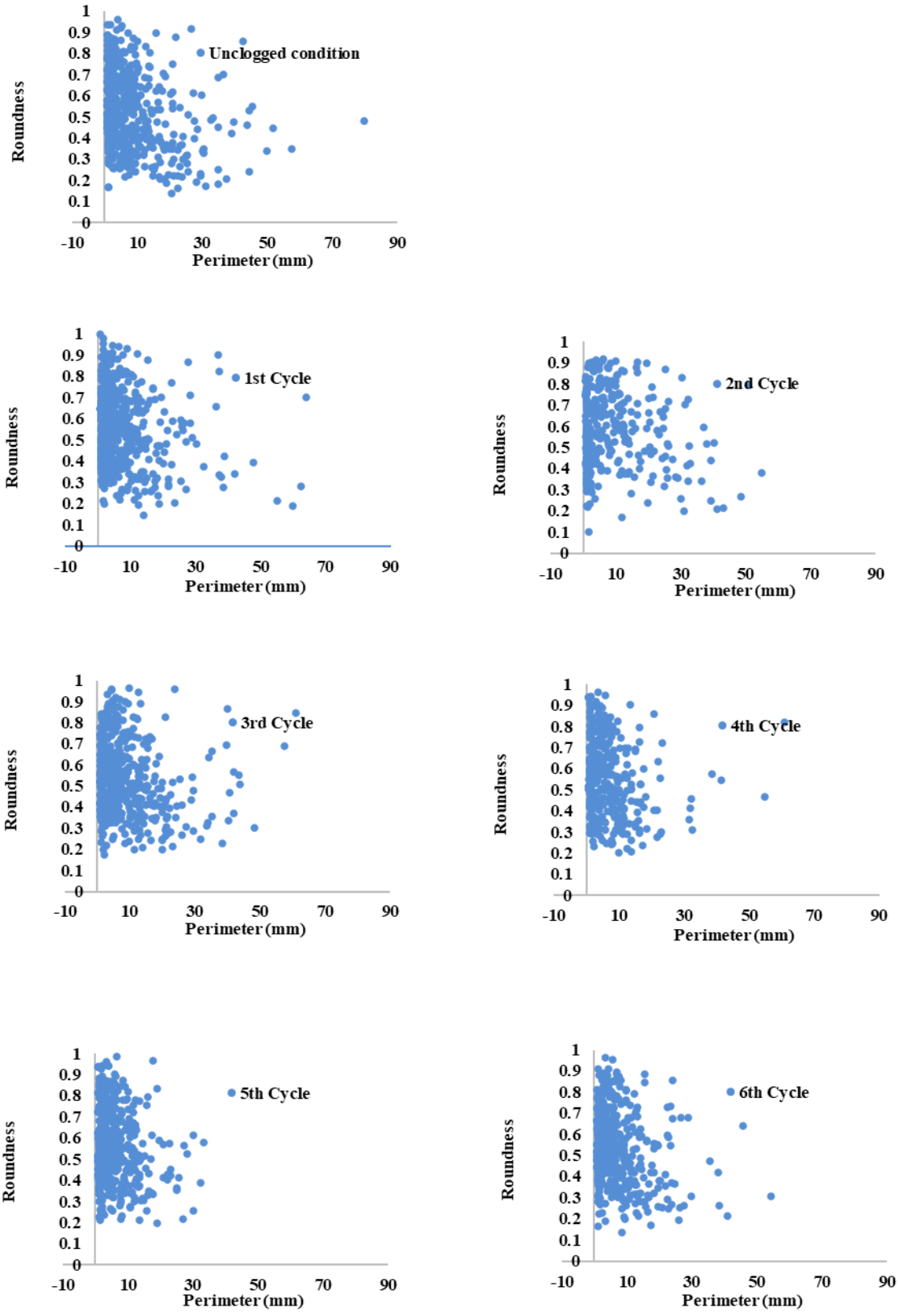

Figure 4.38 Roundness Vs Perimeter for 2.36 - 4.75mm - Clay clogging cycles

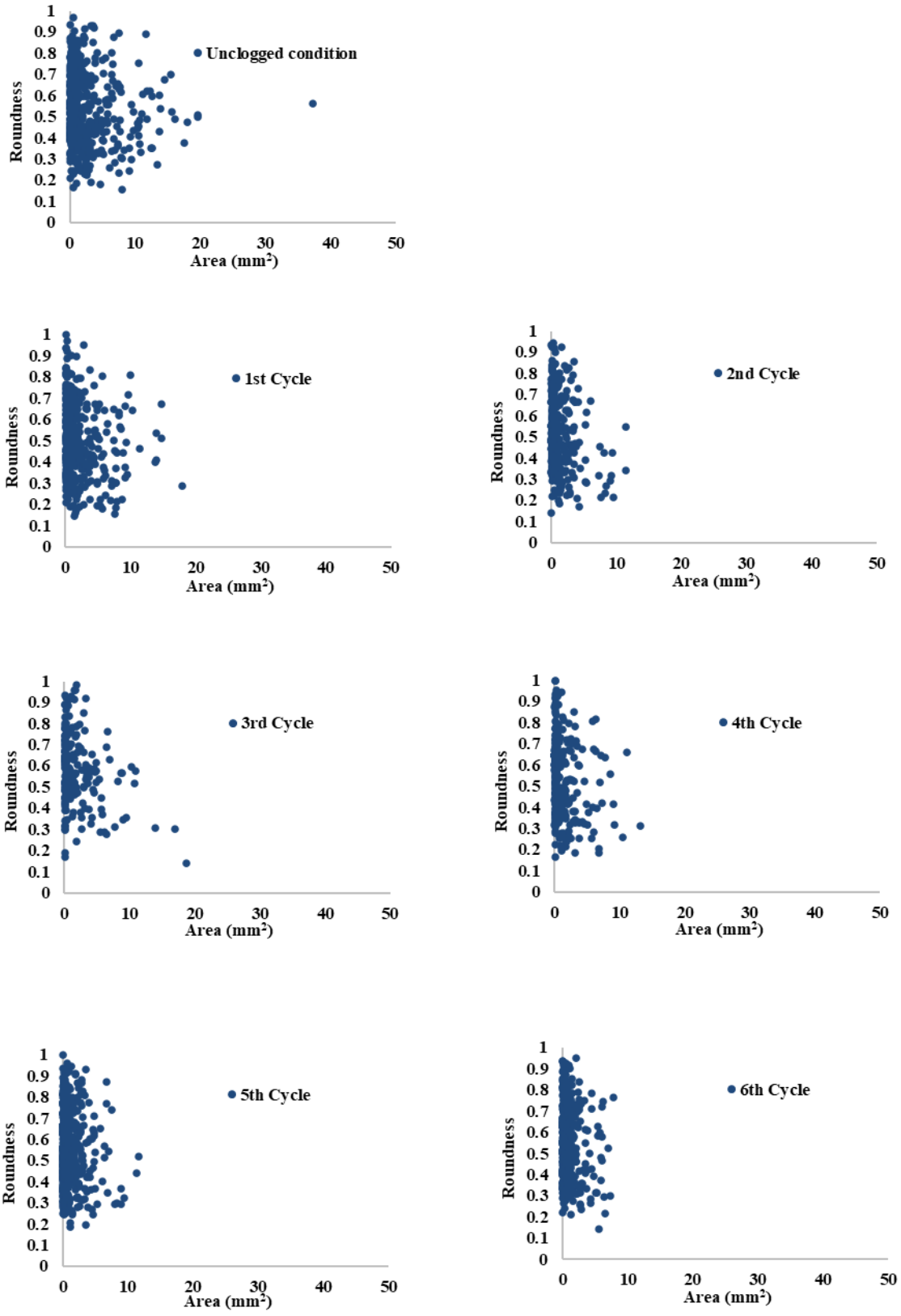

Figure 4.39 Roundness Vs Area for 2.36 - 4.75mm - Sand clogging cycles

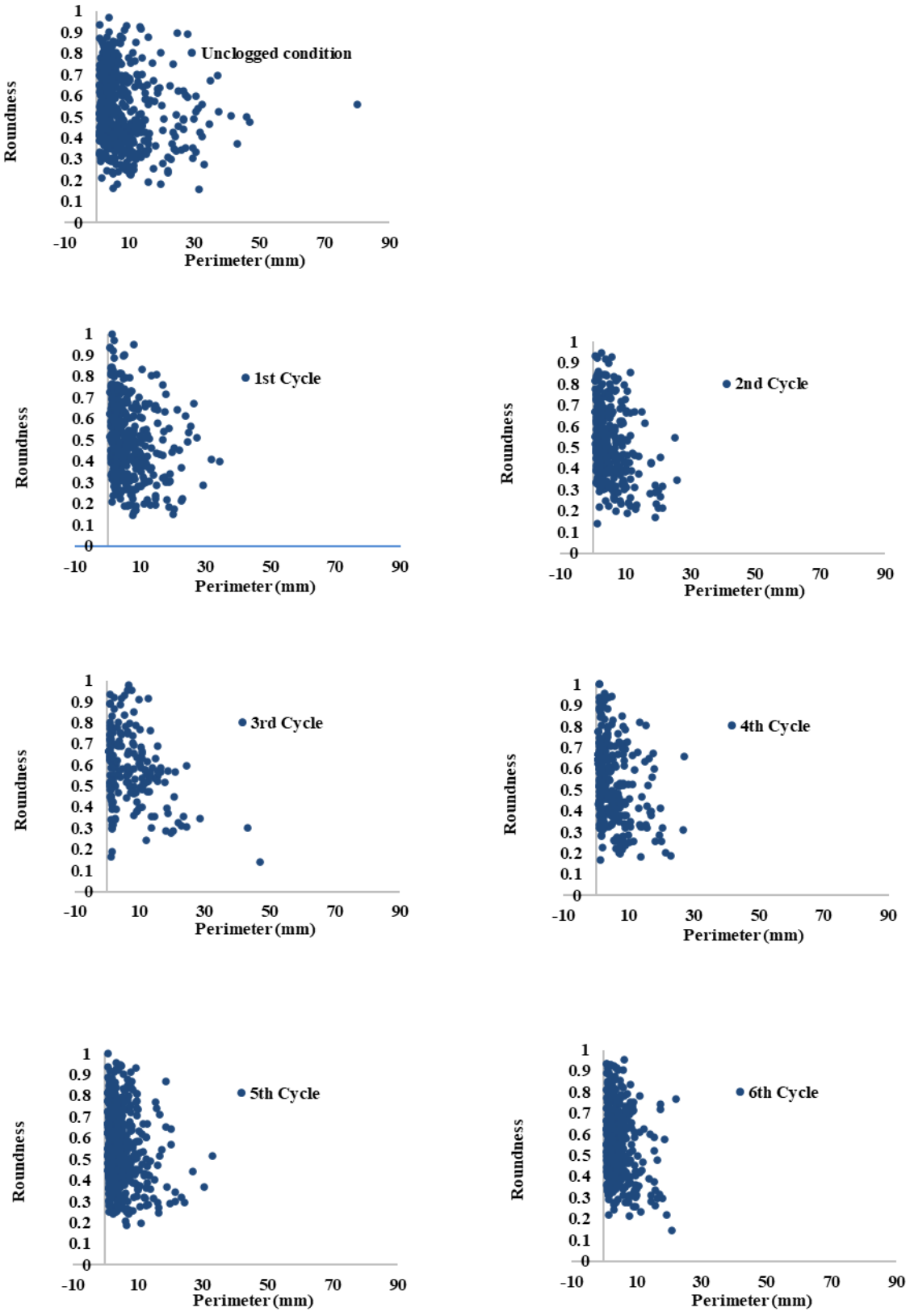

Figure 4.40 Roundness Vs Perimeter for 2.36 - 4.75mm - Sand clogging cycles

The Figure 4.41 shows the relation between roundness and area for clay clogging for 4.75 – 6.30mm, Figure 4.42 shows the relation between roundness and perimeter for clay clogging for 4.75 – 6.30mm, Figure 4.43 shows the relation between roundness and area for sand clogging for 4.75 – 6.30mm, Figure 4.44 shows the relation between roundness and perimeter for sand clogging for 4.75 – 6.30mm. The value of roundness varies from 0.2 to 1. In the clay clogging, the third clogging cycle shows decrease in area and perimeter and also decrease in the number of pores. There is more dispersion in area after the first clogging cycle of clay. Whereas for sand clogging, the first clogging cycle shows the decrease in area and perimeter with the decrease of number of pores. There is no major change in the distribution of roundness values.

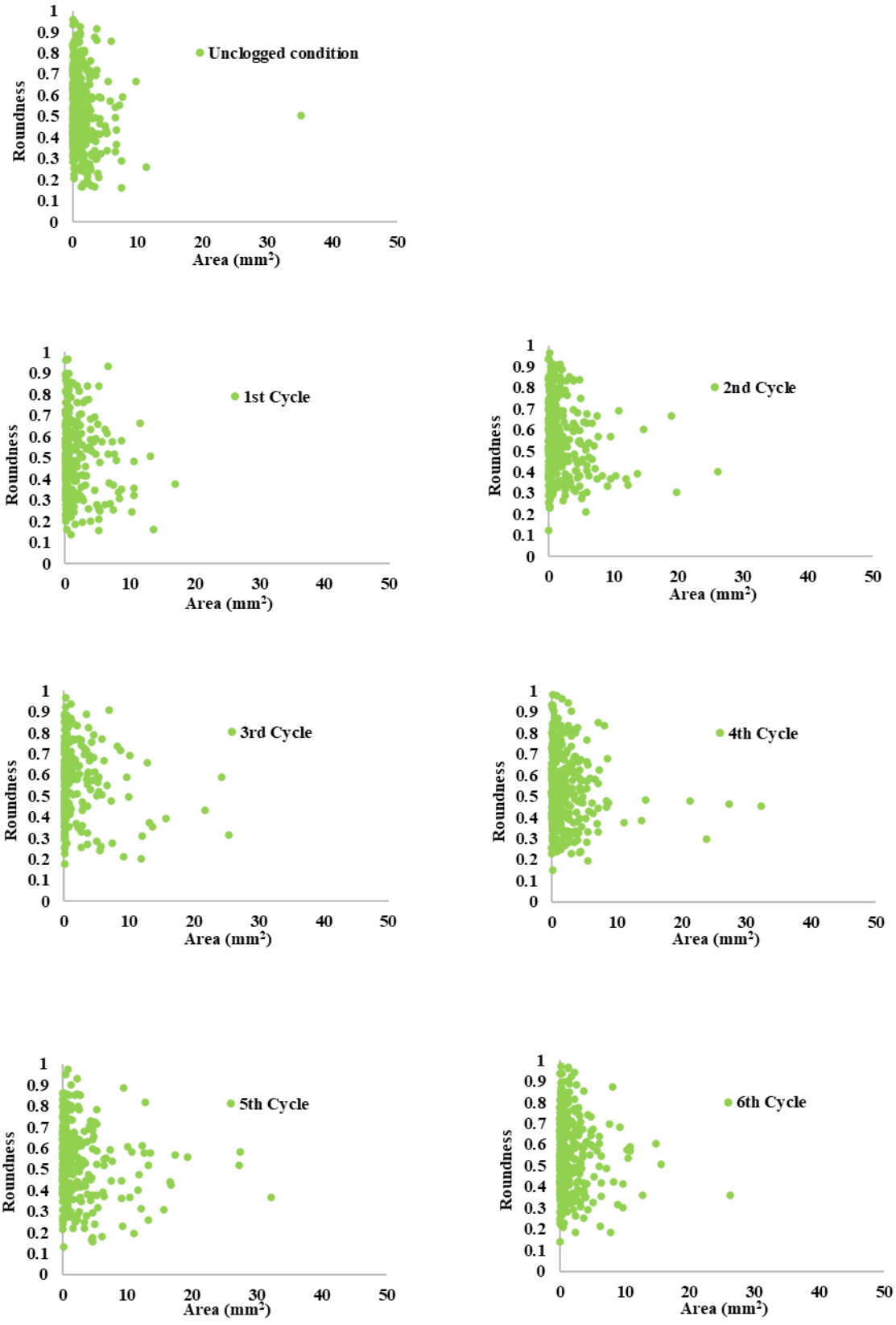

Figure 4.41 Roundness Vs Area for 4.75-6.30mm - Clay clogging cycles

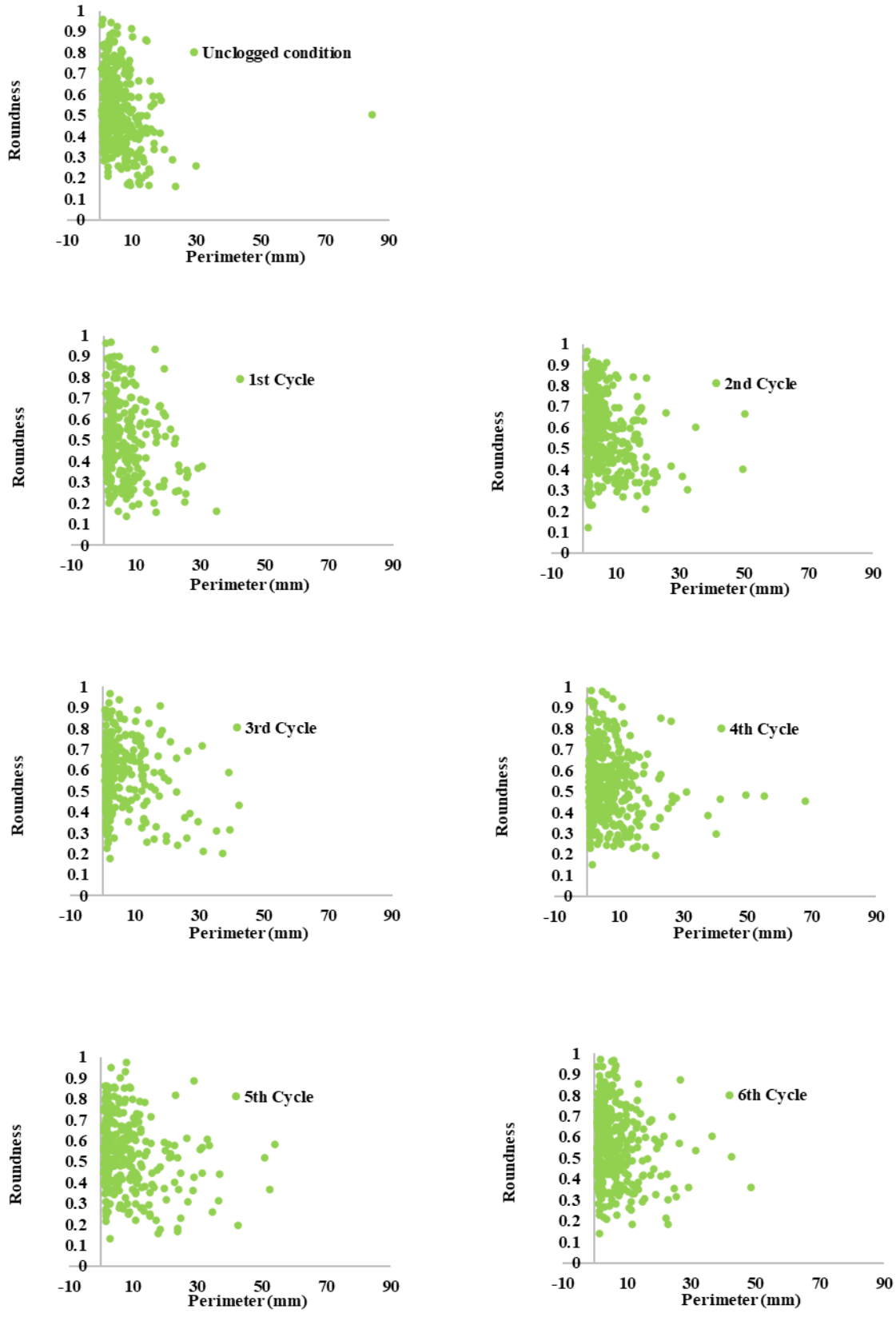

Figure 4.42 Roundness Vs Perimeter for 4.75-6.30mm – Clay clogging cycles

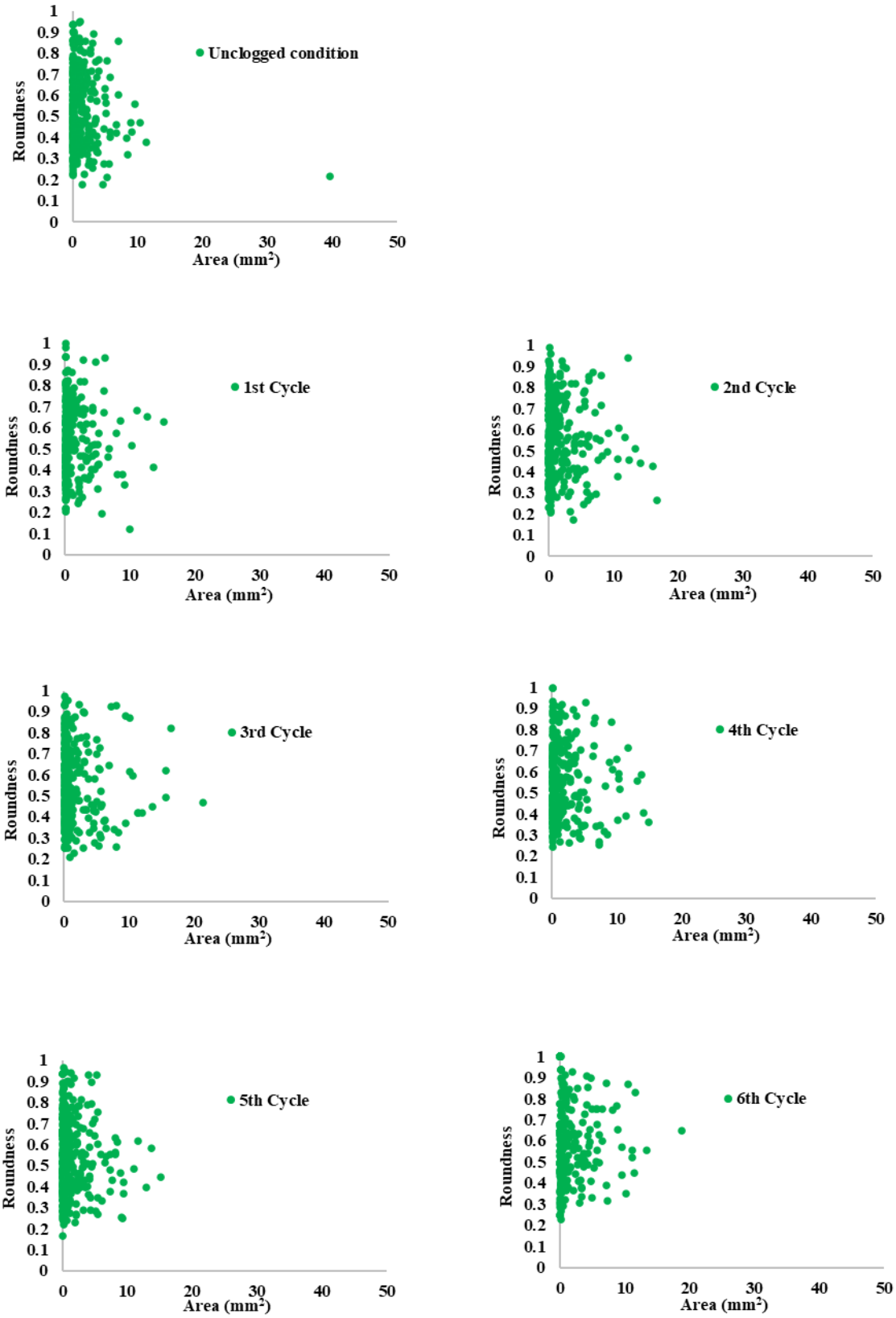

Figure 4.43 Roundness Vs Area for 4.75-6.30mm - Sand clogging cycles

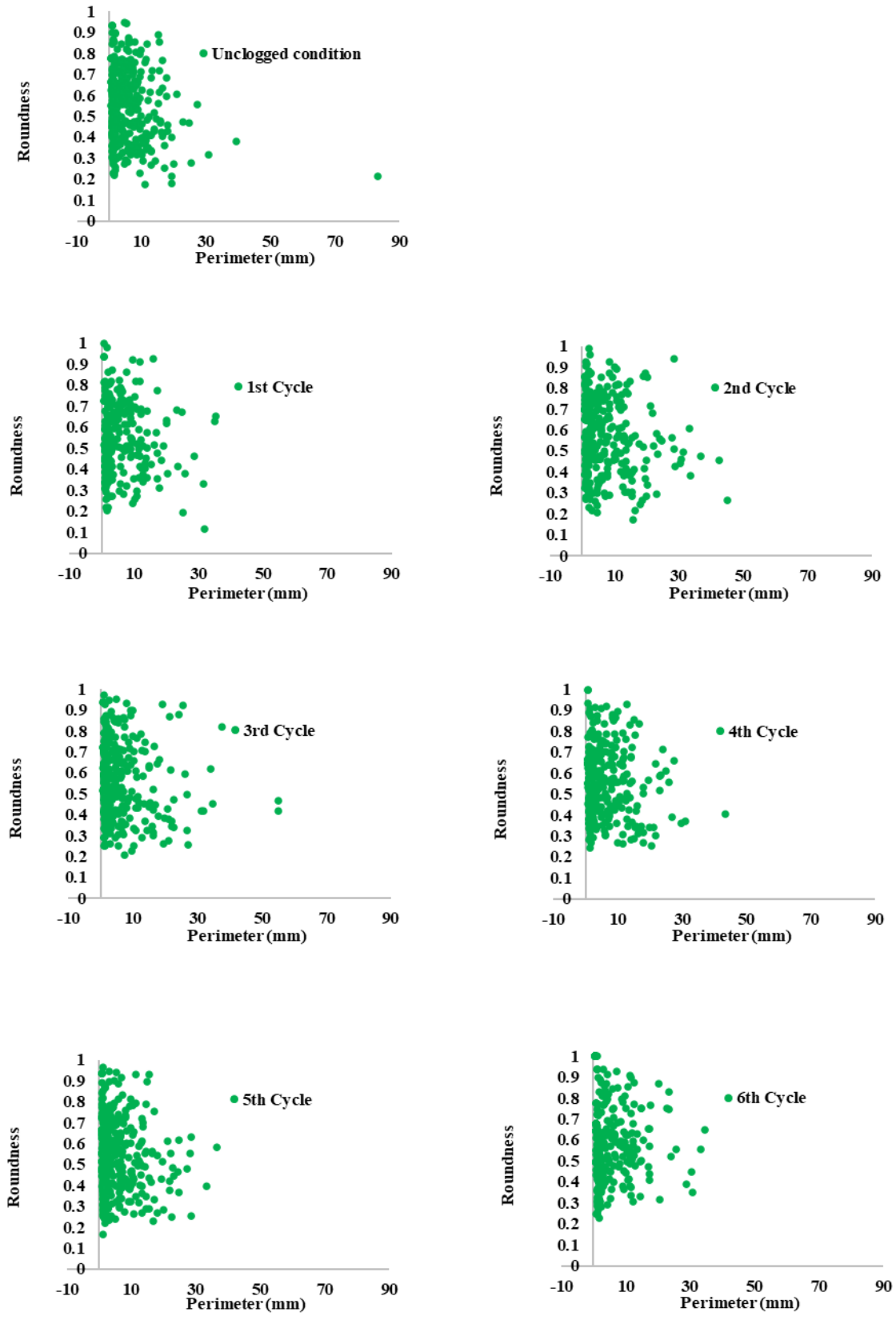

Figure 4.44 Roundness Vs Perimeter for 4.75-6.30mm - Sand clogging cycles

4.12 ANALYSIS OF SOLIDITY OF PORES ON THE TOP SURFACE OF PERVIOUS CONCRETE

Solidity indicates whether a shape is convex or not. As the value approaches 1, it indicates that the shape is convex. As the value deviates from 1, it indicates the concavity of the shape. Table 4.17 tabulates the maximum, minimum, average and standard deviation of the solidity for six cycles of clay and sand clogging for 2.36 – 4.75mm aggregate gradation. The minimum value is 0.36 and max value is 1. The average value of solidity is approximately 0.7 across all cycles.

Table 4.17 Basic statistics of solidity for clay and sand clogging cycles – 2.36 – 4.75mm

S. No	Cycle	Clogging Material	Max	Min	Average	Std. Dev.
1	0	Clay	1.00	0.36	0.71	0.11
2	1	Clay	1.00	0.37	0.66	0.10
3	2	Clay	1.00	0.38	0.67	0.11
4	3	Clay	0.95	0.36	0.68	0.11
5	4	Clay	1.00	0.43	0.71	0.10
6	5	Clay	1.00	0.39	0.70	0.10
7	6	Clay	1.00	0.36	0.71	0.12
8	0	Sand	0.95	0.40	0.72	0.11
9	1	Sand	1.00	0.41	0.77	0.10
10	2	Sand	1.00	0.48	0.73	0.09
11	3	Sand	1.00	0.50	0.72	0.11
12	4	Sand	1.00	0.46	0.74	0.10
13	5	Sand	1.00	0.36	0.73	0.11
14	6	Sand	1.00	0.49	0.75	0.10

Table 4.18 tabulates the maximum, minimum, average and standard deviation of the solidity for six cycles of clay and sand clogging for 4.75 – 6.30mm aggregate gradation. The minimum value is 0.35 and max value is 1. The average value of solidity is approximately 0.7 across all cycles indicating that the perimeter has smoother undulations. Also the standard deviation is approximately equal to 0.10.

Table 4.18 Basic statistics of solidity for clay and sand clogging cycles – 4.75 – 6.30mm

S. No	Cycle	Clogging Material	Max	Min	Average	Std. Dev.
1	0	Clay	1	0.35	0.72	0.10
2	1	Clay	0.95	0.43	0.70	0.10
3	2	Clay	1	0.36	0.70	0.11
4	3	Clay	1	0.38	0.70	0.12
5	4	Clay	1	0.37	0.69	0.11
6	5	Clay	1	0.45	0.70	0.10
7	6	Clay	1	0.43	0.71	0.10
8	0	Sand	1	0.43	0.69	0.10
9	1	Sand	1	0.40	0.69	0.10
10	2	Sand	0.96	0.39	0.68	0.11
11	3	Sand	0.93	0.36	0.69	0.10
12	4	Sand	1	0.42	0.70	0.11
13	5	Sand	1	0.40	0.71	0.11
14	6	Sand	1	0.41	0.76	0.12

Figure 4.45 shows the split violin plot of solidity of the pores for 2.36 – 4.75mm aggregate gradation. It compares the clogging due to clay and sand for six cycles of clogging. The values of solidity are higher in sand clogging compared to clay clogging. Sand clogging scenario also shows variation in the distribution of solidity. The bell curve is unimodal for both the cycles. The pattern of solidity changes across both the clay and sand clogging cases.

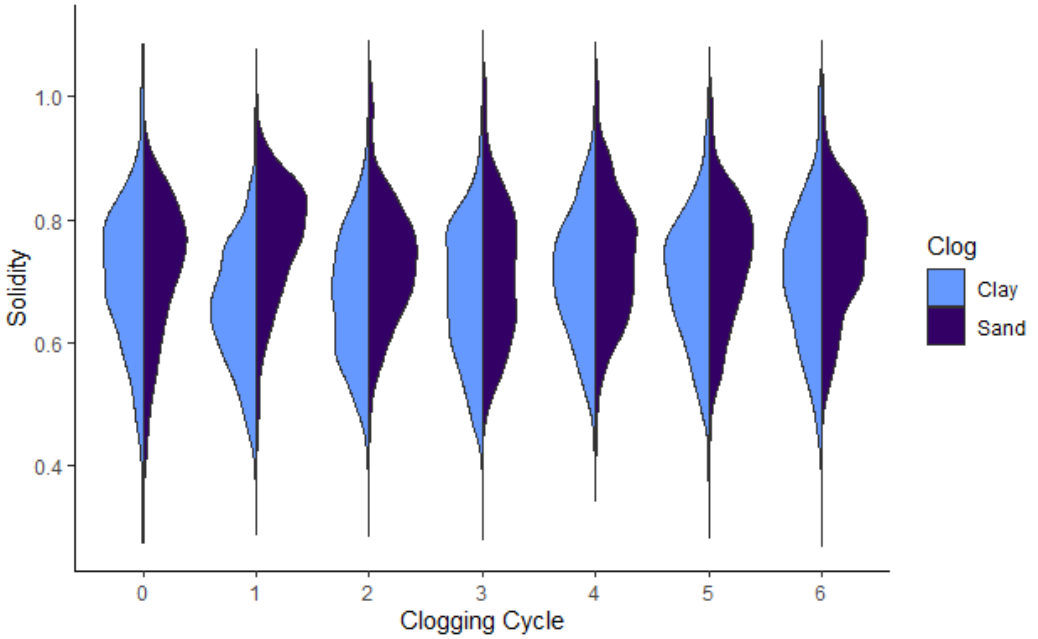

Figure 4.45 Split violin plot of solidity comparing clay and sand clogging – 2.36 – 4.75mm

Figure 4.46 shows the split violin plot of solidity of the pores for 4.75 – 6.30mm aggregate gradation. It compares the clogging due to clay and sand for six cycles of clogging. Sand clogging scenario also shows variation in the distribution of solidity in the sixth clogging cycle. The bell curve is unimodal for clay clogging cycles whereas in clay clogging cycle, there is an appearance of multi-modality in fourth and sixth cycle. The pattern of solidity changes across both the clay and sand clogging cases.

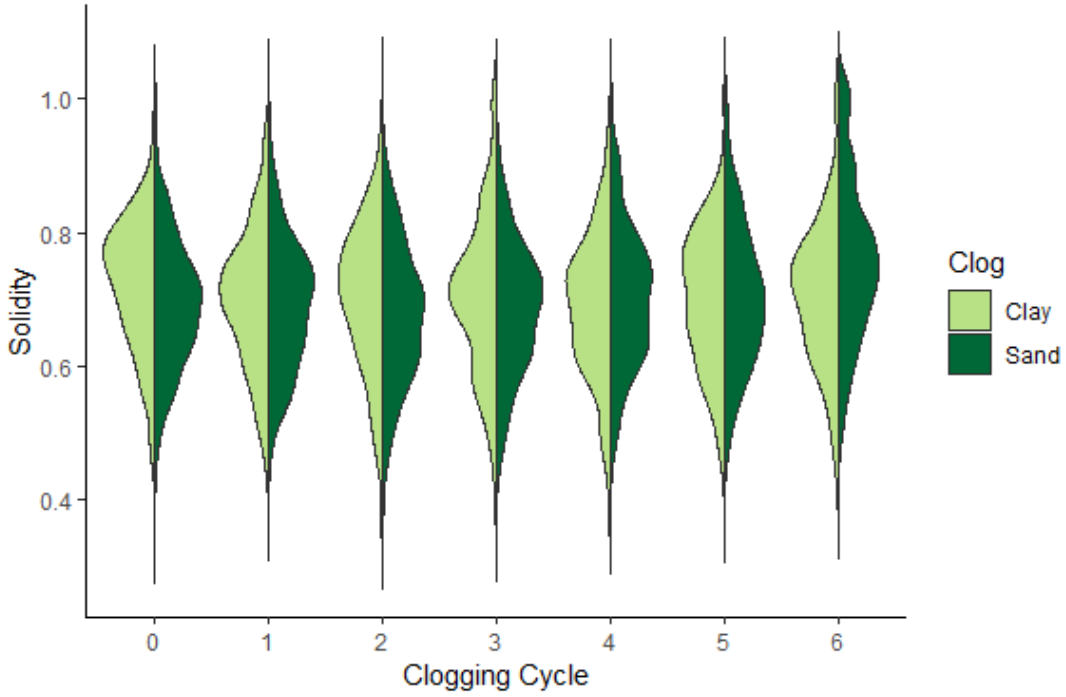

Figure 4.46 Split violin plot of solidity comparing clay and sand clogging – 4.75 – 6.30mm

The below figures given the distribution of the solidity based on the area and perimeter under the conditions of clay and sand clogging for the aggregate size gradations of 2.36 – 4.75mm and 4.75 – 6.30mm. It is colour coded as per the split violin plots. The graphs gives an insight into the clustering of solidity through the progression of clogging cycles. The outliers can be computed easily through the below scatter plots.

The Figure 4.47 shows the relation between solidity and area for clay clogging for 2.36 – 4.75mm, Figure 4.48 shows the relation between solidity and perimeter for clay clogging for 2.36 – 4.75mm, Figure 4.49 shows the relation between solidity and area for sand clogging for 2.36 – 4.75mm, Figure 4.50 shows the relation between solidity and perimeter for sand clogging for 2.36 – 4.75mm. The solidity varies from 0.5 to 1 indicating most of the shapes are convex in nature. A value of 1 indicates a perfectly convex shape. Most of the larger pores have solidity close to 0.5. Convex shapes **ensure** better permeability compared to concave shapes. The dispersion of pore area and perimeter is more in the clay clogging compared to sand clogging.

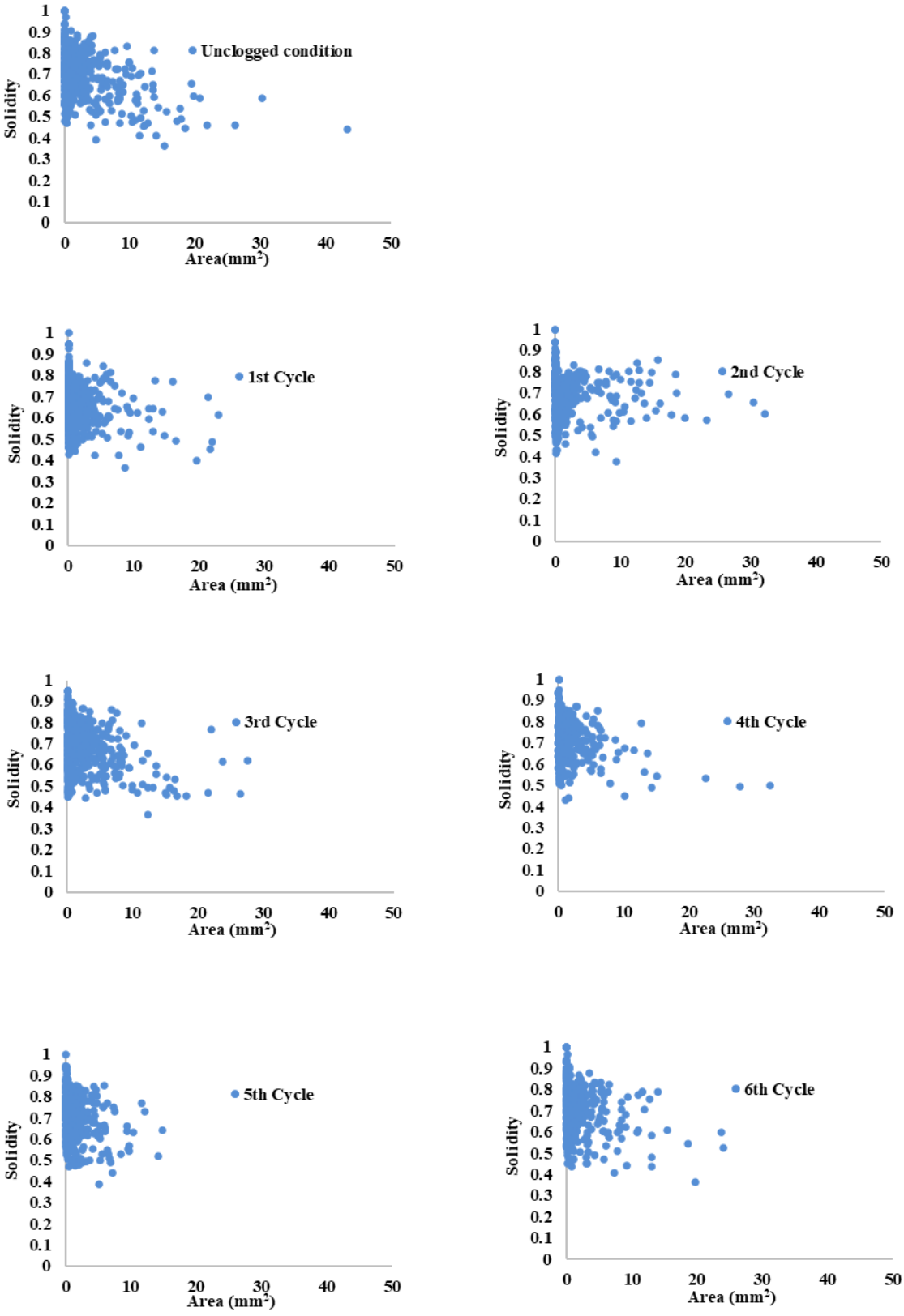

Figure 4.47 Solidity Vs Area for 2.36 - 4.75mm - Clay clogging cycles

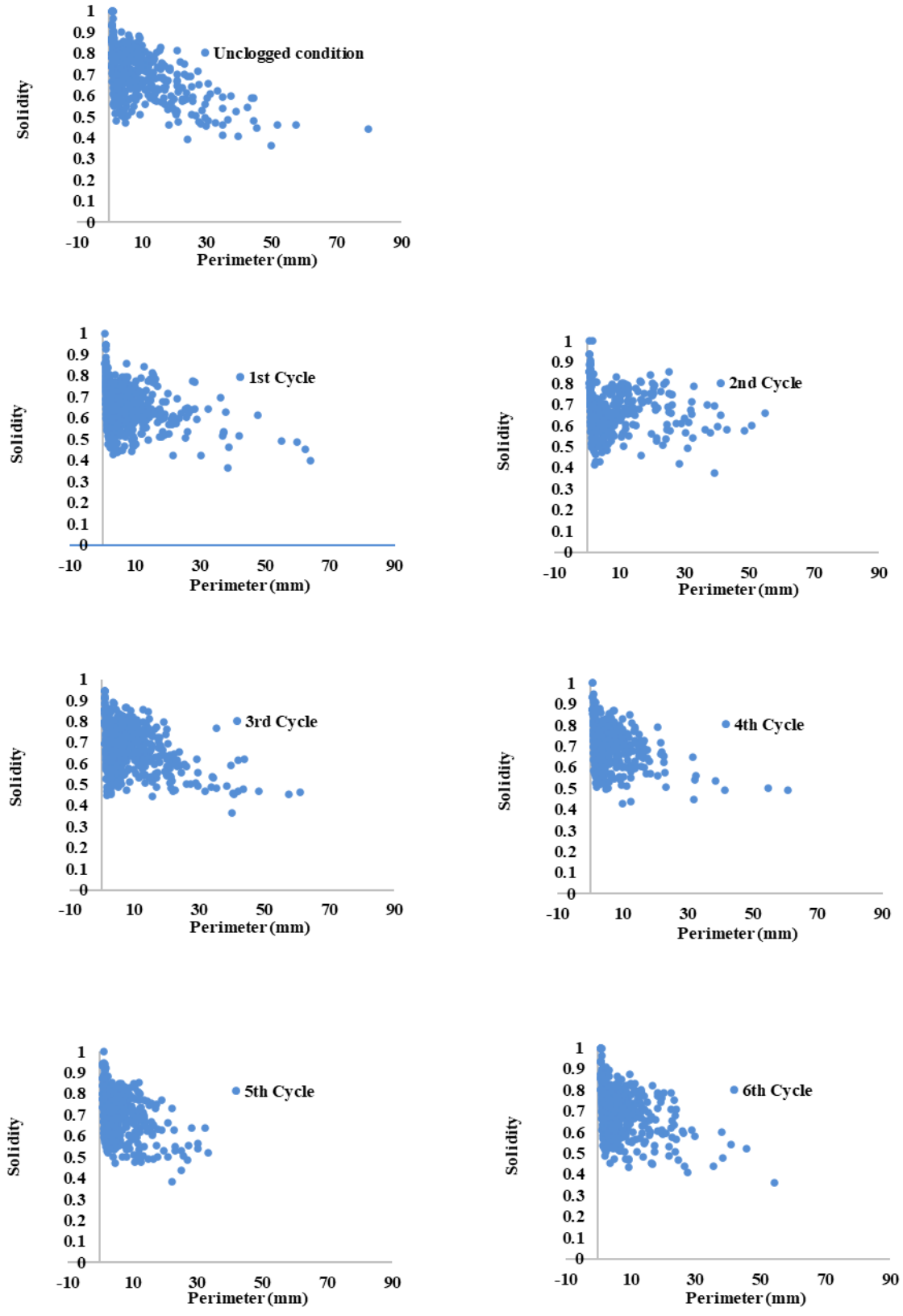

Figure 4.48 Solidity Vs Perimeter for 2.36 - 4.75mm - Clay clogging cycles

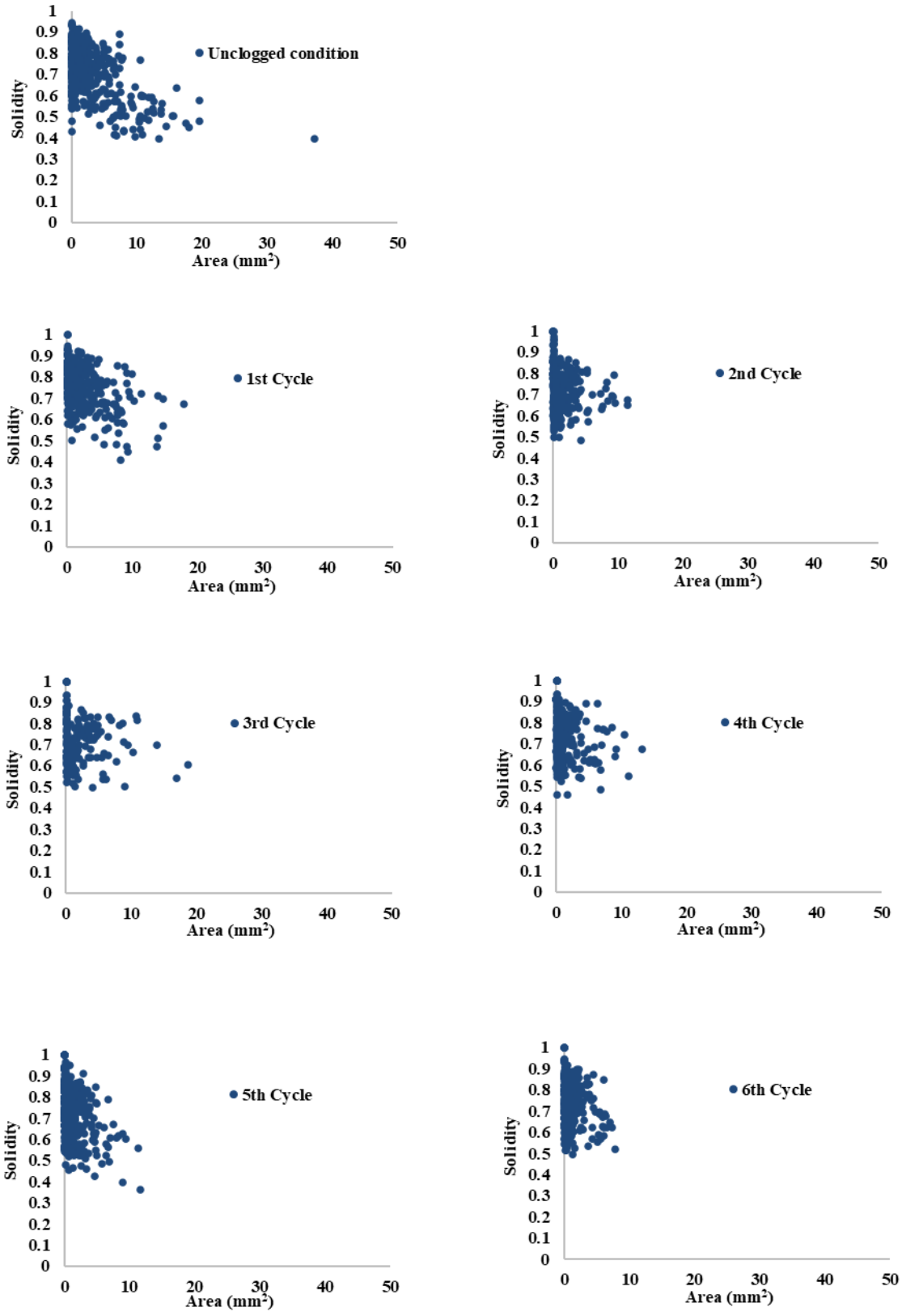

Figure 4.49 Solidity Vs Area for 2.36 - 4.75mm - Sand clogging cycles

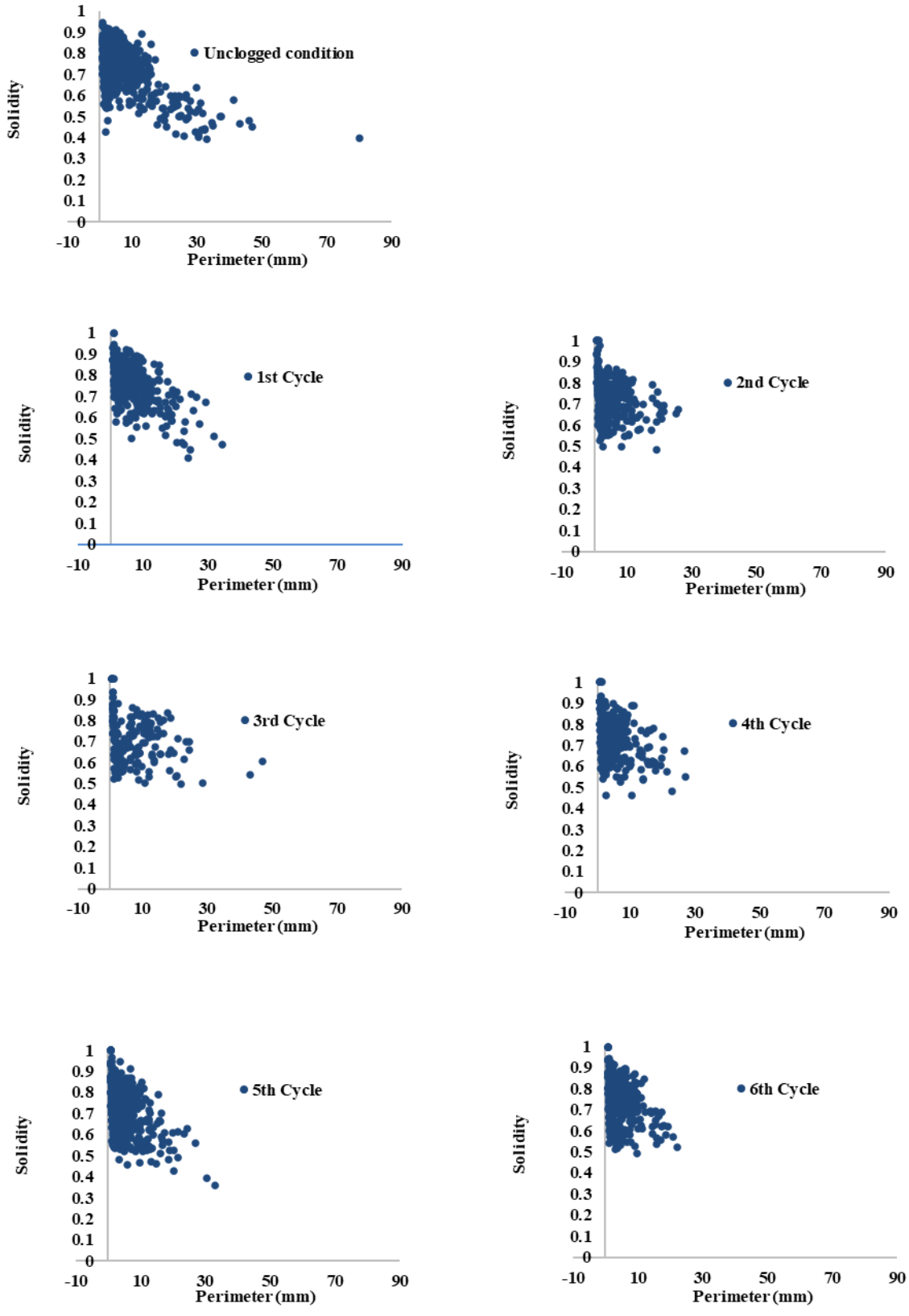

Figure 4.50 Solidity Vs Perimeter for 2.36 - 4.75mm - Sand clogging cycles

The Figure 4.51 shows the relation between solidity and area for clay clogging for 4.75 – 6.30mm, Figure 4.52 shows the relation between solidity and perimeter for clay clogging for 4.75 – 6.30mm, Figure 4.53 shows the relation between solidity and area for sand clogging for 4.75 – 6.30mm, Figure 4.54 shows the relation between solidity and perimeter for sand clogging for 4.75 – 6.30mm. The value of solidity varies from 0.5 to 1. The higher area and perimeter have solidity around 0.5 for both the clogging cycles. The dispersion of pore area and perimeter is almost similar for clay and sand clogging. The dispersion follows a sinusoidal pattern as the clogging progresses.

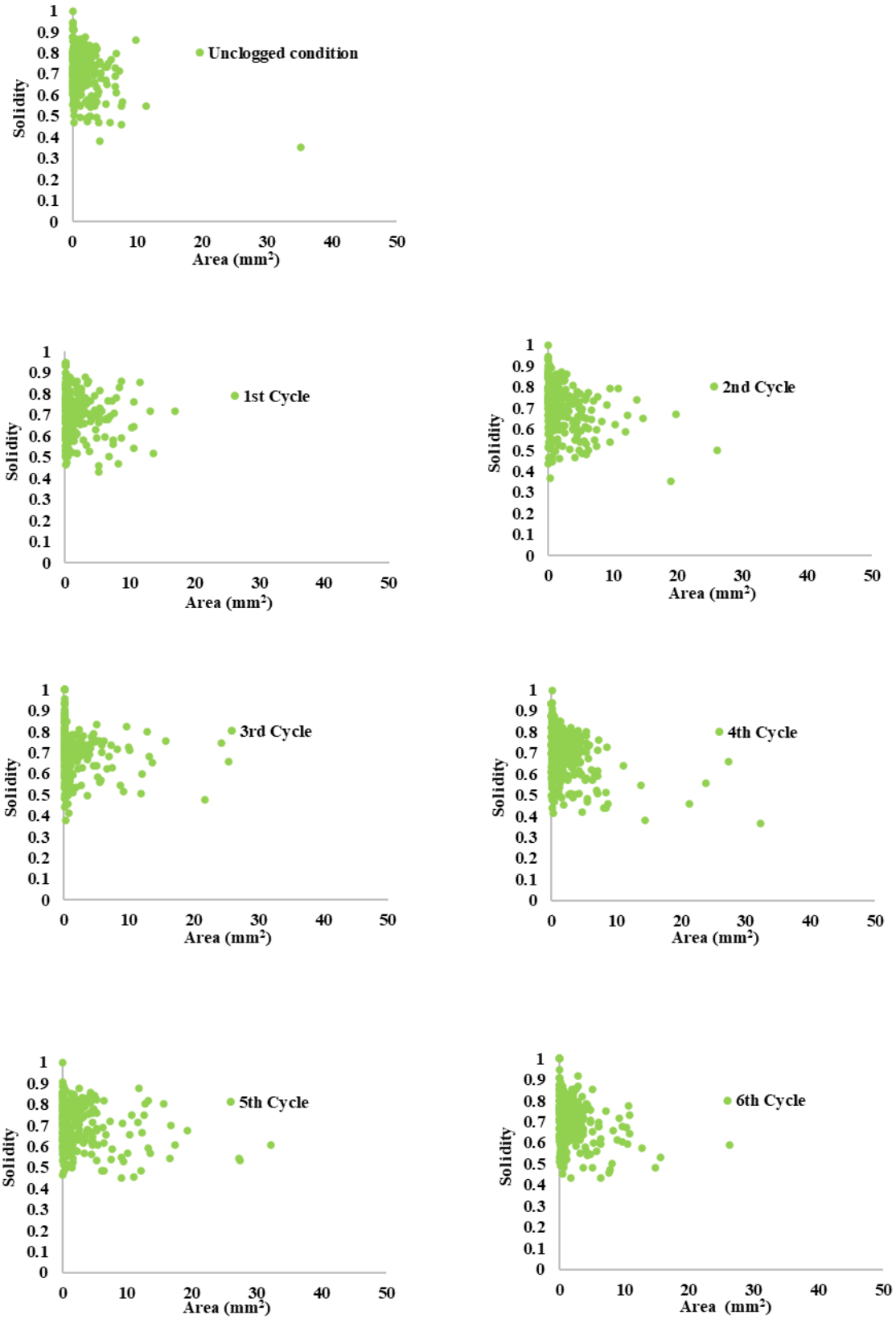

Figure 4.51 Solidity Vs Area for 4.75-6.30mm - Clay clogging cycles

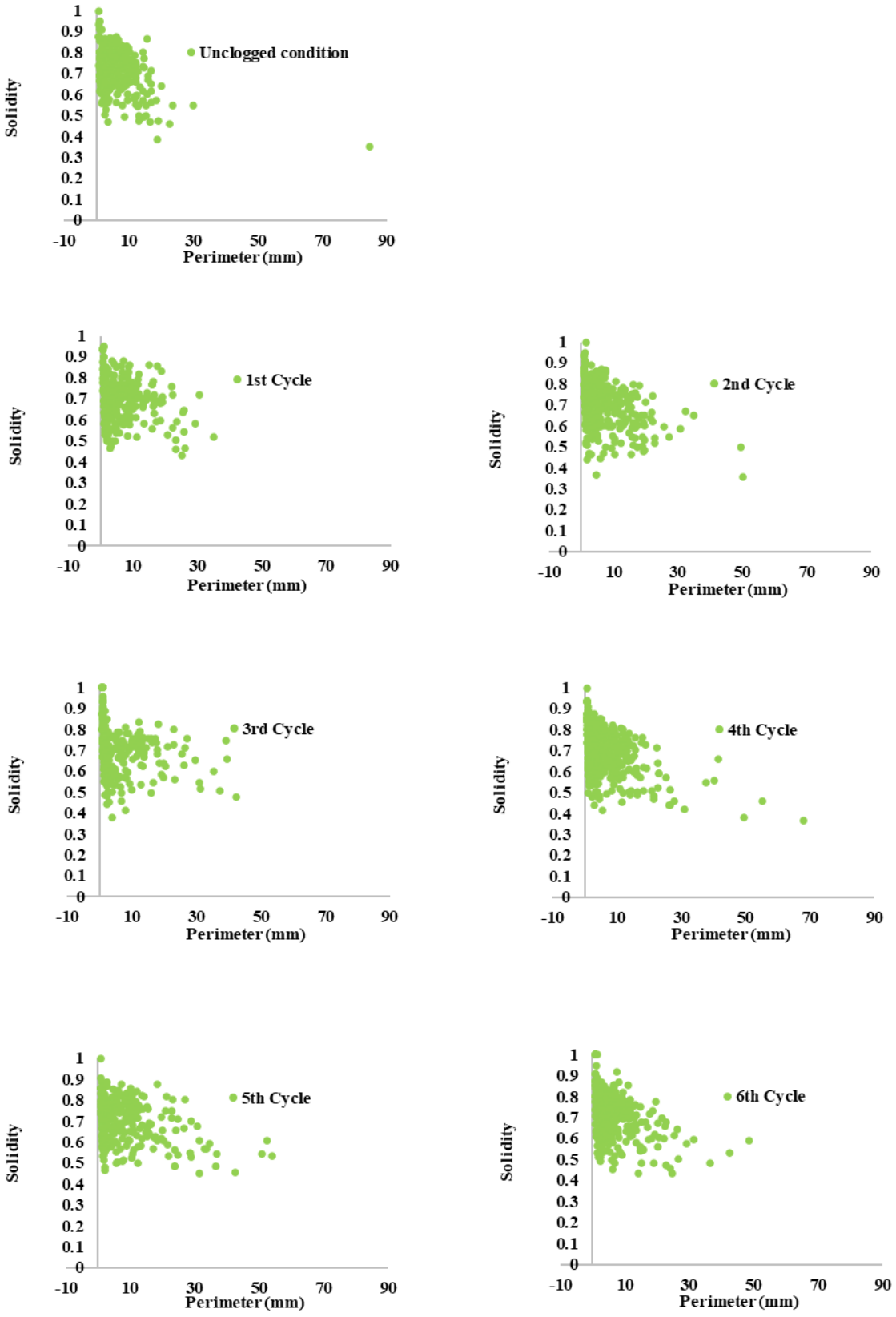

Figure 4.52 Solidity Vs Perimeter for 4.75-6.30mm - Clay clogging cycles

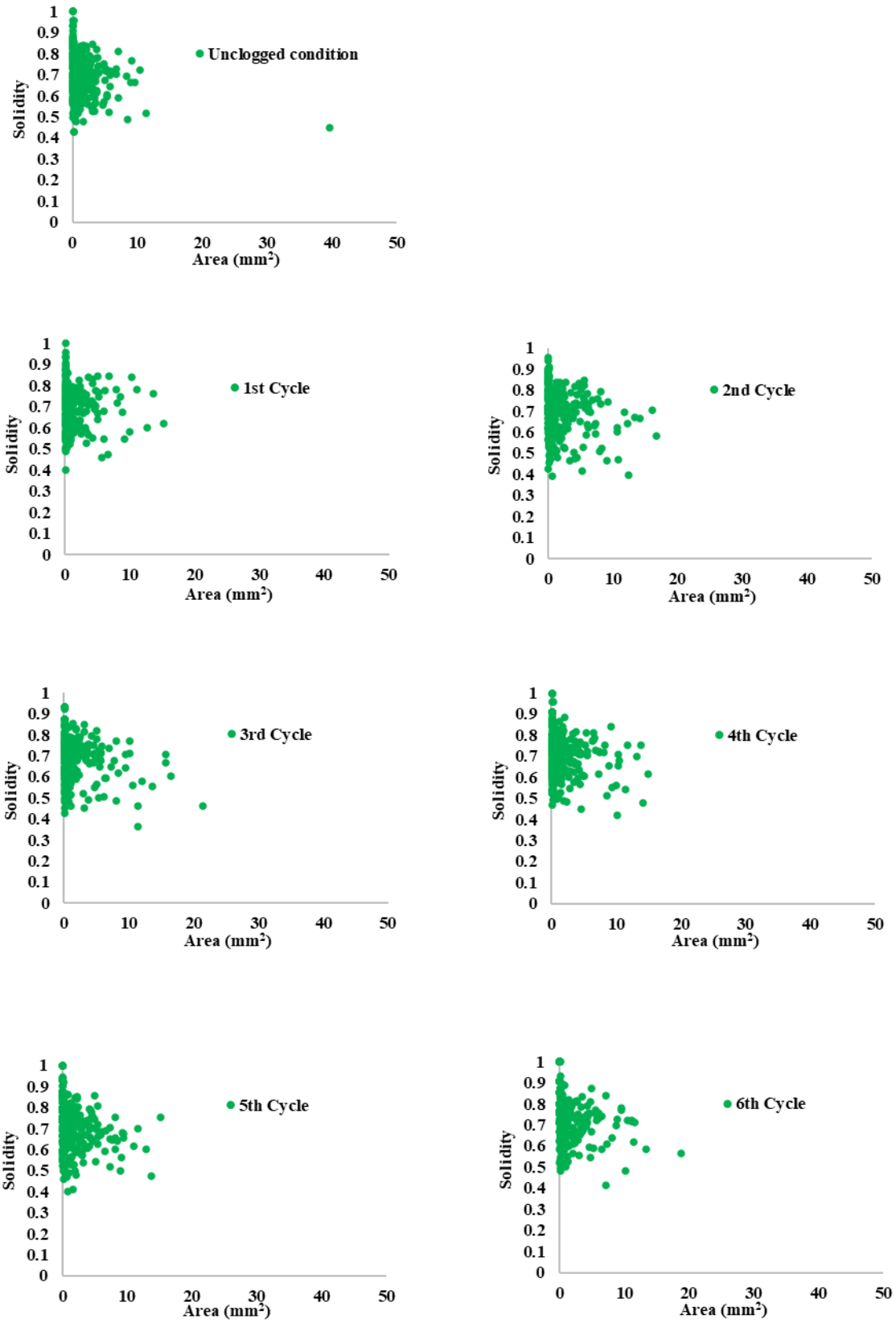

Figure 4.53 Solidity Vs Area for 4.75-6.30mm - Sand clogging cycles

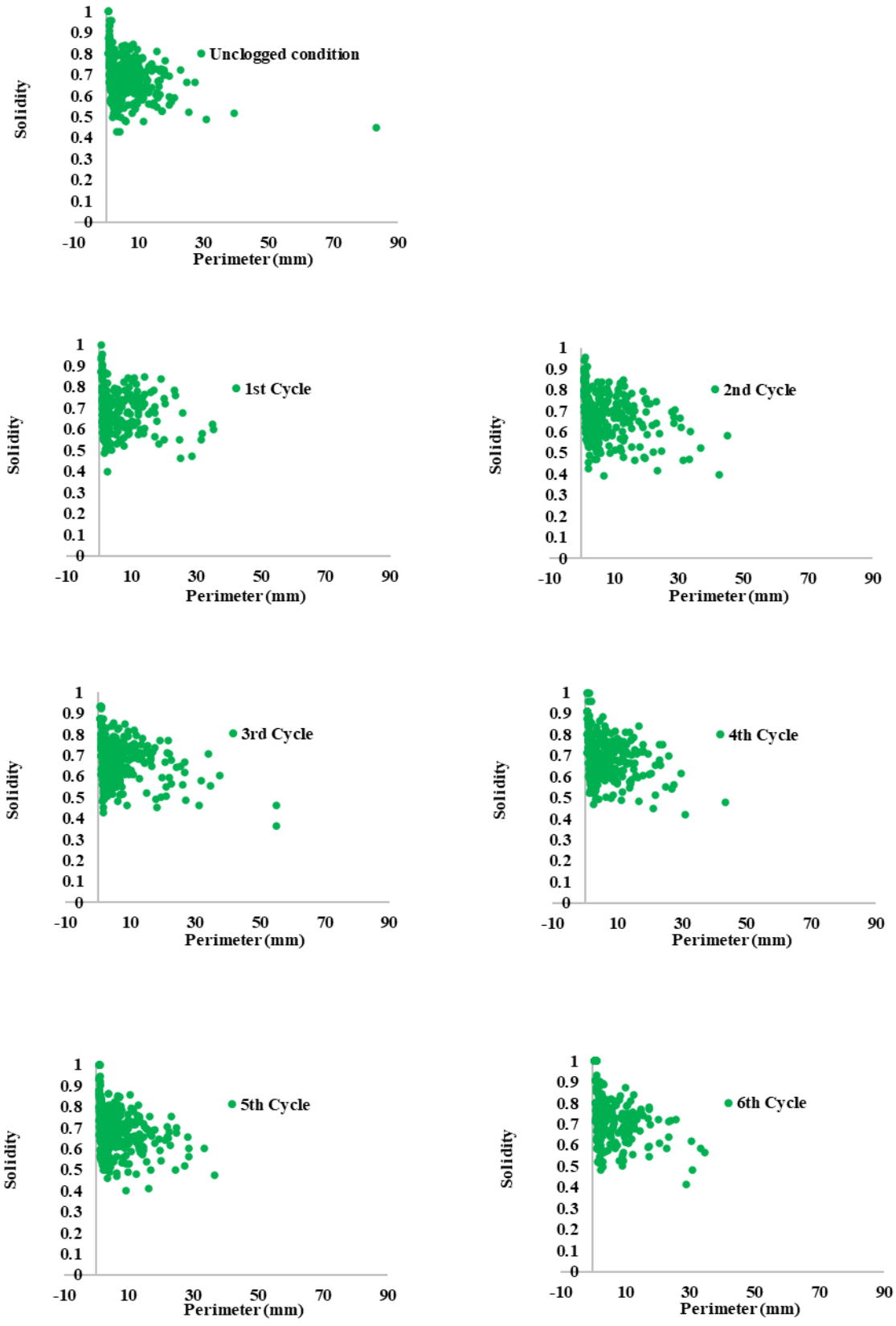

Figure 4.54 Solidity Vs Perimeter for 4.75-6.30mm - Sand clogging cycles

4.13 CLOSURE

In this work, the permeability and clogging of pervious concrete is calculated by falling head method. Clogging as a phenomenon affects the permeability of pervious concrete and reduces the life of pervious concrete. The clogging is maximum after the first cycle of clay and sand slurry introduction. It follows an exponential decreasing pattern as the clogging progresses. For understanding clogging, it is necessary to study the clogging of pores on the top surface. Image analysis of the top surface is undertaken to study in detail the geometric properties of pores namely area, perimeter, aspect ratio, circularity, roundness and solidity. The major pores are non-circular with less elongation and with more inclination towards convex shapes. Such shapes reduce the permeability of the pervious concrete.

CHAPTER 5

CONCLUSIONS

5.1CONCLUSIONS

This study highlights the role of aggregate size gradation on the hydraulic properties of pervious concrete mixes, and the following are the main conclusions drawn from the study.

- The larger aggregate size gradation of 4.75mm - 6.3mm shows higher permeability than the smaller size gradation of 2.36mm - 4.75mm due to the larger pores. The variation of permeability is more in the larger aggregates due to the numerous interconnectivity of pores. It results in varying flow paths and flow directions within the concrete matrix. The vibration of pervious concrete is not recommended as it has a higher chance of paste drain at the bottom. Compaction is a more suitable method. Uniformity in compaction pressure is essential for avoiding variation in porosity.
- The compressive strength, porosity and permeability is compared with the standards and literature using aggregate binder and water binder ratio. The results are in agreement with the literature.
- The relationship between permeability and porosity is established as an exponential equation. The highest reduction in permeability is when the clogging materials are introduced to the specimen. Further degration of permeability has a low impact compared to the initial decrease. The slope of the line drawn is approximately equal to zero, indicating a line drawn parallel to the x-axis.
- The larger particle size of sand clogs the concrete matrix differently from clay particles. The fineness of clay particles causes a part of it to pass through the concrete matrix, whereas, in the case of sand, there is accumulation in the six cycles of the introduction of sand slurry. It is not

recommended to use aggregate size of 2.36 - 4.75mm in the pervious concrete mix when the surrounding area has higher siltation.

- The pores in the pervious concrete are non–circular, less elongated with higher convexity resulting in non-uniform flow pattern with reduced permeability.

5.2 LIMITATIONS

The following are the limitations of the research work:

- The permeability is calculated by the falling head method using Darcy's equation. Darcy's equation is valid when the flow is laminar flow.
- The pre-requisite for using falling head method is that the specimen should be saturated. The experimental calculation was conducted for unsaturated conditions.
- The set up had limitations for calculating high difference in falling head.

5.3 FUTURE WORK

- Improvised set up can be used for evaluating the permeability. Internet of Things (IOT) based instruments can give better results.
- The pore parameters can be correlated to the permeability to understand the influence of the geometric parameters on the permeability.

REFERENCES

Agudelo-vera, C. M., Leduc, W. R. W. A., Mels, A. R., and Rijnaarts, H. H. M. (2012). "Resources , Conservation and Recycling Harvesting urban resources towards more resilient cities." *Resour Conserv Recycl*, 64, 3–12.

Ahiablame, L. M., and Engel, B. A. (2012). "Effectiveness of Low Impact Development Practices : Literature Review and Suggestions for Future Research." *Water Air Soil Pollut*, 223, 4253–4273.

Akand, L., Yang, M., and Gao, Z. (2016). "Characterization of pervious concrete through image based micromechanical modeling." *Constr Build Mater*, 114(July), 547–555.

Azad, A., Mousavi, S., Karami, H., Farzin, S., Kheyroddin, A., and Singh, V. P. (2020). "Properties of metakaolin-based green pervious concrete cured in cold and normal weather conditions." *European Journal of Environmental and Civil Engineering*, 0(0), 1–14.

Barišić, I., Grubeša, I. N., Dokšanović, T., and Zvonarić, M. (2020). "Influence of Clogging and Unbound Base Layer Properties on Pervious Concrete Drainage Characteristics." 1–13.

Bonicelli, A., Giustozzi, F., and Crispino, M. (2015). "Experimental study on the effects of fine sand addition on differentially compacted pervious concrete." *Constr Build Mater*, 91, 102–110.

Buckman, J., Bankole, S. A., Zihms, S., Lewis, H., Couples, G., and Corbett, P. W. M. (2017). "Quantifying Porosity through Automated Image Collection and Batch Image Processing : Case Study of Three Carbonates and an Aragonite Cemented Sandstone." *Geosciences* 7, 70.

Burns, M. J., Fletcher, T. D., Walsh, C. J., Ladson, A. R., and Hatt, B. E. (2012). "Hydrologic shortcomings of conventional urban stormwater management and opportunities for reform." *Landsc Urban Plan*, 105(3), 230–240.

Cai, X., Wu, K., Huang, W., Yu, J., and Yu, H. (2020). “Application of recycled concrete aggregates and crushed bricks on permeable concrete road base.” *Road Materials and Pavement Design*, 0(0), 1–16.

Chai, L., Kayhanian, M., Givens, B., Harvey, J. T., and Jones, D. (2012). “Hydraulic Performance of Fully Permeable Highway Shoulder for Storm Water Runoff Management.” *Journal of Environmental Engineering-Asce*, 138(July), 711–722.

Chandrappa, A. K., and Biligiri, K. P. (2016). “Pervious concrete as a sustainable pavement material-Research findings and future prospects: A state-of-the-art review.” *Constr Build Mater*, 111(March), 262–274.

Chandrappa, A. K., and Biligiri, K. P. (2017). “Investigations on Pervious Concrete Properties Using Ultrasonic Wave Applications.” *J Test Eval*, 45(5), 20160117.

Chen, H. (2017). “An integrated assessment of urban flooding mitigation strategies for robust decision making.” *Environmental Modelling and Software*, 95(June), 143–155.

Chen, Y., Wang, K., Wang, X., and Zhou, W. (2013). “Strength, fracture and fatigue of pervious concrete.” *Constr Build Mater*, 42, 97–104.

Chindaprasirt, P. (2008). “Cement paste characteristics and porous concrete properties.” 22, 894–901.

Ćosić, K., Korat, L., Ducman, V., and Netinger, I. (2015). “Influence of aggregate type and size on properties of pervious concrete.” *Constr Build Mater*, 78, 69–76.

Coughlin, J. P., Asce, M., Campbell, C. D., Mays, D. C., and Asce, M. (2012). “Infiltration and Clogging by Sand and Clay in a Pervious Concrete Pavement System.” (January), 68–73.

Crookes, A. J., Drake, J. A. P., and Green, M. (2017). “Hydrologic and Quality Control Performance of Zero-Exfiltration Pervious Concrete Pavement in Ontario.” *J Sustain Water Built Environ*, 3(3), 1–8.

Crouch, L. K., Pitt, J., and Hewitt, R. (2007). “Aggregate Effects on Pervious Portland Cement Concrete Static Modulus of Elasticity.” 19(July), 561–568.

Cui, X., Zhang, J., Huang, D., Tang, W., Wang, L., and Hou, F. (2016). "Experimental simulation of rapid clogging process of pervious concrete pavement caused by storm water runoff." *International Journal of Pavement Engineering*, 8436(November), 1–9.

Deo, O., Sumanasooriya, M., and Neithalath, N. (2010). "Permeability Reduction in Pervious Concretes due to Clogging: Experiments and Modeling." *Journal of Materials in Civil Engineering*, 22(7), 741–751.

Dierkes, C., Lucke, T., and Helmreich, B. (2015). "General Technical Approvals for Decentralised Sustainable Urban Drainage Systems (SUDS)—The Current Situation in Germany." *Sustainability*, 7, 3031-3051.

Drake, J., Bradford, A., and Seters, T. Van. (2014). "Hydrologic Performance of Three Partial-Infiltration Permeable Pavements in a Cold Climate over Low Permeability Soil." *J Hydrol Eng*, 19(9), 04014016.

El-Hassan, H., and Kianmehr, P. (2018a). "Pervious concrete pavement incorporating GGBS to alleviate pavement runoff and improve urban sustainability." *Road Materials and Pavement Design*, 19(1), 167–181.

El-Hassan, H., and Kianmehr, P. (2018b). "Pervious concrete pavement incorporating GGBS to alleviate pavement runoff and improve urban sustainability." *Road Materials and Pavement Design*, 19(1), 167–181.

Fassman, E. a., and Blackbourn, S. (2010). "Urban Runoff Mitigation by a Permeable Pavement System over Impermeable Soils." *J Hydrol Eng*, 15(6), 475–485.

Fu, T. C., Yeih, W., Chang, J. J., and Huang, R. (2014). "The Influence of Aggregate Size and Binder Material on the Properties of Pervious Concrete.", 963971.

Fwa, T. F., Lim, E., and Tan, K. H. (2015). "Comparison of Permeability and Clogging Characteristics of Porous Asphalt and Pervious Concrete Pavement Materials." *Transportation Research Record: Journal of the Transportation Research Board*, 2511(2511), 72–80.

Gong, L., Nie, L., and Xu, Y. (2020). “Geometrical and topological analysis of pore space in sandstones based on x-ray computed tomography.” *Energies (Basel)*, 13(15).

Gupta, R. (2014). “Monitoring in situ performance of pervious concrete in British Columbia - A pilot study.” *Case Studies in Construction Materials*, 1, 1–9.

Hasan, M. R., Zain, M. F. M., Hamid, R., Kaish, A. B. M. A., and Nahar, S. (2017). “A Comprehensive Study on Sustainable Photocatalytic Pervious Concrete for Storm Water Pollution Mitigation: A Review.” *Mater Today Proc*, 4(9), 9773–9776.

Haselbach, L., Boyer, M., Kevern, J. T., and Schaefer, V. R. (n.d.). “Cyclic Heat Island Impacts on Traditional Versus Pervious Concrete Pavement Systems.” 107–115.

Haselbach, L., Dutra, V. P., Schwetz, P., and Silva Filho, L. C. P. (2015). “A pervious concrete mix design based on clogging performance in Rio Grande do Sul Introduction Problem Statement.” *International Conference on Best Practices for Concrete Pavements*, (1), 1–11.

Haselbach, L. M., Dutra, V. P., and Schwetz, P. F. (2015). “A pervious concrete mix design based on clogging performance in Rio Grande do Sul A pervious concrete mix design based on clogging performance in Rio Grande do Sul.” (October).

Hatanaka, S., Kamalova, Z., and Harada, M. (2019). “Construction of a nonlinear permeability model of pervious concrete and drainage simulation of heavy rain in a residential area.” *Results in Materials*, 3(October), 100033.

Hintze, J. L., and Nelson, R. D. (1998). *Violin Plots: A Box Plot-Density Trace Synergism. Source: The American Statistician*.

Huang, B., Wu, H., Shu, X., and Burdette, E. G. (2010). “Laboratory evaluation of permeability and strength of polymer-modified pervious concrete.” *Constr Build Mater*, 24(5), 818–823.

Huang, J., Luo, Z., Basit, M., and Khan, E. (2020). “Impact of aggregate type and size and mineral admixtures on the properties of pervious concrete : An experimental investigation.” *Constr Build Mater*, 265, 120759.

Ibrahim, A., Mahmoud, E., Yamin, M., and Chowdary, V. (2014). “Experimental study on Portland cement pervious concrete mechanical and hydrological properties.” *Constr Build Mater*, 50, 524–529.

Jagadeesh, A., Asce, S. M., Ong, G. P., Ph, D., Asce, A. M., Su, Y., Ph, D., and Asce, A. M. (2019). “Development of Discharge-Based Thresholding Algorithm for Pervious Concrete Pavement Mixtures.” 31(9), 1–12.

Jo, M., Soto, L., Arocho, M., St John, J., and Hwang, S. (2015). “Optimum mix design of fly ash geopolymer paste and its use in pervious concrete for removal of fecal coliforms and phosphorus in water.” *Constr Build Mater*, 93, 1097–1104.

Kayhanian, M., Anderson, D., Harvey, J. T., Jones, D., and Muhunthan, B. (2012). “Permeability measurement and scan imaging to assess clogging of pervious concrete pavements in parking lots.” *J Environ Manage*, 95(1), 114–123.

Ketcheson, S., and Price, J. (2014). “Transport and Retention of Water and Salt within Pervious Concrete Pavements Subjected to Freezing and Sand Application.” *Journal of Hydrologic …*, 19(Marsalek 2003), 1–7.

Kevern, J. T. (2015). “Operation and Maintenance of Pervious Concrete Pavements Operation and Maintenance of Pervious Concrete Pavements.” (December 2010).

Kia, A., Wong, H. S., and Cheeseman, C. R. (2017). “Clogging in permeable concrete : A review.” *J Environ Manage*, 193, 221–233.

Kia, A., Wong, H. S., and Cheeseman, C. R. (2018). “Defining clogging potential for permeable concrete.” *J Environ Manage*, 220(February), 44–53.

Kia, A., Wong, H. S., and Cheeseman, C. R. (2019). “High-strength clogging resistant permeable pavement.” *International Journal of Pavement Engineering*, 0(0), 1–12.

Kytyr, D., and Valach, J. (2010). “Assessment of pore size distribution using image analysis.” (January), 3–6.

Lang, L., Duan, H., and Chen, B. (2019). “Properties of pervious concrete made from steel slag and magnesium phosphate cement.” *Constr Build Mater*, 209, 95–104.

Lee, J. G., Borst, M., Brown, R. A., Rossman, L., and Simon, M. A. (2015). “Modeling the Hydrologic Processes of a Permeable Pavement System.” *J Hydrol Eng*, 20(5), 04014070.

Li, H., Harvey, J. T., Holland, T. J., and Kayhanian, M. (2013). “The use of reflective and permeable pavements as a potential practice for heat island mitigation and stormwater management.” *Environmental Research Letters*, 8(1).

Liao, Z., Chen, H., Huang, F., and Li, H. (2016). “Cost – effectiveness analysis on LID measures of a highly urbanized area.” *Desalination Water Treat*, 56(11), 2809–2815.

Lin, W., Park, D. G., Ryu, S. W., Lee, B. T., and Cho, Y. H. (2016). “Development of permeability test method for porous concrete block pavement materials considering clogging.” *Constr Build Mater*, 118, 20–26.

Liu, R., Chi, Y., Chen, S., Jiang, Q., Meng, X., Wu, K., and Li, S. (2020). “Influence of Pore Structure Characteristics on the Mechanical and Durability Behavior of Pervious Concrete Material Based on Image Analysis.” *Int J Concr Struct Mater*, 14(1), 1–16.

Lori, A. R., Bayat, A., and Azimi, A. (2019). “Influence of the replacement of fine copper slag aggregate on physical properties and abrasion resistance of pervious concrete.” *Road Materials and Pavement Design*, 1–17.

Marcaida, A. K., and Nguyen, T. H. (2018). “Investigation of Particle-Related Clogging of Sustainable Concrete Pavements.” *Sustainability*, 10(12), 4845.

Martin, W. D., Putman, B. J., and Kaye, N. B. (2013). “Using image analysis to measure the porosity distribution of a porous pavement.” *Constr Build Mater*, 48, 210–217.

Mohammed, B. S., Liew, M. S., and Alaloul, W. S. (2018). “Case Studies in Construction Materials Properties of nano-silica modi fi ed pervious concrete.” *Case Studies in Construction Materials*, 8(January), 409–422.

Neithalath, N., Sumanasooriya, M. S., and Deo, O. (2010). “Characterizing pore volume, sizes, and connectivity in pervious concretes for permeability prediction.” *Mater Charact*, 61(8), 802–813.

Nguyen, D. H., Sebaibi, N., Boutouil, M., Leleyter, L., and Baraud, F. (2014). “A modified method for the design of pervious concrete mix.” *Constr Build Mater*, 73, 271–282.

Nnadi, E. O., Newman, A. P., Coupe, S. J., and Mbanaso, F. U. (2015). “Stormwater harvesting for irrigation purposes: An investigation of chemical quality of water recycled in pervious pavement system.” *J Environ Manage*, 147, 246–256.

Ong, S. K., Wang, K., Ling, Y., and Shi, G. (2016). “Pervious Concrete Physical Characteristics and Effectiveness in Stormwater Pollution Reduction.” (April), 57.

Opiso, E. M., Supremo, R. P., and Perodes, J. R. (2019). “Effects of coal fly ash and fine sawdust on the performance of pervious concrete.” *Heliyon*, 5(11), e02783.

Page, J. L., Winston, R. J., Mayes, D. B., Perrin, C., and Hunt, W. F. (2015). “Retrofitting with innovative stormwater control measures: Hydrologic mitigation of impervious cover in the municipal right-of-way.” *J Hydrol (Amst)*, 527, 923–932.

Palla, A., and Gnecco, I. (2016). “Assessing the urban catchment hydrologic response under different environmental scenarios.” *Novatech 2016, 28 juin - 1er juillet 2016, Lyon, France (FRA)*, 1–8.

Pavičić, I., Briševac, Z., Vrbaški, A., Grgasović, T., Duić, Ž., Šijak, D., and Dragičević, I. (2021). “Geometric and Fractal Characterization of Pore Systems in the Upper Triassic Dolomites Based on Image Processing Techniques (Example from Žumberak Mts, NW Croatia).” *Sustainability*, 13(14), 7668.

Qin, Y., Yang, H., Deng, Z., and He, J. (2015). “Water permeability of pervious concrete is dependent on the applied pressure and testing methods.” *Advances in Materials Science and Engineering*, 2015(January).

Sai, V., and Kothala, K. (2018). “Use of Image Analysis as a Tool for Evaluating Various Construction Materials Recommended Citation.”

Sandoval, G. F. B., Galobardes, I., Schwantes-cezario, N., and Berenice, M. (2019). “Correlation between permeability and porosity for pervious concrete Correlación de la permeabilidad y la porosidad para el concreto permeable (CoPe).” 86(209), 151–159.

Schaefer, V. R., and Kevern, J. T. (2011). “An Integrated Study of Pervious Concrete Mixture Design for Wearing Course Applications An Integrated Study of Pervious Concrete Mixture Design for Wearing.”

Schwartz, S. S., and Asce, A. M. (2010). “Effective Curve Number and Hydrologic Design of Pervious Concrete Storm-Water Systems.”

Shen, J., Zhang, Q., and Engineering, I. (2016). “m nl ad in e e V by e th rsio is n fil O e is nly m nl ad in e e V by e th rsio is n fil O e is nly.” 9(11), 25–34.

Tan, Y., Zhu, Y., and Xiao, H. (2020). “Applied sciences Evaluation of the Hydraulic , Physical , and Mechanical Properties of Pervious Concrete Using Iron Tailings as Coarse Aggregates.” *Appl. Sci.*, *10*, 2691.

Valeo, C. (2018). “Determining Surface Infiltration Rate of Permeable Pavements with Digital Imaging.” *Water*, *10*, 133.

Vázquez-Rivera, N. I., Soto-Pérez, L., St John, J. N., Molina-Bas, O. I., and Hwang, S. S. (2015). “Optimization of pervious concrete containing fly ash and iron oxide nanoparticles and its application for phosphorus removal.” *Constr Build Mater*, 93, 22–28.

Walsh, S. P., Rowe, A., Ph, D., Asce, A. M., Guo, Q., and Asce, M. (2014). “Laboratory Scale Study to Quantify the Effect of Sediment Accumulation on the Hydraulic Conductivity of Pervious Concrete.” *Journal of Irrigation and Drainage Engineering*, 140(6), 1–7.

Wang, H., Li, H., Liang, X., Zhou, H., Xie, N., and Dai, Z. (2019). “Investigation on the mechanical properties and environmental impacts of pervious concrete containing fly ash based on the cement-aggregate ratio.” *Constr Build Mater*, 202, 387–395.

Welker, A., Jenkins, J., McCarthy, L., and Nemirovsky, E. (2013). “Examination of the Material Found in the Pore Spaces of Two Permeable Pavements.” *Journal of Irrigation and Drainage Engineering*, 139(4), 278–284.

Winston, R. J., Al-Rubaei, A. M., Blecken, G. T., Viklander, M., and Hunt, W. F. (2016). “Maintenance measures for preservation and recovery of permeable pavement surface infiltration rate - The effects of street sweeping, vacuum cleaning, high pressure washing, and milling.” *J Environ Manage*, 169, 132–144.

Xie, X., Zhang, T., Yang, Y., Lin, Z., Wei, J., and Yu, Q. (2018). “Maximum paste coating thickness without voids clogging of pervious concrete and its relationship to the rheological properties of cement paste.” *Constr Build Mater*, 168, 732–746.

Yang, J., and Jiang, G. (2003). “Experimental study on properties of pervious concrete pavement materials.” 33, 381–386.

Yekkalar, M., Haselbach, L., and Langfitt, Q. (2018). “Impacts of a Pervious Concrete Retention System on Neighboring Clay Soils.” *Journal of Cold Regions Engineering*, 32(1), 04017023.

Zhong, R., and Wille, K. (2015). “Material design and characterization of high performance pervious concrete.” *Constr Build Mater*, 98, 51–60.

Zhou, H., Li, H., Abdelhady, A., Liang, X., Wang, H., and Yang, B. (2019). “Experimental investigation on the effect of pore characteristics on clogging risk of pervious concrete based on CT scanning.” *Constr Build Mater*, 212, 130–139.

Zhou, J., Zheng, M., Wang, Q., Yang, J., and Lin, T. (2016). “Flexural fatigue behavior of polymer-modified pervious concrete with single sized aggregates.” *Constr Build Mater*, 124, 897–905.

Zhu, H., Wen, C., Wang, Z., and Li, L. (2020). “Study on the Permeability of Recycled Aggregate Pervious Concrete with Fibers.” Jan 10;13(2):321.

LIST OF PUBLICATIONS

JOURNAL

- Mulu, A., Jacob, P., and Dwarakish, G. S. (2022). “Hydraulic Performance of Pervious Concrete Based on Small Size Aggregates.” *Advances in Materials Science and Engineering*, (D. Foti, ed.), 2022, 2973255. (https://doi.org/10.1155/2022/2973255)

BOOK CHAPTER

- Jacob, P., Dwarakish, G. S., Sharath, G. O., and Ramesh, G. N. (2022). “Pervious Concrete as an Effective Urban Flood Management Tool.” *River and Coastal Engineering: Hydraulics, Water Resources and Coastal Engineering*, R. Jha, V. P. Singh, V. Singh, L. B. Roy, and R. Thendiyath, eds., Cham: Springer International Publishing, 145–159. (https://doi.org/10.1007/978-3-031-05057-2_13)

INTERNATIONAL CONFERENCE

- Jacob, P., Dwarakish, G. S., Sharath, G. O., and Ramesh, G. N. S (2018), “Pervious Concrete as an effective Urban Flood Management Tool”. *HYDRO 2018 International Conference*, National Institute of Technology Patna, 19 to 21 December 2018.

BIO – DATA

Name	:	Preeti Jacob
Date of Birth	:	15-02-1985
Address	:	10, 4th Cross, Ramanujappa Layout, B Narayanapura Extn., Udayanagar, Bangalore - 560016
Mobile	:	8050258880
Email	:	pmj285@gmail.com, preeti.j@cmrit.ac.in
Qualifications	:	B. Tech - Civil Engineering - Government Engineering College, Thrissur, Calicut University M. Tech - Water Resources Engineering and Management, NITK Surathkal
Publications	:	Journal - 1, Book Chapter - 1, International Conference - 2